



UNIVERSIDAD AUTÓNOMA DE SAN LUIS POTOSÍ

FACULTAD DE CIENCIAS QUÍMICAS

Centro de Investigación y Estudios de Posgrado

Posgrado en Ciencias en Ingeniería Química



UNIVERSIDAD DE GRANADA

FACULTAD DE CIENCIAS

Departamento de Química Inorgánica

Programa de Doctorado en Química

**Adsorción de compuestos farmacéuticos en solución
acuosa sobre arcillas naturales y nanomateriales de
carbono**

Tesis en cotutela internacional que para obtener los grados de:

Doctor en Ciencias en Ingeniería Química

por la Universidad Autónoma de San Luis Potosí

Doctor en Química

por la Universidad de Granada

Presenta:

ORTIZ RAMOS UZIEL

Directores de Tesis:

Dr. Roberto Leyva Ramos

Dr. Francisco Carrasco Marín

SAN LUIS POTOSÍ, S. L. P.

AGOSTO, 2024

Esta tesis está enmarcada en el Convenio de Cotutela de Tesis Doctoral Suscrito entre la Universidad de Granada, España (UGR) y la Universidad Autónoma de San Luis Potosí, México (UASLP), de fecha 19 de noviembre de 2021.



REPOSITORIO INSTITUCIONAL



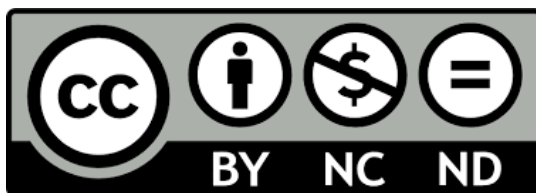
**UASLP-Sistema de Bibliotecas
Repositorio Institucional Tesis digitales Restricciones de uso**

DERECHOS RESERVADOS

PROHIBIDA SU REPRODUCCIÓN TOTAL O PARCIAL

Todo el material contenido en este Trabajo Terminal está protegido por la Ley Federal de Derecho de Autor (LFDA) de los Estados Unidos Mexicanos.

El uso de imágenes, fragmentos de videos, y demás material que sea objeto de protección de los derechos de autor, será exclusivamente para fines educativos e informativos y deberá citar la fuente donde se obtuvo, mencionando el autor o autores. Cualquier uso distinto o con fines de lucro, reproducción, edición o modificación será perseguido y sancionado por el respectivo titular de los Derechos de Autor.



ADSORCIÓN DE COMPUESTOS FARMACÉUTICOS SOBRE ARCILLAS
NATURALES Y NANOMATERIALES DE CARBONO © 2024 by UZIEL ORTIZ
RAMOS is licensed under Creative Commons Attribution-NonCommercial-
NoDerivatives 4.0 International. To view a copy of this license visit

<https://creativecommons.org/licenses/by-nc-nd/4.0/>

La primera parte de la tesis doctoral se realizó en el Laboratorio de Ingeniería Química Ambiental perteneciente a la Facultad de Ciencias Químicas de la Universidad Autónoma de San Luis Potosí (México), en el periodo comprendido entre agosto 2020 y julio 2022, bajo la dirección del Dr. Roberto Leyva Ramos. La segunda parte de la tesis doctoral se llevó a cabo en el grupo de investigación Materiales Polifuncionales Basados en Carbono (UGR-Carbon) perteneciente a la Facultad de Ciencias de la Universidad de Granada (España), en el periodo comprendido entre agosto 2022 y julio 2024, bajo la dirección del Dr. Francisco Carrasco Marín. Este trabajo de investigación ha sido financiado por la Asociación Universitaria Iberoamericana de Postgrado, España con la beca de movilidad *PMA2-2022-123-14* en Andalucía – Segundo Plazo 2022, la Consejería de Universidad, Investigación e Innovación (Junta de Andalucía) 2021-2027 por el proyecto *C-EXP-247-UGR23*, el Ministerio de Ciencia e Innovación / Agencia Estatal de Investigación / 10.13039/501100011033 y el Fondo Europeo de Desarrollo Regional Una manera de hacer Europa por el proyecto *PID2021-127803OB-I00*



El programa de Doctorado en Ciencias en Ingeniería Química de la Universidad Autónoma de San Luis Potosí pertenece al Sistema Nacional de Posgrados de Calidad (SNP) del Consejo Nacional de Humanidades, Ciencias y Tecnologías (CONAHCyT), registro 000897 en el nivel SNP Consolidado.

Número de la beca otorgada por CONAHCYT: 780307

Número de CVU: 930155

Los datos del trabajo titulado “Adsorción de Compuestos Farmacéuticos en Solución Acuosa sobre Arcillas Naturales y Nanomateriales de Carbono” se encuentran bajo el resguardo de la Universidad Autónoma de San Luis Potosí y de la Universidad de Granada.

Solicitud de Registro de Tesis Doctorado

San Luis Potosí SLP a 04/ agosto /2024

Comité Académico

En atención a: Coordinador/a del Posgrado

Por este conducto solicito a Usted se lleve a cabo el registro de título de tesis de Doctorado, el cual quedo definido de la siguiente manera:

“Adsorción de compuestos farmacéuticos en solución acuosa sobre arcillas naturales y nanomateriales de carbono”

que desarrollará el/la estudiante: Uziel Ortiz Ramos

bajo la dirección y/o Co-dirección de los Drs.: Roberto Leyva Ramos y Francisco Carrasco Marín

Asimismo, le comunico que el proyecto en el cual trabajará el alumno involucrará el manejo de animales de experimentación, estudios con seres humanos o muestras derivadas de los mismos, el manejo y/o generación de organismos genéticamente modificados y requiere de aval de Comité de Ética e investigación de la FCQ.

(Complete la opción que aplique en su caso):

() Sí debido a que: _____

() No

(X) No Aplica

Sin otro particular, quedo de Usted.

ATENTAMENTE

Uziel Ortiz Ramos

Dr. Roberto Leyva Ramos

Dr. Francisco Carrasco Marín

Nombre y firma del estudiante Nombre y firma de los Directores de Trabajo Terminal



UNIVERSIDAD AUTÓNOMA DE SAN LUIS POTOSÍ
FACULTAD DE CIENCIAS QUÍMICAS
Centro de Investigación y Estudios de Posgrado
Posgrado en Ciencias en Ingeniería Química



UNIVERSIDAD DE GRANADA
FACULTAD DE CIENCIAS
Departamento de Química Inorgánica
Programa de Doctorado en Química

**Adsorción de compuestos farmacéuticos en solución
acuosa sobre arcillas naturales y nanomateriales de
carbono**

Tesis que para obtener los grados de:

Doctor en Ciencias en Ingeniería Química
Doctor en Química

Presenta:

ORTIZ RAMOS UZIEL

SINODALES:

Presidente:

Secretario:

Secretario:

Vocal:

Vocal:

San Luis Potosí, S.L.P., México

Agosto, 2024

Integrantes del comité tutorial académico:

Dra. Paola Elizabeth Díaz Flores: Presidenta. Adscrita al Programa de Doctorado en Ciencias en Ingeniería Química de la Universidad Autónoma de San Luis Potosí, San Luis Potosí, México.

Dr. Francisco Carrasco Marín: Secretario. Adscrito al Programa de Doctorado en Química de la Universidad de Granada, España.

Dr. Erik César Herrera Hernández: Secretario. Adscrito al Programa de Doctorado en Ciencias en Ingeniería Química de la Universidad Autónoma de San Luis Potosí, San Luis Potosí, México.

Dra. Damarys Haidee Carrales Alvarado: Vocal. Adscrita al Programa de Doctorado en Ciencias en Ingeniería Química de la Universidad Autónoma de San Luis Potosí, San Luis Potosí, México.

Dr. Antonio Aragón Piña: Vocal. Adscrita al Instituto de Metalurgia de la Universidad Autónoma de San Luis Potosí, San Luis Potosí, México.



Carta Cesión de Derechos

San Luis Potosí SLP a 04/ agosto /2024

En la ciudad de San Luis Potosí, S.L.P., el día 04 del mes de agosto del año 2024 El que suscribe Uziel Ortiz Ramos alumno(a) del programa de posgrado Doctorado en Ciencias en Ingeniería Química adscrito a la Universidad Autónoma de San Luis Potosí manifiesta que es autor(a) intelectual del presente trabajo terminal, realizado bajo la dirección de: Dr. Roberto Leyva Ramos y Dr. Francisco Carrasco Marín y cede los derechos del trabajo titulado Adsorción de compuestos farmacéuticos en solución acuosa sobre arcillas naturales y nanomateriales de carbono a la **Universidad Autónoma de San Luis Potosí y a la Universidad de Granada**, para su difusión con fines académicos y de investigación.

Los usuarios de la información no deben reproducir de forma total o parcial texto, gráficas, imágenes o cualquier contenido del trabajo si el permiso expreso del o los autores. Éste, puede ser obtenido directamente con el autor o autores escribiendo a la siguiente dirección uzielrms@hotmail.com. Si el permiso se otorga, el usuario deberá dar el agradecimiento correspondiente y citar la fuente del mismo.

Uziel Ortiz Ramos

Nombre y firma del alumno

Carta de Análisis de Similitud

San Luis Potosí SLP a 08/julio/2024

L.B. María Zita Acosta Nava
Biblioteca de Posgrado FCQ

Asunto: Reporte de porcentaje de similitud de tesis de grado

Por este medio me permito informarle el porcentaje de similitud obtenido mediante Ithenticate para la tesis titulada: **Adsorción de compuestos farmacéuticos en solución acuosa sobre arcillas naturales y nanomateriales de carbono**, presentada por el autor **Uziel Ortiz Ramos**. La tesis es requisito para obtener el grado de Doctorado el Posgrado en Ciencias en Ingeniería Química. El análisis reveló un porcentaje de similitud de **31%** excluyendo referencias y metodología.

Agradezco sinceramente su valioso tiempo y dedicación para llevar a cabo una revisión exhaustiva de la estructura de la tesis. Quedo a su disposición para cualquier consulta o inquietud que pueda surgir en el proceso.

Sin más por el momento, le envió un cordial saludo.

A T E N T A M E N T E

Dr. Erik César Herrera Hernández
Coordinador Académico del Posgrado
en Ciencias en Ingeniería Química

*“A bit of science distances one from God,
but much science nears one to him”*

Louis Pasteur

Agradecimientos

Quiero agradecer en primer lugar a Dios por todas sus bendiciones y por permitirme culminar una de las etapas más importantes de mi vida.

Muy especialmente, quiero expresar mi gratitud a mis directores de tesis, Dr. Roberto Leyva Ramos y Dr. Francisco Carrasco Marín, por su guía en esta tesis. Su experiencia, paciencia y motivación fueron esenciales para la culminación exitosa de este trabajo.

Agradezco infinitamente al Dr. Roberto Leyva Ramos por darme la oportunidad de formar parte del grupo de investigación de Ingeniería Química Ambiental de la Universidad Autónoma de San Luis Potosí en México, y a su esposa, la Sra. Rosa María Guerrero Coronado. El constante apoyo, experiencia, sabios consejos, disponibilidad, paciencia y confianza que me brindaron fueron fundamentales para concluir esta etapa. Muchas gracias a ambos por su preocupación y por tratarme como a un hijo, mis padres académicos, personas maravillosas y grandes ejemplos a seguir.

Al Dr. Francisco Carrasco Marín, Dr. Agustín Francisco Pérez Cadenas y Dra. Esther Bailón García, por permitirme formar parte del grupo de investigación Materiales Polifuncionales Basados en Carbono (UGR-Carbon) de la Universidad de Granada en España. Su vasta experiencia, conocimiento y consejos me han inspirado mucho a continuar en el camino científico. Muchas gracias por el seguimiento, apoyo, disponibilidad y paciencia que me brindaron durante mi etapa doctoral en Granada.

A mi comité de evaluación tutorial, Dra. Esmeralda Mendoza Mendoza, Dr. Antonio Aragón Piña, Dr. Erik César Herrera Hernández y Dra. Diana Elizabeth Villela Martínez, por su seguimiento durante mi etapa doctoral. Sus consejos, recomendaciones y correcciones han sido cruciales para la realización de este trabajo.

Una mención muy especial a la Dra. Esther Bailón García. Gran parte de este trabajo es gracias a usted. Muchas gracias por toda su dedicación y disponibilidad en el desarrollo de esta investigación, por compartir sus conocimientos, por transmitirme el amor por la ciencia, por sus consejos y charlas motivacionales, y también por sus regaños. Todo esto me ha inspirado a querer continuar en el camino de la ciencia y

me ha ayudado a forjarme como investigador. Le agradezco infinitamente por creer en mi y por su gran amistad. Siempre será una inspiración para mí.

A todos mis colegas y amigos que conocí durante mi etapa doctoral. En el laboratorio de Ingeniería Química Ambiental, a Carolina, Brenda, Génesis, Vianey, Cecilia, Diana, Damarys, Lupita, Alberto. Muchas gracias por hacer los días en el laboratorio muy divertidos, por su grata compañía y por su ayuda en la resolución de todas mis dudas. En el grupo UGR-Carbon, a Lilian, Adriana, John, Edgar, Diego, Lady, Daniel y a los doctores Cristian, Adriana, Juan, Hakim y María. Muchas gracias por hacerme sentir como en casa, por todas esas mañanas de café y charlas. De cada uno aprendí mucho, y espero que nuestras colaboraciones sigan adelante.

Finalmente, agradezco a familia que me acompañó durante esta travesía. A mis padres, Yolanda y Pablo, por todo su apoyo, confianza, amor, por ayudarme a seguir cumpliendo mis sueños y metas y por hacer de mí una mejor persona a través de sus consejos y enseñanzas. A mis hermanos, Luis Ángel, Sarai y Lupita, y a mi sobrina Grecia, que, aunque aún no te conozco, gracias por ser mi apoyo diario.

*A mis padres, Yolanda Ramos y Pablo Ortiz,
pilares fundamentales en mi vida. A mis
hermanos, Luis Ángel, Sarai, Lupita y mi sobrina
Grecia, por todo su apoyo incondicional. Gracias a
todos ustedes he logrado cumplir este sueño.*

Resumen

Este trabajo se centra en el desarrollo de materiales basados en arcillas naturales y en la fabricación de estructuras monolíticas de carbono con porosidad y geometrías de canales controladas por impresión 3D, aplicados para eliminar contaminantes farmacéuticos del agua. Se estudió la adsorción de tetraciclina, trimetoprima y clorfenamina en varias arcillas, destacando la bentonita por su alta capacidad de adsorción gracias a su estructura laminar y propiedades de hinchamiento. La adsorción de trimetoprima y tetraciclina está gobernada por difusión superficial, y la de clorfenamina por difusión en el volumen del poro. En la adsorción binaria de tetraciclina y cadmio se encontraron efectos competitivos y sinérgicos en función del pH de la solución. La organobentonita híbrida mostró altas capacidades de adsorción según la carga iónica y naturaleza hidrofóbica del fármaco. Los resultados indicaron que las interacciones electrostáticas son el principal mecanismo de adsorción y que la velocidad de adsorción se debe al transporte externo de masa.

Se diseñaron y fabricaron innovadores adsorbentes monolíticos de carbono con diferentes texturas porosas y geometrías avanzadas de canales mediante impresión 3D. Las variables de síntesis analizadas incluyeron la relación resorcinol/catalizador, el agente activante (CO_2 y H_2O), tiempos de activación y geometrías de canales. Estas variables se evaluaron en la adsorción de sulfametoxazol. Los monolitos de carbono mostraron una integración óptima de alta resistencia mecánica con geometrías de canales avanzadas controladas y replicadas fielmente por la impresión 3D, con una macroestructura porosa de baja resistencia al flujo. Las variables de síntesis afectaron significativamente la morfología, logrando una estructura porosa jerárquica con alta área superficial, superando la capacidad de adsorción de muchos materiales adsorbentes existentes. Las geometrías de canales influyeron drásticamente en las curvas de ruptura: monolitos de canales rectos, hexagonales y romboidales tuvieron tiempos de ruptura tempranos por efectos de canalización, mientras que los de red interconectada mostraron mayores tiempos de ruptura, mitigando estos efectos gracias a la turbulencia y mezclado, confirmados por simulaciones CFD.

Palabras clave: adsorción, fármacos, arcillas, monolitos de carbono, impresión 3D.

Abstract

This work focuses on the development of clay-based materials and the fabrication of carbon monolithic structures with controlled porosity and channel geometries using 3D printing, aimed at removing pharmaceutical contaminants from water. The adsorption of tetracycline, trimethoprim and chlorphenamine on various clays was studied, with bentonite showing high adsorption capacity due to its laminar structure and swelling properties. The adsorption of trimethoprim and tetracycline is governed by surface diffusion, while chlorphenamine adsorption is controlled by pore volume diffusion. Binary adsorption of tetracycline and cadmium revealed competitive and synergistic effects depending on solution pH. Hybrid organobentonite exhibited high adsorption capacities based on the ionic charge and hydrophobic nature of the drug. Results indicated that electrostatic interactions are the primary adsorption mechanism, and that adsorption rate is due to external mass transport.

Innovative carbon monolithic adsorbents with different porous textures and advanced channel geometries were designed and fabricated using 3D printing. The synthesis variables analyzed included resorcinol/catalyst ratio, activating agents (CO₂ and H₂O), activation times and channel geometries. These variables were evaluated in sulfamethoxazole adsorption. Carbon monoliths showed optimal integration of high mechanical strength with advanced channel geometries, faithfully replicated by 3D printing, and a porous macrostructure with low flow resistance. Synthesis variables significantly affected morphology, achieving a hierarchical porous structure with high surface area, surpassing the adsorption capacity of many existing adsorbent materials. Channel geometries drastically influenced breakthrough curves: monoliths with straight, hexagonal and rhomboidal channels had early breakthrough times due to channeling effects, while interconnected network channel showed longer breakthrough times, mitigating these effects through turbulence and mixing, confirmed by CFD simulations.

Keywords: adsorption, pharmaceuticals, clays, carbon monoliths, 3D printing.

TABLE OF CONTENTS	PAGE
List of tables	iv
List of figures	v
CHAPTER 1. INTRODUCTION	1
CHAPTER 2. BACKGROUND OF THE RESEARCH AND OBJECTIVES	4
2.1 Water contamination	5
2.2 Emerging contaminants	5
2.3 Contamination by pharmaceutical compounds	7
2.3.1 Antihistamines	8
2.3.2 Antibiotics	9
2.3.3 Nonsteroidal anti-inflammatories	10
2.3.4 Antiepileptics	11
2.4 Methods for the removal of pharmaceutical compounds from water solutions	12
2.4.1 Adsorption	15
2.5 Adsorbent materials	17
2.5.1 Natural clays	18
2.5.2 Organoclays	22
2.5.3 Carbon xerogels	27
2.6 Objectives	33
2.6.1 General objective	33
2.6.2 Specific objectives	33
CHAPTER 3. EXPERIMENTAL METHODS	35
3.1 Preparation and synthesis of clay-based materials and carbon monolithic structures	36
3.1.1 Clay minerals preconditioning	36
3.1.2 Preparation of clay samples with different uptakes of pharmaceuticals adsorbed	36

3.1.3 Synthesis of hybrid hexadecyltrimethylammonium bromide-modified organobentonite	36
3.1.4 Synthesis of nanostructured carbon xerogels	36
3.1.5 Design of 3D geometries using Computer-Aided Design (CAD)	37
3.1.6 Fabrication of 3D-printed carbon monoliths	37
3.1.7 Activation of 3D-printed carbon monoliths using CO ₂ and H ₂ O	37
3.2 Characterization techniques	37
3.3 Adsorption tests	37
CHAPTER 4. REMOVAL OF TETRACYCLINE FROM AQUEOUS SOLUTIONS BY ADSORPTION ON RAW Ca-BENTONITE. EFFECT OF OPERATING CONDITIONS AND ADSORPTION MECHANISM	38
4.1 Introduction	39
4.2 Experimental methodology	41
4.2.1 Materials	41
4.2.2 Clay minerals preconditioning	42
4.2.3 Characterization of bentonite and bentonite with TC adsorbed	43
4.2.4 Quantification of TC concentration in water samples	44
4.2.5 Technique for conducting the adsorption equilibrium experiments	44
4.2.6 Technique for performing the desorption equilibrium experiments	46
4.2.7 Procedure for determining the amounts of cations adsorbed during adsorption of TC	46
4.3 Results and discussion	48
4.3.1 Cation exchange capacity, chemical composition, textural characteristics and morphology of bentonite	48
4.3.2 Zeta potential distribution	50

4.3.3 X-ray diffraction testing	53
4.3.4 Infrared spectroscopy analysis	54
4.3.5 Thermogravimetric analysis	56
4.3.6 Adsorption isotherms of TC	58
4.3.7 Comparing the adsorption capacity of TC on various raw clays	59
4.3.8 Influence of solution pH upon the capacity of bentonite for adsorbing TC	60
4.3.9 Analysis of cations exchanged during adsorption of TC	62
4.3.10 Variation of the adsorption capacity of bentonite with the ionic strength	64
4.3.11 Variation of the bentonite adsorption capacity with temperature	65
4.3.12 Desorption of TC adsorbed on bentonite	66
4.3.13 Adsorption mechanisms of TC on bentonite	68
4.4 Conclusions	69
References	71

LIST OF TABLES	PAGE
Table 4.1. Physicochemical properties of TC.	42
Table 4.2. Chemical composition and textural properties of Bent and B-TC (pH 3).	48
Table 4.3. Adsorption isotherm parameters and average percentage deviation for the adsorption of TC on raw clays.	59
Table 4.4. Adsorption capacities of several adsorbent materials towards TC.	61
Table 4.5. Exchangeable cations and H ⁺ concentration at the beginning and the end of the adsorption of TC on Bent and uptake of TC adsorbed on Bent.	63
Table 4.6. Desorption percentages of TC from Bent at T = 25 °C.	68

LIST OF FIGURES	PAGE
Figure 2.1. Tetrahedral sheet of clays.	19
Figure 2.2. Octahedral sheet of clays.	19
Figure 2.3. Trilaminar structure 2:1 (T:O:T) of a bentonite clay.	21
Figure 2.4. Chemical structures of the cationic surfactants HDTMA (a), DDTMA (b) and BTMA (c).	23
Figure 2.5. Structural arrangements of organoclays: monolayer (a), bilayer (b), pseudotrimolecular layer (c) and inclined paraffin-like structures (d, e).	24
Figure 2.6. Variation of basal space, d_{001} , with cationic surfactant alkyl chain length, n_c , due to monolayer, bilayer, and pseudotrimolecular layer formation.	25
Figure 2.7. Stages of synthesis of carbon gels by the sol-gel method.	28
Figure 2.8. Polymerization mechanisms of resorcinol and formaldehyde.	30
Figure 4.1. Chemical structure of TC (a) and speciation diagram of TC (b) as a function of solution pH.	42
Figure 4.2. Batch adsorbers.	45
Figure 4.3. Adsorption-desorption isotherms of N_2 on Bent and B-TC (pH 3) at $-195.15\text{ }^\circ\text{C}$.	49
Figure 4.4. The cumulative pore volume percentage of Bent and B-TC (pH 3).	50
Figure 4.5. SEM images of Bent and B-TC (pH 3) recorded at 500X (a), 3000X (b) and 5000X (c).	51
Figure 4.6. Zeta potential distribution of Bent as a function of TC initial concentration (a) and Zeta potential difference of Bent as a function of the uptake of TC adsorbed (b) at $T = 25\text{ }^\circ\text{C}$ and pH of 3 and 7.	52
Figure 4.7. X-ray patterns obtained for Bent, B-TC (pH 3) and B-TC (pH 7) (a). Enlargement of the area depicting the (001) reflection of Bent (b).	54
Figure 4.8. FT-IR spectra of Bent, B-TC (pH 3), B-TC (pH 7) and TC (a). The amplification of the spectra selected by the blue dashed line showing the TC bands (b).	55

Figure 4.9. TGA (red line) and DTG (black dashed line) curves obtained for Bent (a), B-TC (pH 7) (b) and B-TC (pH 3) (c).	57
Figure 4.10. Effect of the type of raw clay on the adsorption isotherms of TC at pH = 3 and T = 25 °C (a). Amplification in the uptake of TC adsorbed range from 0 to 70 mg/g (b). The lines represent the best-fit isotherm.	60
Figure 4.11. Effect of the solution pH on the adsorption isotherms of TC on Bent at T = 25 °C. The lines represent the Langmuir isotherm.	62
Figure 4.12. Effect of the solution ionic strength on the adsorption isotherms of TC on Bent at T = 25 °C and pH = 3 (a) and pH = 7 (b). The lines represent the Langmuir isotherm.	64
Figure 4.13. Effect of the temperature on the adsorption isotherms of TC on Bent at pH = 7. The lines represent the Langmuir isotherm.	65
Figure 4.14. Adsorption isotherm of TC on Bent at pH = 3 and T = 25 °C; and desorption isotherm of TC at pH of 3 and 7. The lines represent the Langmuir isotherm.	67
Figure 4.15. Adsorption mechanisms of TC on Bent at pH = 3 (a) and pH = 7 (b).	69

CHAPTER

INTRODUCTION

1

Water is essential for life and ecosystems across the planet. It is the most important natural resource and also one of the most vulnerable. In recent years, the development of human activities has led to the emergence of new contaminants known as emerging contaminants (ECs). ECs include pharmaceutical compounds, personal care products, endocrine disruptors, dyes and agricultural chemicals. These contaminants can enter the environment through discharges of hospital, industrial and domestic wastewater. ECs are transported to wastewater treatment plants, continuously released into surface and groundwater systems, and detected in a wide range of concentrations, from ng/L to µg/L (Chaturvedi et al., 2021).

It is known that ECs can cause sexual disorders in marine organisms, neurological, reproductive and immunological alterations in animals, cancer, the development of antibiotic-resistant bacterial genes, and congenital heart disease, among other toxic effects (Gogoi et al., 2018). However, precise information on the toxic effects of ECs in water systems is limited.

One category of ECs that has gained priority is pharmaceuticals (Ahuja, 2021). Pharmaceuticals are widely used in the diagnosis, treatment, cure and prevention of various diseases in humans and animals due to their different physicochemical and biological properties. Most pharmaceuticals experience transformations in the body when ingested, resulting in the release of a large number of metabolites into surface and groundwater systems during wastewater treatment and cause irreparable harm to humans and ecosystems (Bexfield et al., 2019).

Currently, wastewater treatment plants play a crucial role in removing various contaminants, such as suspended particles, dissolved organic compounds, nutrients, and pathogens. These plants employ different treatment stages involving processes like sieving, coagulation/flocculation, centrifugation, sedimentation and biological treatments. However, current conventional technologies have limitations in reducing the concentrations of pharmaceutical compounds present in wastewater. To address this challenge, recent years have seen the development and implementation of more effective and specific treatment technologies. Among these technologies are methods

such as chlorination, ozonation, adsorption, advanced oxidation processes and visible light photodegradation.

Adsorption processes have been widely used and stand out as a promising and effective alternative for removing pharmaceuticals from wastewater. This technology offers a wide range of significant advantages, marking it an attractive option compared to other treatment techniques. Key advantages include ease of operation, low cost, reproducibility, high efficiency and the absence of toxic byproduct generation. Additionally, it offers flexibility in utilizing a wide range of adsorbent materials, from natural micrometric materials to advanced nanostructured synthetic materials (Cooney, 1998).

The aim of this thesis is to develop clay-based adsorbent materials and to fabricate nanostructured carbon monolith adsorbents with controlled porosity and channel geometries using 3D printing technology combined with sol-gel polymerization, both for the removal of pharmaceutical compounds from water. The study will focus on the effect of the chemical, textural and swelling properties of natural clays with distinct structural arrangements on the adsorption capacity of pharmaceutical compounds, as well as the impact of operational parameters on adsorption capacity. Furthermore, for the first time, the mass transport mechanisms controlling the overall adsorption rate of pharmaceutical compounds on natural clays will be elucidated by obtaining kinetic data under different experimental conditions.

In addition, hybrid materials will be prepared by intercalating organic molecules of cationic surfactants within the interlayer space of the clays to modify their surface chemistry and provide additional functional properties that enable the adsorption of pharmaceuticals in aqueous solution.

Furthermore, the fabrication of integral monoliths of carbon xerogels is proposed by combining sol-gel polymerization and 3D printing technology to be applied as adsorbents in continuous adsorption systems. The effect of synthesis conditions and channel geometry will be investigated to obtain monolithic structures with an appropriate and highly controlled chemical composition, porous structure and channel geometries for adsorption purposes.

CHAPTER

**BACKGROUND OF THE
RESEARCH AND OBJECTIVES**

2

2.1 Water contamination

Water is essential for sustaining life and ecosystems worldwide, making it one of the most crucial yet vulnerable natural resources. Recent official figures estimate that each person consumes approximately 227 liters of water per day, contributing to the alarming rise of water pollution, a pressing global environmental concern (Vasilachi et al., 2021).

Water pollution can stem from both natural factors and various anthropogenic sources, including industrial dischargers, agricultural runoff, untreated sewage, oil spills, and chemical releases, among others. These pollutants can adversely impact water quality, aquatic ecosystems, and human health.

In recent years, human activities have given rise to the emergence of new organic pollutants known as “emerging contaminants”. This term is used when there is limited information available about the extent and frequency of the risks these contaminants pose to human health and the environment (Lofrano et al., 2020). Generally, emerging contaminants encompass a broad range of human-produced organic compounds considered essential for modern society but can pose long-term dangers to ecosystems and human health when present in water. According to the 2016 Global Burden of Diseases, Injuries, and Risk Factors Study (GBD), an estimated 1.3 million deaths were linked to 12 synthetic substances present in environment (Naghavi, 2017). In 2021, during the 5th United Nations Environment Assembly (UNEA5), environmental pollution was categorized as one of the top global challenges, alongside biodiversity loss and climate change. Consequently, it is evident that urgent action is required to address this global issue and implement effective measures to protect our ecosystems and ensure the health of future generations.

2.2 Emerging contaminants

Emerging contaminants (ECs), as defined by the United States Geological Survey (USGS), are synthetic chemicals that are not regularly monitored in the environment but have the potential to cause adverse effects on ecology and human health.

According to the database of the Network of Laboratories, Research Centers, and related organizations for monitoring emerging environmental substances (NORMAN network), over 700 compounds of emerging concern have been identified. These compounds are classified into different categories depending on their use and origin:

- i) Persistent Organic Pollutants (POPs).
- ii) Pharmaceuticals and Personal Care Products (PPCPs).
- iii) Endocrine-Disrupting Chemicals (EDCs).
- iv) Agricultural chemicals (herbicides, pesticides).

These contaminants enter the environment through various pathways, such as hospitals, industrial facilities, and households. Subsequently, they are transported to wastewater treatment plants and continuously released into surface and groundwater systems. This is because wastewater treatment plants are not designed to remove these contaminants due to their low concentrations, wide variety and different physical properties that pose when are present in water (Lin et al., 2020; Parida et al., 2021; Riva et al., 2019; Taheran et al., 2018).

The presence of ECs has been detected in surface water systems (rivers and lakes), groundwater, drinking water, wastewater, and effluents from wastewater treatment plants, with concentrations ranging from nanograms per liter (ng/L) to micrograms per liter (µg/L) (Chaturvedi et al., 2021; López-Pacheco et al., 2019; Sharma et al., 2019). They have been found in areas where they have never used, as some ECs are persistent and bio accumulative.

The lack of information on the origin, behavior, impact, and risks of ECs in the environment poses a significant challenge for governments worldwide in terms of controlling and regulating these contaminants. Currently, there are no laws establishing maximum concentrations of ECs in surface and groundwater, drinking water, and the environment. However, some countries have implemented strategies to observe, identify, control and monitor the presence of ECs. For example, the European Union has established different directives and regulations for the control of pesticides (Regulation (EC) No. 1107/2009), pharmaceuticals (Directive 2001/82/EC), and

industrial chemicals (Regulation (EC) No. 1907/2006). It has also listed 45 priority compounds and set environmental quality standards for water systems, in addition to adding another 10 to the contemporary monitoring list (Decision (EU) 2015/495).

In recent decades, advances in environmental ecotoxicology have shown that, even at low concentrations in water sources, ECs pose a potential risk to ecosystem integrity. ECs have been reported to cause sexual disorders in marine organisms (Azizi-Lalabadi and Pirsahab, 2021), neurological, reproductive, and immunological disturbances in animals (Furian et al., 2022), cancer (Lei et al., 2015), the development of antibiotic-resistant bacterial genes (Chaturvedi et al., 2021), congenital heart disease (Gorini et al., 2014), among other toxic effects. However, precise information on the toxic effects of ECs in water systems remains limited and is linked to the complex physicochemical characteristics of ECs, resulting in unpredictable behaviors when present in the environment (Gogoi et al., 2018; Wilkinson et al., 2017).

The United Nations General Assembly adopted the 2030 Agenda for Sustainable Development, recognizing the importance of preventing, controlling, and managing ECs to protect marine biodiversity (Goal No. 14), terrestrial life (Goal No. 15), water quality (Goal No. 6), and to promote responsible consumption and sustainable production (Goal No. 12).

2.3 Contamination by pharmaceutical compounds

Currently, a category of ECs that has gained priority is that of pharmaceuticals (Ahuja, 2021). Pharmaceuticals are widely used in the diagnosis, treatment, cure, and prevention of various diseases in humans and animals, owing to their diverse physicochemical and biological properties. These drugs encompass a wide range of substances, including non-steroidal anti-inflammatory drugs, antihistamines, antibiotics, antiepileptics, β -blockers, and more.

Most pharmaceutical compounds undergo transformations in the body when ingested, leading to the release of a large number of metabolites into surface and groundwater systems (Bexfield et al., 2019; Zhou et al., 2019). These metabolites may undergo additional transformations during wastewater treatment (Ramírez-Morales et

al., 2020). Moreover, they can be degraded by photolysis or hydrolysis, generating degradation by-products with similar or even higher toxicity than the original compounds, posing a risk to humans and ecosystems (Hossain et al., 2018; Nantaba et al., 2020; Serwecińska, 2020). Therefore, reducing the concentrations of pharmaceutical compounds in water systems is of paramount importance.

Although information on the potential toxic effects caused by the presence of pharmaceutical compounds in water is still limited, studies have reported that water contamination with these compounds can lead to the development of antibiotic-resistant bacterial genes (Amarasiri et al., 2020), genotoxic effects (Phong Vo et al., 2019), hormonal disorders (Schaefer and Zito, 2023), and disruptions in the reproduction, growth, and mortality of aquatic organisms (Nkoom et al., 2019).

2.3.1 Antihistamines

Antihistamines are widely used medications for treating allergic diseases. However, their applications have also been discovered in the treatment of inflammatory, autoimmune, and neurological disorders (Pearlman, 1976). Since their introduction to the market in the 1940s, more than 45 classes of antihistamines have been developed, including notable ones such as chlorpheniramine, ranitidine, cetirizine, loratadine, and diphenhydramine. Unfortunately, their presence has been frequently observed in various water bodies worldwide (Kristofco and Brooks, 2017). For instance, Guruge et al. (2019) found chlorpheniramine in surface waters in Sri Lanka, with concentrations of 1.36 ng/L. Other studies reported the presence of chlorpheniramine in the effluent of a wastewater treatment plant in Australia, with concentrations of 4.9 ng/L (Roberts et al., 2016). The presence of antihistamines in water has proven to be a serious environmental risk, especially for aquatic life (Berninger et al., 2011; Isidori et al., 2009; Schaefer and Zito, 2023; Teixeira et al., 2017). One study found that chlorpheniramine induces hormonal disruptions and other negative effects, such as central nervous system depression and dangerous hyperpyrexia (Schaefer and Zito, 2023). Moreover, most antihistamines in water have been found to have the ability to generate toxic by-products, such as nitrosamines,

particularly N-nitrosodimethylamine (NDMA). This substance forms during disinfection/oxidation treatment in wastewater treatment plants (Lv et al., 2015; White and Hernandez, 2021) and has been classified as a Category B2 carcinogenic compound by the United States Environmental Protection Agency (USEPA).

2.3.2 Antibiotics

Antibiotics constitute a class of drugs with a significant impact on the quality of water systems. Due to their potent ability to inhibit and eliminate bacterial growth, these substances are widely used to treat infectious diseases in both humans and animals. Global antibiotic consumption is estimated to range between 100,000 and 200,000 tons annually (Milić et al., 2013; Ngigi et al., 2020). Some commonly used antibiotics include trimethoprim, sulfamethoxazole, tetracycline, metronidazole, ronidazole, and ciprofloxacin.

Most antibiotics exhibit low absorption in the human body, meaning that approximately 80 % of the antibiotic is released in its active form or as a metabolite into water systems. These substances are transported through sewer networks and discharged into surface and groundwater systems. Antibiotic concentrations in various water bodies worldwide have been shown to exceed safe levels by up to 300 times (Vasilachi et al., 2021). For instance, concentrations of trimethoprim in surface water have been detected ranging from 0.5 to 27.43 ng/L (Chernova et al., 2021; Letsinger et al., 2019; Zhang et al., 2018), and in effluents from wastewater treatment plants, concentrations range from 33 to 788 ng/L (Biel-Maeso et al., 2018; Chernova et al., 2021). On the other hand, tetracycline has been found in different water bodies at concentrations ranging from 0.11 to 1300 µg/L (Chernova et al., 2021; Gao et al., 2012; Lin et al., 2009; Zhang et al., 2018). Hospital waste also represents a significant source of water pollution (Halling-Sørensen, 2000; Jjemba, 2006; Lofrano et al., 2020).

The presence of antibiotics in water can lead to mutagenic reactions, giving rise to new antibiotic-resistant bacterial genes. These genes can spread to other bacterial strains, affecting the growth and reproduction of aquatic species (Brain et al., 2004; Lützhøft et al., 1999; Yılmaz and Özcengiz, 2017). Additionally, antibiotics can inhibit

crop growth (Farkas et al., 2007) and have detrimental effects on human health (Amarasiri et al., 2020), rendering them potentially hazardous contaminants.

2.3.3 Nonsteroidal anti-inflammatories

Nonsteroidal anti-inflammatory drugs (NSAIDs) are a common group of medications used to treat inflammations and musculoskeletal pain, such as rheumatoid arthritis, fever, headaches, colds, toothaches, etc. In recent years, they have also been frequently used to treat infections caused by Covid-19 (Micallef et al., 2020; Wojcieszńska et al., 2022). Due to their low cost, accessibility, and availability as over-the-counter medications, NSAIDs are widely consumed globally, raising concerns about river and lake pollution (Madikizela and Ncube, 2021; Rastogi et al., 2021).

Currently, there are more than 100 NSAID compounds, with ibuprofen, naproxen, diclofenac, and acetaminophen being prominent among them. These compounds are released from various pollution sources and are found in significant concentrations in surface water and the effluents of wastewater treatment plants. For example, diclofenac has been detected in surface water at concentrations ranging from 1.0 to 51.4 ng/L, while acetaminophen at concentrations of 31.5 to 902 ng/L (Chernova et al., 2021; Kondor et al., 2020; Letsinger et al., 2019; Zhang et al., 2018). Furthermore, diclofenac and acetaminophen have been located in effluents from wastewater treatment plants at concentrations of 38 to 1020 ng/L and 17 to 441 ng/L, respectively (Biel-Maeso et al., 2018; Chernova et al., 2021).

While the presence of NSAIDs in water bodies is widely acknowledged, information on their ecotoxicological risk is still limited. A study by Sathishkumar et al. (2020) revealed that diclofenac causes adverse effects on the reproduction of griffon vultures, as well as cardiotoxic, hepatotoxic, nephrotoxic, neurotoxic, genotoxic, and hematotoxic effects in mammals. It has also been observed to affect the liver, kidneys, and gills of fish, as well as cytotoxicity and genotoxicity in plants, and a decrease in the survival and reproduction of invertebrate organisms. On the other hand, acetaminophen has been found to alter the genetic code and cellular function in both

humans and aquatic animals, depending on the level of exposure to the contaminant (Phong Vo et al., 2019).

2.3.4 Antiepileptics

Epilepsy is one of the most common neurological disorders, characterized by frequent seizures, loss of consciousness, and gastrointestinal dysfunction (Kwan and Brodie, 2001). According to the World Health Organization (WHO), over 50 million people worldwide are affected by epilepsy. Antiepileptic medications are used to treat seizures associated with epilepsy, but they are also employed for other conditions such as migraines, chronic neuropathic pain, and mood disorders, leading to a significant increase in their consumption in recent years (Carmland et al., 2022; Ho et al., 2021; Parikh and Silberstein, 2019).

Carbamazepine, gabapentin, lamotrigine, and primidone are the antiepileptics most frequently detected and found in elevated concentrations in rivers and lakes worldwide (Anim et al., 2020; Challis et al., 2018; Ebele et al., 2020; Kondor et al., 2020; Park and Lee, 2018; Sanz-Prat et al., 2020; White et al., 2019). In a study, Kondor et al. (2020) reported high concentrations of carbamazepine in the Danube River, with value of 47.6 ng/L. Generally, carbamazepine has been detected in various water bodies at concentrations ranging from 3.0 to 72.01 ng/L (Chernova et al., 2021; Zhang et al., 2018). Additionally, it has been found in effluents from wastewater treatment plants at concentrations of 21 to 657 ng/L (Biel-Maeso et al., 2018; Chernova et al., 2021).

Antiepileptics, especially carbamazepine, are contaminants that rise significant environmental concerns due to their toxic effects on aquatic ecosystems. Numerous studies have been reported that carbamazepine has severe effects on aquatic organisms, including impacts on the reproduction rate, growth, and mortality of planktonic crustaceans, algae, and invertebrates (Nkoom et al., 2019; Zhang et al., 2012; Zind et al., 2021). Additionally, genetic alterations and acute toxic effects have been observed in rainbow trout exposed to this compound (Li et al., 2010, 2011), increased mortality of zebrafish embryos and larvae (da Silva Santos et al., 2018; Pohl

et al., 2019), as well as morphological changes in cnidarians (Quinn et al., 2009). On the other hand, little research has been conducted on the toxic effects of antiepileptics on human health. Some authors have examined the effects of carbamazepine on human health when present in water, and although it is concluded that carbamazepine does not pose a potential risk to human health, continued monitoring of its behavior is necessary due to the adverse effects it may have when consumed for medical purposes (Cunningham et al., 2010; Houeto et al., 2012). For example, Abuzneid et al. (2022) reported that the ingestion of carbamazepine by 23-year-old patient led to the development of Stevens-Johnson syndrome and toxic epidermal necrolysis, which are skin reactions causing high fever and ulcers in the mouth and face. Additionally, carbamazepine has been found to cause congenital malformations when consumed during pregnancy (Andrade, 2018; Jentink et al., 2010; Jones et al., 1989; Sutcliffe et al., 1998).

2.4 Methods for the removal of pharmaceutical compounds from water solutions

Currently, wastewater treatment plants play a crucial role in eliminating various contaminants, such as suspended particles, dissolved organic compounds, nutrients, and pathogens. These plants employ different treatment stages involving processes like screening, coagulation/flocculation, centrifugation, sedimentation, and biological treatments. However, current conventional technologies have limitations in reducing concentrations of pharmaceutical compounds in wastewater (Rout et al., 2021). To address this challenge, there has been ongoing work in the development and implementation of more effective and specific treatment technologies. Notable among these technologies are methods such as chlorination, ozonation, adsorption, advanced oxidation processes, and visible light photodegradation (Ahmed et al., 2021; Kavitha, 2022; Krakkó et al., 2022; Liu et al., 2019; Obradović et al., 2022; Wang et al., 2023). These innovative technologies have shown promise in the removal of pharmaceutical compounds and other persistent contaminants in wastewater, undergoing continuous research and development.

Ozonation relies on ozone as strong oxidizing and disinfecting agent to degrade organic contaminants. Recently, catalytic and photocatalytic ozonation techniques have been proposed to enhance the formation of hydroxyl radicals, favoring the degradation and mineralization of pharmaceutical compounds (Issaka et al., 2022). A study by Li et al. (2022) investigated the degradation of trimethoprim through catalytic ozonation using a ceramic membrane functionalized with manganese-iron binary oxides (Mn/FeOx). The results showed a 98.6 % removal of trimethoprim. However, the study also detected the formation of hard-to-mineralize intermediate products, achieving only around 50 % mineralization of trimethoprim.

Chlorination involves the use of free chlorine and chlorine dioxide (ClO₂) to degrade active organic compounds (Crain and Gottlieb, 1935). In a recent study, simultaneous or multicomponent chlorination of sulfamethoxazole, acetaminophen, and diclofenac in acidic, neutral, and alkaline solutions was investigated. The study revealed that degradation capacity depended on the solution pH, decreasing in the order of sulfamethoxazole > diclofenac > acetaminophen in acidic solution, sulfamethoxazole > acetaminophen > diclofenac in alkaline solution. Additionally, the study discovered the formation of unknown dimers, sulfamethoxazole-acetaminophen and sulfamethoxazole-diclofenac, as degradation byproducts during simultaneous chlorination (Liu et al., 2019). These findings highlight the complexity of chlorination processes and their effects on the formation of undesirable byproducts, which may have significant implications for the safety and effectiveness of pharmaceutical compound removal through this method.

Visible light photodegradation is an emerging technology for water treatment capable of completely breaking down organic contaminants in aqueous solutions. In this process, an oxidant is used to break down pharmaceutical compounds into short-chain organic acids, inorganic acids, and CO₂, generating hydroxyl radicals (Kavitha, 2022). A study by Guo et al. (2021) evaluated the photocatalytic activity of tubular hollow graphene carbon nitride decorated with copper phosphide nanoparticles (Cu₃P/HTCN) in the visible light photodegradation of tetracycline. The results demonstrated that Cu₃P/HTCN exhibited high photocatalytic efficiency in tetracycline

degradation, achieving a 96.9 % efficiency in just 40 minutes. Despite the advantages of visible light photodegradation in removing pharmaceutical compounds from water (Kutuzova et al., 2021; Li et al., 2019; Xu et al., 2021), this technology still faces challenges requiring thorough study before large-scale implementation. These challenges include the cost of photocatalysts, chemical stability, infrastructure needed for identification and analysis of degradation byproducts, large-scale reactor design, and environmental efficacy. These factors limit its implementation compared to other water treatment technologies.

Advanced Oxidation Processes (AOPs) are innovative and highly effective strategies for wastewater treatment. These processes accelerate the degradation rate of organic contaminants and promote mineralization by generating intense hydroxyl radicals (Glaze et al., 1987; Klavarioti et al., 2009; Legrini et al., 1993; Malato et al., 2009). Examples of AOPs for the oxidation of organic contaminants include photocatalysis using titanium dioxide (TiO₂) and zinc oxide (ZnO) (Panwar et al., 2022), solar-assisted electrooxidation (Ding et al., 2021), ozone-based electrochemical processes (Bavasso et al., 2022), hydrogen peroxide (Wang et al., 2023), UV chlorination photolysis (Guo et al., 2022), and Fenton processes (Dargahi et al., 2021). Numerous studies have been conducted on the use of these advanced oxidation processes for the removal of pharmaceutical compounds from aqueous solutions. For instance, Nguyen et al. (2022) investigated the degradation of antibiotics cephalexin and tetracycline using novel Ni-doped TiO₂-based photocatalysts. The results showed that the photocatalytic degradation of cephalexin and tetracycline reached 91.6 % and 82.5 %, respectively, and after 5 reuse cycles, the degradation capacity remained above 75 %. In another study, the degradation of acetaminophen by ultrasound-assisted electro-Fenton using iron oxide nanoparticles as a catalyst (HNPs) was reported. The photocatalytic activity of HNPs was found to be superior to other photocatalysts prepared with different transition metals. For example, at an initial concentration of 20 mg/L of acetaminophen, degradation reached 98.9 %, decreasing by at least 14 % after the fourth reuse cycle (Ghanbari et al., 2021). Despite the high degradation capacity of pharmaceutical compounds demonstrated by advanced

oxidation processes (AOPs), concerns arise due to the formation of degradation byproducts that may be more toxic than the original pharmaceutical. Liu et al. (2016) identified the presence of at least 31 degradation byproducts of oxytetracycline, generated through reaction mechanisms including hydroxylation, secondary alcohol oxidation, demethylation, decarbonylation, and dehydration. This raises issues about the potential environmental impact of these toxic byproducts. Additionally, AOPs face limitations in water with high organic content and turbidity, which hinders the penetration of UV radiation (Homem and Santos, 2011). Furthermore, the high consumption of chemicals in AOPs can lead to significant secondary contamination concerns and increased treatment costs in the medium term (Martínez-Huitle and Ferro, 2006).

Adsorption processes emerge as a highly promising and effective alternative for the removal of pharmaceuticals from wastewater. This technology presents several advantages, making it an appealing choice when compared to other treatment techniques. Noteworthy features include ease of operation, cost-effectiveness, reproducibility, high efficiency, and the absence of toxic byproduct generation (Sophia A. and Lima, 2018). Moreover, it offers flexibility in utilizing a broad range of adsorbent materials, ranging from natural micrometric substances to advanced nanostructured synthetic materials (Carrales-Alvarado et al., 2020; García-Reyes et al., 2021; Maggio et al., 2022; Moral-Rodríguez et al., 2020; Ortiz-Ramos et al., 2022).

2.4.1 Adsorption

Adsorption is a surface process involving the accumulation of a substance, called the solute, on the surface of a typically porous solid. The substance adhering to the solid is known as the adsorbate and can be an ion or a molecule, while the solid where adsorption occurs is termed the adsorbent (Cooney, 1998).

Adsorption of the adsorbate onto the surface of the adsorbent can occur due to physical or chemical interactions and is classified as either physical adsorption or chemical adsorption. Physical adsorption arises from molecular interactions between the solid surface and the adsorbate molecules. These interactions can be electrostatic,

van der Waals forces, hydrogen bonding, or London dispersion forces. Due to these weak interactions, the adsorbate can move freely on the surface, rendering the adsorption reversible. In contrast, chemical adsorption involves a strong chemical interaction between specific active sites on the adsorbent and adsorbate molecules. In this case, the chemical interaction typically involves the formation of chemical bonds, resulting in irreversible adsorption. Additionally, the heat of adsorption in chemical adsorption is high, exceeding 40 kJ/mol, similar to that of chemical reaction (Leyva-Ramos, 2010).

Liquid-phase adsorption is influenced by various factors affecting interactions between the adsorbate and the adsorbent, including:

- i) *Morphology and textural properties of the adsorbent:* The adsorption capacity depends on the textural and morphological properties of the adsorbent, such as specific surface area, pore volume and diameter, and pore size distribution. These properties impact the availability and accessibility of the area where adsorption occurs.
- ii) *Surface charge and zero-point charge.* The adsorbent in an aqueous solution can acquire a charge on its surface, which can be positive, neutral, or negative, depending on the solution pH. Studying the distribution of surface charge and the zero-point charge of the adsorbent is crucial for understanding adsorption mechanisms.
- iii) *Concentration and type of active sites.* The adsorbent material has functional groups on its surface that can donate or accept protons depending on the solution pH. Proton-donating sites are acidic, while proton-accepting sites are basic. The concentration and type of active sites are fundamental characteristics for adsorbing cations or anions.
- iv) *Nature of the adsorbate.* The adsorption capacity is strongly influenced by the physicochemical properties of the adsorbate, such as concentration, molecular size, polarity, solubility, composition, and chemical speciation.
- v) *Liquid phase characteristics.* Properties of the liquid phase, such as pH, temperature, ionic strength, and solvent type, affect the adsorption capacity. In

particular, the pH of the solution plays a crucial role since the surface charge of the adsorbent depends on the pH. Furthermore, for compounds that ionize in aqueous solution by donating or accepting protons, the adsorption capacity varies considerably with pH.

- vi) *Presence of other substances.* The presence of additional contaminants can harm, not affect, or enhance the adsorption capacity of the organic compound under study. When an additional adsorbate hinders the adsorption of the target adsorbate, a competitive or antagonistic effect occurs. Conversely, when the presence of another adsorbate promotes adsorption capacity, a cooperative or synergistic effect takes place. Finally, when the adsorption capacity is unaffected by the presence of another adsorbate, the multicomponent adsorption system is said to have a non-interactive effect.

2.5 Adsorbent materials

Activated carbon stand out as the primary adsorbent material widely used in industrial wastewater treatment (Perrich, 1981). However, ongoing research is exploring numerous natural and synthetic adsorbent materials for the removal of pharmaceutical contaminants from aqueous solutions. These materials include natural soils (Rodríguez-López et al., 2022), natural clays (Ortiz-Ramos et al., 2022), organoclays with Gemini surfactants (Guo et al., 2019), magnetic biocarbonized materials (Dai et al., 2020), magnetite-doped graphene oxides (Lin et al., 2019), metal-organic frameworks (Cheng et al., 2022), molecularly imprinted polymers (Cantarella et al., 2019), carbon xerogels (Moral-Rodriguez et al., 2020), and carbon nanotubes (Carrales-Alvarado et al., 2020).

In general, the activity and capacity of an adsorbent material depend on its physicochemical properties, influenced by the nature of the raw material, the separation process, and the synthesis parameters used. There are certain key characteristics that an adsorbent material should possess:

- i) Low cost and abundant availability.
- ii) Ease of synthesis and manipulation.

- iii) Chemical, thermal and mechanical stability.
- iv) Appropriate chemical, texture, and particle size properties.
- v) High adsorption capacity and rate.
- vi) Easy regeneration and reusability.

2.5.1 Natural clays

Clays are a category of hydrated phyllosilicates that constitute a significant portion of the fine-grained fraction found in rocks, sediments, and soils. These natural materials are predominantly composed of silicon, aluminum, oxygen, and hydrogen (Domínguez and Schiffer, 1992). They are characterized by negative surface charges and a colloidal structure, providing them with chemical stability and expansive capacity. These properties enable clays to retain and trap metallic cations and certain organic compounds on their surface (Chaari et al., 2019; Padilla-Ortega et al., 2013).

The structure of clays is marked by an organized arrangement of tetrahedral (T) and octahedral (O) layers. Each layer consists of tetrahedra formed by a cation coordinated with four oxygen atoms. These tetrahedra are connected through three shared corners with adjacent tetrahedra, creating a two-dimensional hexagonal lattice pattern along the crystallographic directions a and b (T-layer). The tetrahedron contains a silicon (SiO_4^{4-}) or aluminum (AlO_4^{5-}) atom at its center (Figure 2.1). On the other hand, the octahedral layer is composed of octahedra formed by a cation coordinated with six oxygen and hydroxyl atoms. These octahedra are connected sharing oxygens and hydroxyls at the edges of one octahedron with those at the edges of another octahedron. The octahedra exhibit two different topologies based on the position of the hydroxyl group, cis and trans. As a result, the octahedral layer can display a hexagonal or pseudo-hexagonal structure (O-layer) (Figure 2.2). The central cation in each octahedron can be aluminum, iron, or magnesium, resulting in the following chemical composition: $[(\text{Al}/\text{Fe})\text{O}_n (\text{OH})_m]^-$ or $[(\text{Mg}/\text{Fe})\text{O}_n (\text{OH})_m]^-$. In these formulas, $n + m = 6$ (Brigatti et al., 2013).

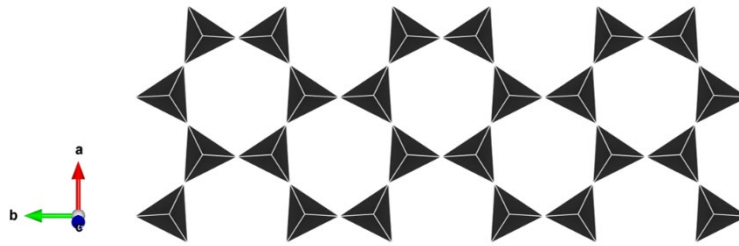


Figure 2.1. Tetrahedral sheet of clays.

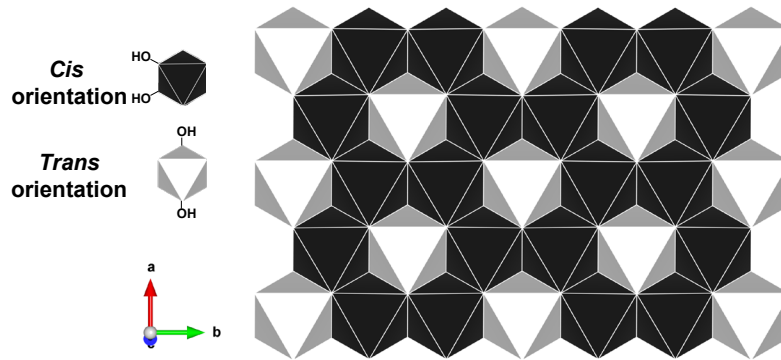


Figure 2.2. Octahedral sheet of clays.

The T and O sheets in clays can join through the oxygen atoms at the vertices of the tetrahedra and octahedra, forming a planar arrangement of laminar structures. The combination of one T sheet with the one O sheet results in T:O or 1:1 lamellar block, known as bilaminar structures. Alternatively, two T sheets can join with one O sheet to form T:O:T or 2:1 trilaminar structures. The clay structure can be dioctahedral or trioctahedral, depending on how the octahedral and tetrahedral sheets are joined. In a dioctahedral structure, two-thirds of the octahedral sites are occupied by trivalent atoms such as Al^{3+} or Fe^{3+} . In trioctahedral sheets, all octahedral sites are occupied by divalent atoms such as Mg^{2+} and Fe^{2+} (Velde, 1992).

The formed lamellar blocks can be electrically neutral or negatively charged. Electrical neutrality occurs when: i) the octahedral sheet contains trivalent cations (Al^{3+} or Fe^{3+}) in two octahedral sites and a vacancy in the third octahedron; ii) all octahedral sites are occupied by divalent cations (Mg^{2+} or Fe^{2+}); and iii) the tetrahedral sheet contains Si^{4+} in all tetrahedral sites. On the other hand, the negative charge in clays is

due to i) the substitution of Si^{4+} by Al^{3+} in tetrahedral sites; ii) the substitution of Al^{3+} or Fe^{3+} by lower charged cations in octahedral sites, usually Mg^{2+} or Fe^{2+} ; and iii) the presence of vacancies. These substitutions are known as isomorphic substitutions, as they do not alter the morphology of the lamellar block (Brigatti et al., 2013).

Clays, especially those with a 2:1 layered structure such as smectites, vermiculites, and micas, are characterized by their charge variability, enabling the occupation of spaces between each laminar block by exchangeable cations. In addition to this characteristic, clays possess other distinctive properties:

- i) Lamellar structure on a nanometric scale: Bilaminar blocks 1:1 (T:O) have an approximate thickness of 0.7 nm, while trilaminar blocks 2:1 (T:O:T) have a thickness close to 1 nm (Moore and Hower, 1986).
- ii) Capacity to exchange cations.
- iii) Hydration, plasticity, and swelling.
- iv) Different types of surfaces: external surface, edge surfaces, and interlayer space surface.
- v) Surface modification: Clay surfaces are easily modifiable, allowing the creation of hybrid materials with additional functionalities.

Bentonite is a natural clay primarily found in the form of montmorillonite and belongs to the smectite group (Figure 2.3). Its 2:1 layered structure comprises an octahedral sheet, primarily containing trivalent Al^{3+} cations (dioctahedral structure), situated between two tetrahedral sheets of Si^{4+} . Isomorphous substitutions of cations in the sheets generate an excess of negative charge, balanced by exchangeable and hydratable cations such as Na^+ , Ca^{2+} , K^+ , and Mg^{2+} present in the interlayer space, forming weak bonds. Hydration of interlayer cations can occur in two ways: inner-sphere hydration and outer-sphere hydration. In inner-sphere hydration, the cation interacts with the clay surface on one side and with water molecules on the other side. In contrast, in outer-sphere hydration, the cation is fully surrounded by water molecules interacting with the clay surface through hydration water.

The capacity of bentonite to adsorb cations is attributed to its Cation Exchange Capacity (CEC), expressed in units of centimoles of positive charge per kilogram of

clay (cmol(+)/kg). CEC exhibits the following characteristics: i) it is reversible; ii) it is stoichiometric; and iii) it shows selectivity of one cation over another.

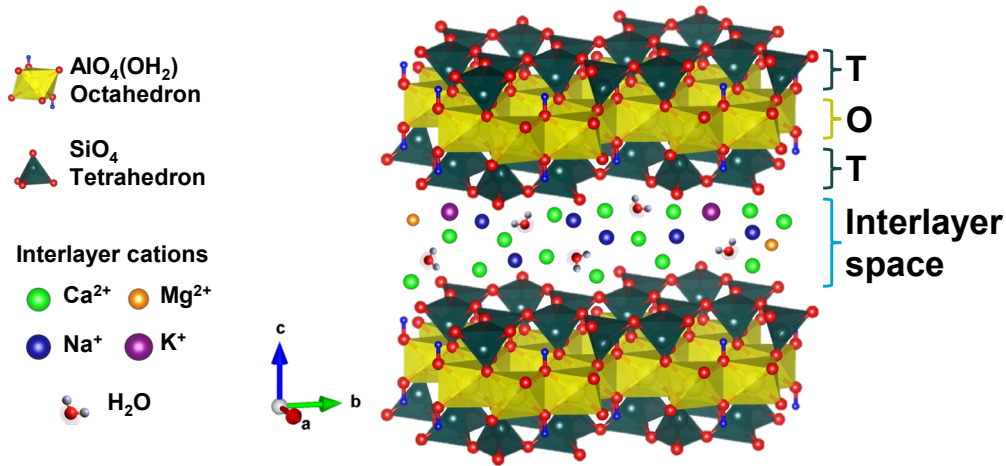


Figure 2.3. Trilaminar structure 2:1 (T:O:T) of a bentonite clay.

Concerning the removal of pharmaceutical compounds by adsorption on natural clays, there is a lack of significant studies in this area. Most research has concluded that natural clays do not exhibit a high adsorption capacity for pharmaceutical compounds. For instance, Thiebault and Boussafir (2019) studied the adsorption of diazepam on montmorillonite and found a low adsorption capacity of 10.2 mg/g at pH = 7.5. In another recent study, Vallova et al. (2022) investigated the ability of montmorillonite to adsorb the analgesics paracetamol, diclofenac, and ibuprofen. The results showed that the clay failed to completely remove the analgesics from the aqueous solution, obtaining adsorption capacities of 3.9, 18.0 and 15 mg/g for paracetamol, diclofenac, and ibuprofen, respectively. These studies conclude that the negative and hydrophilic surface of natural bentonite inhibits the adsorption capacity of pharmaceutical compounds. However, it is important to note that previous research has demonstrated that bentonite can adsorb tetracycline through electrostatic attraction, cation exchange, and complexation, achieving a high adsorption capacity of 283.5 mg/g at pH = 3 (Ortiz-Ramos et al., 2022). Similar results were obtained in a study by Wu et

al. (2019), where the adsorption of the antibiotic ciprofloxacin on montmorillonite was investigated.

These findings suggest that, although natural clays generally have limitations in the adsorption of pharmaceutical compounds, specific mechanisms and particular conditions can influence their adsorption capacity. Further research is needed to understand and optimize the adsorption capacity of natural clays for pharmaceutical compounds, as well as to explore possible surface modifications that may enhance their effectiveness in removing these compounds.

2.5.2 Organoclays

Organoclays are highly innovative and of great interest, obtained by modifying natural clays with organic compounds. This surface modification provides them with new functionalities, making them applicable in various fields such as rheological control agents, paints, cosmetics, refractory varnishes, and thixotropic fluids (de Paiva et al., 2008). In recent years, organoclays have been found to exhibit a remarkable adsorption capacity for organic molecules in aqueous solutions (Martín et al., 2019; Martínez-Costa et al., 2018; Shah et al., 2018; Shen and Gao, 2019; Tariq et al., 2022). This discovery has opened up new opportunities for their application in the removal of pharmaceutical contaminants from wastewater.

The synthesis of organoclays is based on reactions involving clays and organic compounds and can occur through two different reaction routes: i) solid-state reactions and ii) cation exchange reactions. In the first case, organic molecules can be intercalated into dry clay without the use of solvents, thanks to ion-dipole interactions, where the polar groups of the organic compound interact with the interlayer cations (Garikoé and Guel, 2022; Lagaly et al., 2013). In the second case, interlayer cations are exchanged for cationic surfactants, such as quaternary ammonium salts, in an aqueous solution (Leyva-Ramos et al., 2021). Additionally, in some cases, other types of organic compounds such as Gemini surfactants (Shen and Gao, 2019), amino acids (Imanipour et al., 2021), phospholipids (Liu et al., 2017), and even polymeric macromolecules (Kausar et al., 2019) can be used to achieve clay modification.

Cation exchange reactions with cationic surfactants enable the preparation of organoclays, modifying the surface nature of the clay from hydrophilic to hydrophobic and organophilic, simultaneously generating positively charged anionic sites on its surface. Cationic surfactants consist of a quaternary ammonium group attached to an organophilic chain and are represented by the general formula $(\text{CH}_3)_3\text{NR}^+$, where R can be an alkyl chain or a benzyl group. Among the most commonly used surfactants for organoclay preparation are hexadecyltrimethylammonium bromide (HDTMA), dodecyltrimethylammonium bromide (DDTMA), and benzyltrimethylammonium bromide (BTMA) (Leyva-Ramos et al., 2021; Martinez-Costa and Leyva-Ramos, 2017). Their chemical structures are illustrated in Figure 2.4.

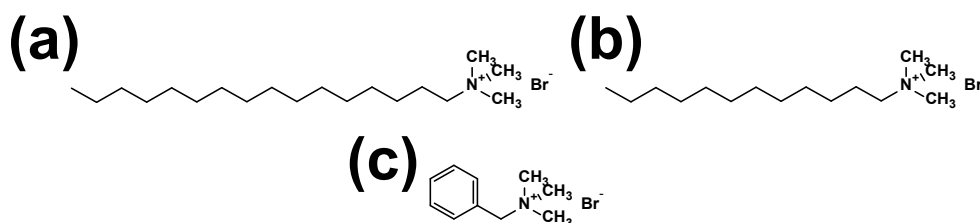


Figure 2.4. Chemical structures of the cationic surfactants HDTMA (a), DDTMA (b) and BTMA (c).

The structural arrangement of organoclays is primarily determined by the packing density of interlayer cations and the length of the alkyl chain of the cationic surfactant. However, other factors such as surface geometry and the cation exchange capacity of the clay can also influence this structure. As a result, organoclays can adopt various structural configurations, including monolayers, bilayers, pseudotrimolecular layers, and paraffin-like structures. Figure 2.5 illustrates some of these structural configurations (Lagaly et al., 2013).

The structural configuration of organoclays can be determined by measuring the basal spacing (d_{001}) of the organoclay, which is influenced by the length of the cationic surfactant chain, as shown in Figure 2.6. According to Lagaly et al. (2013), a monolayer arrangement will form when the alkylammonium chains are short ($n_c < 6$), while a bilayer will form when the alkylammonium chains are long ($n_c > 7$). In both cases, the

alkylammonium chains are arranged parallel to the clay layers. The d_{001} distance in a monolayer is generally 1.35 nm, and the interaction occurs at the negatively charged cationic sites of the clay layers, attributed to electrostatic attraction and cation exchange. The bilayer has a d_{001} value of 1.77 nm and interacts with the previously adsorbed monolayer through van der Waals interactions between the alkyl chains of the cationic surfactant (Leyva-Ramos et al., 2021). As the length of the alkyl chain increases ($n_c > 14$), a transition to a pseudotrimolecular structural configuration occurs, along with an increase in the d_{001} value. In this case, the positive group $(\text{CH}_3)_3\text{N}^+$ is located near to the cationic sites of the clay layer, and the chains arrange in a “twisted” trimolecular arrangement. The pseudotrimolecular structure typically exhibits a d_{001} value of 2.15 nm. Increasing the length of the alkyl chain and the cationic surfactant/clay ratio has been observed to make organoclays more hydrophobic (Martinez-Costa and Leyva-Ramos, 2017). Finally, the paraffin-like arrangement is found in quaternary ammonium surfactants that contain two or more long alkyl chains, such as phospholipids (Wicklein et al., 2010).

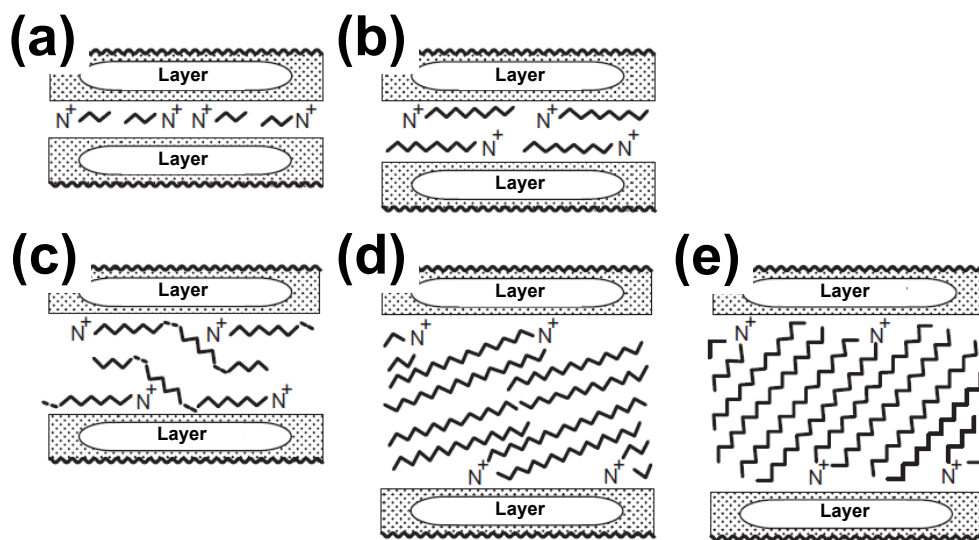


Figure 2.5. Structural arrangements of organoclays: monolayer (a), bilayer (b), pseudotrimolecular layer (c) and inclined paraffin-like structures (d, e). (Lagaly et al., 2013).

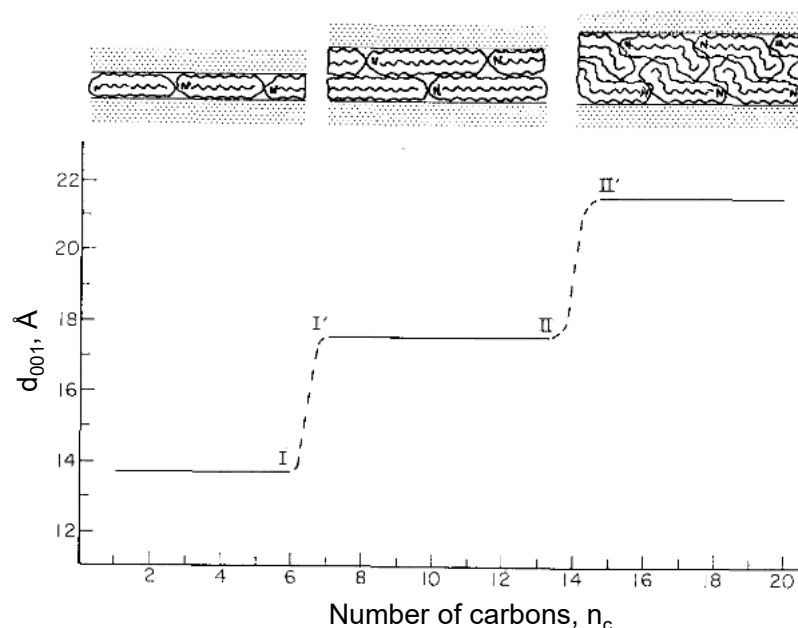


Figure 2.6. Variation of basal space, d_{001} , with cationic surfactant alkyl chain length, n_c , due to monolayer, bilayer, and pseudotrimolecular layer formation (Lagaly et al., 2013).

Several studies have investigated the adsorption of pharmaceutical compounds on organoclays, yielding varied results. For instance, De Oliveira et al. (2017) examined the adsorption of diclofenac on organomontmorillonite modified with two different surfactants: benzyldimethyltetradecylammonium bromide (BDTA) and hexadecyltrimethylammonium bromide (HDTMA). They found that the adsorption capacity of diclofenac varied slightly depending on the surfactant used. Materials prepared with BDTA and HDTMA showed diclofenac adsorption capacities of 56.3 and 44.4 mg/g, respectively. However, another study obtained a much higher diclofenac adsorption capacity of 361.3 mg/g on HDTMA-modified bentonite (Martinez-Costa et al., 2018). Both works concluded that adsorption is attributed to electrostatic attraction between the anionic species of diclofenac and the anionic and positively charged sites of organoclays. In another recent investigation, the adsorption of paracetamol on organobentonites modified with different surfactants, both anionic (sodium dodecyl sulfate and dodecyl benzene sulfonic acid) and cationic (dodecyltrimethylammonium

bromide and dodecylpyridinium chloride), was studied. The adsorption capacity was found to depend on the type of ionic surfactant used. The organoclay modified with dodecyltrimethylammonium bromide showed the highest paracetamol adsorption capacity of 32.4 mg/g, while the adsorption capacities decreased in the following order: dodecylpyridinium bromide > sodium dodecyl sulfate > dodecyl benzene sulfonic acid (Çalışkan Salihi et al., 2023). The hydrophobic effect on the surfactant chains in the clay was found to play a significant role.

While numerous studies have concluded that organoclays exhibit high adsorption capacities for pharmaceutical compounds (França et al., 2020; Imanipoor et al., 2021; Malvar et al., 2020; Saitoh and Shibayama, 2016; Vallova et al., 2022; Zhang et al., 2021), contradictory results have also been obtained where the organic modification of the clay does not increase or even decreases the adsorption capacity. For example, Yang et al. (2020) analyzed the adsorption of tetracycline on organovermiculite modified with the surfactant dodecyl dimethyl betaine (DDB) and found that the adsorption capacity did not significantly increase with organic modification. At pH = 7, the adsorption capacities were 8.8 and 11.1 mg/g for natural vermiculite and organovermiculite, respectively. Another study investigated the simultaneous adsorption of sulfamethoxazole and trimethoprim on HDTMA-modified organobentonite and found that the organobentonite exhibited high individual adsorption capacity for sulfamethoxazole but not for trimethoprim. The individual adsorption capacities were 55.7 and 8.7 mg/g for sulfamethoxazole and trimethoprim, respectively (Martínez-Costa et al., 2018).

Despite numerous studies on the adsorption of pharmaceutical compounds on organoclays, the reasons why organoclays inhibit or decrease the adsorption capacity for certain pharmaceutical compounds have not been thoroughly investigated. Therefore, further research in this field is crucial to better understand the adsorption mechanisms and optimize the use of organoclays in pharmaceutical compound removal from water.

2.5.3 Carbon xerogels

Carbon gels are nanostructured materials with highly controlled chemical composition and porous structure. These materials are formed by the carbonization of an organic gel, commonly synthesized through the sol-gel method (Pekala, 1989). They have found extensive use in various applications (da Cunha et al., 2021; Elmouwahidi et al., 2021; Haye et al., 2020; Prokić et al., 2022; Yang et al., 2020; Zainol et al., 2021). The sol-gel method involves the polymerization of a hydroxylated benzene derivative (such as resorcinol, phenol, cresol, among others) and an aldehyde (such as formaldehyde, furfural, among others) in the presence of a solvent (water, ethanol, methanol, acetone). Once the solvent is removed, the resulting solid organic polymer is called organic gel. Resorcinol, formaldehyde, and water are the most commonly used reagents by various authors (Gaikwad et al., 2019; Ibarra Torres et al., 2021; Job et al., 2005; Li et al., 2019; Lu et al., 2018; Ptaszkowska-Koniarz et al., 2018).

The synthesis of carbon gels through sol-gel method consists of three stages (Figure 2.7): i) polymerization, ii) drying of the solvent-saturated gel, and iii) carbonization with or without activation of the gel. In the first stage, resorcinol (R) and formaldehyde (F), dissolved in a reaction medium, undergo addition and condensation polymerization in the presence of a catalyst. The addition and condensation polymerization mechanisms are depicted in Figure 2.8. During this stage, a suspension of colloidal solid particles (sol) forms, which tend to grow and create a three-dimensional polymeric network of interconnected spherical particles (gel) with suitable chemical characteristics and porosity. Synthesis parameters, such as the nature, ratio, and concentration of reagents, catalyst, solvent, and pH of the reaction medium, are crucial for controlling the meso and macroporosity of the gel. The catalyst plays a fundamental role in polymerization, as its nature determines the pH of the reaction medium. Alkali metal carbonates (Li_2CO_3 , Na_2CO_3 , K_2CO_3 , Rb_2CO_3 , Cs_2CO_3 , Fr_2CO_3) are the most commonly used as catalysts in this method (Alegre et al., 2019; Eckert et al., 2022; Medina et al., 2021; Moral-Rodriguez et al., 2020; Shouman and Fathy, 2018; Yang et al., 2020).

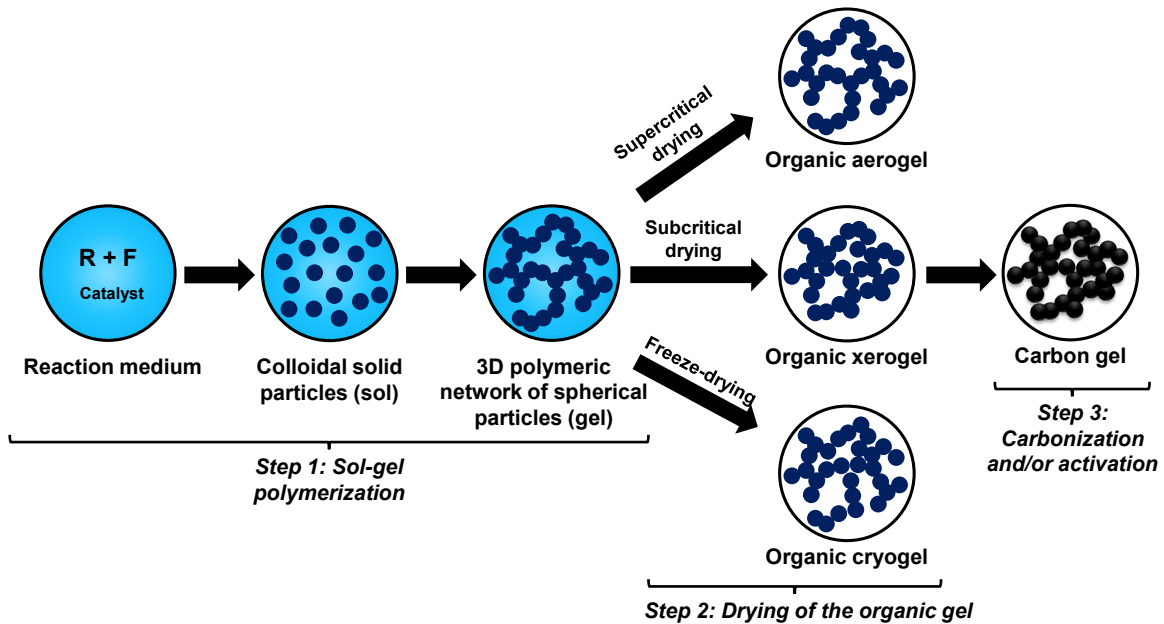


Figure 2.7. Stages of synthesis of carbon gels by the sol-gel method (Arenillas et al., 2019).

The drying of the solvent-saturated gel is a crucial stage in synthesis, as it plays a determining role in preserving the porosity of the final organic gel. Capillary forces generated between the solvent and the pore walls can lead to the collapse of the porous structure of the gel. In the literature, three conventional drying methods have been reported: supercritical drying, subcritical drying, and freeze-drying, which differ in the pressure and temperature conditions used to remove the solvent (Gizli et al., 2022; Job et al., 2005). Depending on the drying method employed, the final organic gel may receive different designations. In the case of supercritical drying, an aerogel is obtained, while subcritical drying results in a xerogel, and freeze-drying leads to a cryogel. These designations reflect the specific characteristics of each gel in terms of its porosity and structure.

Supercritical drying is widely employed by various researchers as one of the most common methods. It involves the use of CO₂ under elevated pressure and temperature conditions to remove the solvent (Bakos et al., 2018; Jayaseelan et al., 2018; Li et al., 2019; Liu et al., 2021; Sam et al., 2020; Wang et al., 2022). In the case

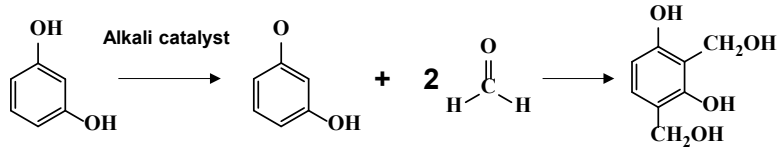
where water is the solvent, it is necessary to replace it first with an organic solvent (acetone, methanol, etc.) due to the high solubility of CO₂ in water. During the drying process, CO₂ replaces the organic solvent and is removed in gas form, minimizing capillary forces and preserving much of the original porosity of the gel. The resulting organic gel is known as an aerogel. On the other hand, freeze-drying involves drying the organic gel under cryogenic conditions (Babić et al., 2004; Okay and Lozinsky, 2014). In this case, the solvent is frozen and then removed by sublimation. Similar to supercritical drying, if the solvent is water, it must be exchanged first with an organic solvent to prevent the formation of ice crystals that could significantly impact the porosity of the gel. After solvent removal, the organic gel is referred to as a cryogel. Although these two drying methods are highly effective in preserving the porosity of the final organic gel, they are also expensive and challenging to handle, limiting their application on a large scale.

In contrast, subcritical drying is a straightforward and cost-effective method for obtaining organic xerogels on a large scale. It relies on the direct evaporation of the solvent under normal pressure and temperature conditions. Although a liquid-vapor interface forms during the drying process, which can potentially lead to collapse of the gel structure due to surface tension, it has been demonstrated that, under controlled operating conditions, it is possible to minimize such collapse and obtain organic xerogels with very well-controlled porosity (Bailón-García et al., 2020; Castelo-Quibén et al., 2019; Medina et al., 2021; Moral-Rodríguez et al., 2020; Pérez-Cadenas et al., 2009; Segovia-Sandoval et al., 2020; Vivo-Vilches et al., 2018).

The carbonization of the organic xerogel constitutes the final stage of synthesis and plays a fundamental role in developing the microporosity of the carbon xerogel. In this stage, the xerogel undergoes an initial thermal stabilization process to eliminate water residues or unreacted reagents present during synthesis. Thermal stabilization occurs at temperatures ranging from 100 to 200 °C, resulting in a hydrophilic xerogel with elevated oxygen content. Carbonization involves exposing the organic xerogel to an inert gas stream, such as N₂, He, or Ar, at elevated temperatures ranging from 600 to 1000 °C, using a slow heating ramp. During this process, a significant amount of

oxygen is removed, resulting in a thermally stable nanostructured carbon xerogel with well-developed microporosity, without altering the structural design established during the sol-gel polymerization.

1. Addition reaction



2. Condensation reaction

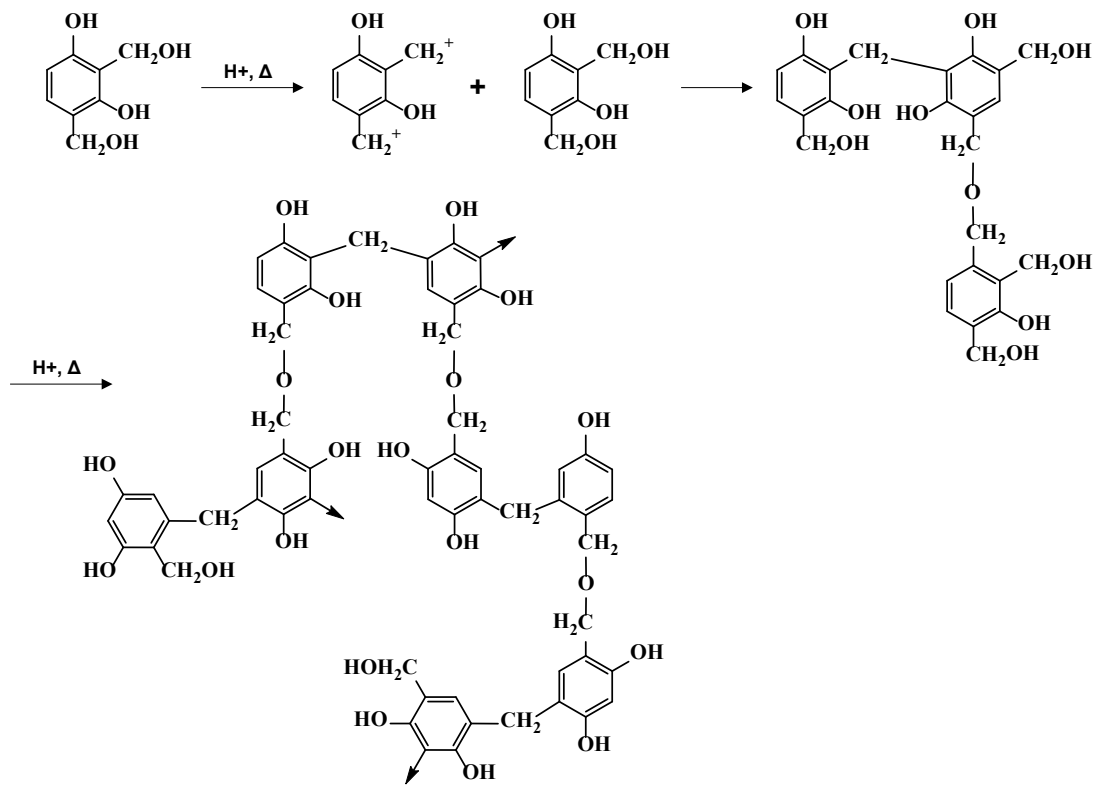


Figure 2.8. Polymerization mechanisms of resorcinol and formaldehyde (Arenillas and Fernández, 2022).

The carbon xerogel can undergo an activation process, either chemical or physical, to increase its microporosity and, consequently, its specific surface area. Chemical activation involves impregnating the carbon xerogel with activating chemicals such as H_3PO_4 , KOH , $ZnCl_2$, $NaOH$, among others, followed by thermal treatment at

temperatures ranging from 400 to 850 °C. This process has certain disadvantages, including the use of high concentrations of activating agent, the need for additional washes to recover the activating agent, and the possibility of partial material dissolution. On the other hand, physical activation is the most commonly used method and is based on controlled thermal treatment of the carbon xerogel with oxidizing agents such as CO₂ or water vapor. This treatment is carried out at temperatures ranging from 700 to 900 °C.

The sol-gel polymerization is a technique that allows obtaining carbon xerogels in various forms, such as microspheres (Bailón-García et al., 2014), films (Espinosa-Iglesias et al., 2015), pellets (Moral-Rodríguez et al., 2020), monoliths (Morales-Torres et al., 2012), and microbeads (Eskenazi et al., 2018). Monolithic carbon xerogels offer numerous advantages compared to other forms, such as low pressure drops, especially at high fluid flows, a larger exposed external surface area, greater accessibility to active sites, and a reduction in mass transport limitations. Therefore, these novel and highly promising materials are very interesting for a wide range of applications, including catalysis, adsorption, and energy storage.

Integral carbon xerogel monoliths are nanostructured porous materials, characterized by a single structure composed of thin, vertical, parallel channels separated by walls and a complex network of macropores that reduce flow resistance. However, existing technology has limited the geometry of these channels. Traditionally, extrusion has allowed the development of monoliths with straight channel geometry, resulting in laminar fluid flow through the channels and limited contact between the fluid and active sites (Morales-Torres et al., 2012; Moreno-Castilla and Pérez-Cadenas, 2010). To improve this aspect, the design of complex or tortuous channels has been explored, inducing turbulent fluid flow within the channels and significantly increasing contact between the fluid and the active sites of the monolith (Chaparro-Garnica et al., 2021a, 2021b). This has sparked great interest in the development of new technologies that allow designing and shaping channels with complex, specific, and highly controlled geometries.

The combination of 3D printing technology with sol-gel polymerization offers an innovative strategy for synthesizing integral carbon xerogel monoliths with a controlled channel configuration. In this method, 3D printed templates with a suitable architectural design of channels are used, which are placed in molds during the first stage of the sol-gel polymerization. During the carbonization process, the template is removed from the xerogel structure, resulting in the formation of the carbon monolith and the shaping of channels with the designed geometry.

The adsorption of pharmaceutical compounds on carbon xerogels has been the subject of limited research. Nevertheless, some studies have yielded promising results. Moral-Rodriguez et al. (2020) investigated the impact of the resorcinol/catalyst molar ratio (R/Cat) on the adsorption of diclofenac in aqueous solution using carbon xerogel pellets. They observed that the highest adsorption capacity was achieved with an R/Cat ratio of 500, reaching an adsorption capacity of 184.6 mg/g at pH = 7. This material exhibited a larger volume and mesoporous area, favoring π - π dispersive interactions. In another study, Segovia-Sandoval et al. (2020) explored the adsorption of metronidazole on hybrid materials of carbon xerogels and graphene (CX-GO). They found that the adsorption capacity of CX-GO for metronidazole significantly increased with the increment of graphene content. The maximum adsorption capacity was 160 mg/g in CX-1.0GO, where the number indicates the graphene oxide content. This increase in adsorption capacity was attributed to the rise in the BET area, promoting π - π dispersive interactions. Carabineiro et al. (2012) compared the adsorption capacities of activated carbons (AC), carbon xerogels (CX), and carbon nanotubes (CNT) for ciprofloxacin adsorption. They found that the maximum adsorption capacity was obtained in AC (230 mg/g), followed by CNT and CX in decreasing order. This decrease in adsorption capacity is directly related to the BET area of the carbonaceous materials.

Until now, there has been a notable absence of studies exploring the application of 3D printing technology for the fabrication of carbon monolith adsorbents with precisely controlled channel morphologies, specifically designed for the removal of pharmaceutical compounds from water. This unexplored field represents an exceptionally intriguing area of research, distinguished by its low cost, straightforward

handling, and potential for industrial scalability, particularly in the context of continuous adsorption systems. The novelty of this research direction not only underscores its scientific significance but also emphasizes its practical appeal, offering a promising platform to address water pollution challenges associated with pharmaceutical contaminants.

2.6 Objectives

2.6.1 General objective

The aim of this thesis is to develop clay-based adsorbent materials and to fabricate nanostructured carbon monolith adsorbents with controlled porosity and channel morphologies using 3D printing technology combined with sol-gel polymerization, both for the removal of pharmaceutical compounds from aqueous solutions.

2.6.2 Specific objectives

The objectives are described as follows:

- i) Investigate the influence of structural characteristics and nature of diverse raw clays (sepiolite, vermiculite, bentonite, halloysite, phlogopite and kaolinite) on their adsorption capacity for tetracycline from aqueous solutions.
- ii) Examine the impact of the chemical, textural, and swelling properties of bentonite on the adsorption of trimethoprim and chlorphenamine from water.
- iii) Elucidate the mass transport mechanisms controlling the overall adsorption rates of three pharmaceutical compounds, trimethoprim, tetracycline and chlorphenamine on natural bentonite clay.
- iv) Analyze the binary adsorption of tetracycline and cadmium (II) on natural bentonite clay under different solution pH conditions and elucidate the binary adsorption mechanisms.
- v) Synthesize hybrid clay-based adsorbents through a cation exchange reaction with hexadecyltrimethylammonium bromide and investigate the impact of surface chemistry on the adsorption capacity for several pharmaceuticals,

including carbamazepine, tetracycline, sulfamethoxazole and chlorphenamine, each possessing different chemical properties.

- vi) Optimize the synthesis conditions of carbon xerogels to achieve synthetic materials with tailored morphology and well-defined pore size distributions, specifically designed for the removal of sulfamethoxazole from water.
- vii) Design and fabricate integral carbon xerogel monoliths with precisely engineered channel geometries, utilizing a combination of sol-gel polymerization with 3D printing technology, for the efficient removal of sulfamethoxazole from water. Furthermore, evaluate the impact of synthesis conditions on adsorption performance.
- viii) Investigate the effect of CO₂ and H₂O activation time on the chemical and textural properties of carbon monoliths and evaluate its influence on the adsorption of sulfamethoxazole from aqueous phase.
- ix) Explore the effects of diverse channel geometries on breakthrough curves for the adsorption of sulfamethoxazole from aqueous solutions and corroborate the results with Computational Fluid Dynamics (CFD) calculations.

CHAPTER

EXPERIMENTAL METHODS

3

3.1 Preparation and synthesis of clay-based materials and carbon monolithic structures

3.1.1 Clay minerals preconditioning

Calcium bentonite was sourced from a mineral deposit in San Luis Potosi, Mexico. Vermiculite was supplied by Virginia Vermiculite Company, Louisa, Virginia, USA. Phlogopite was obtained from RENAGO in Oaxaca de Juarez, Oaxaca, while kaolinite, sepiolite and halloysite were provided by Synerplus, Sepiolsa and Merck, respectively. All clay minerals were ground and sieved to -200 +400 mesh sizes. The preconditioning of the clay is described in Chapter 4, Section 4.4.2.

3.1.2 Preparation of clay samples with different uptakes of pharmaceuticals adsorbed

Clay samples were saturated with pharmaceuticals at various adsorption levels. The nomenclature and specifications of these prepared samples are detailed in Chapter 5, Table 5.2.

3.1.3 Synthesis of hybrid hexadecyltrimethylammonium bromide-modified organobentonite

Organobentonite was prepared through a cation exchange reaction between bentonite and the cationic surfactant hexadecyltrimethylammonium bromide. The detailed methodology is outlined in Chapter 8, Section 8.2.1.

3.1.4 Synthesis of nanostructured carbon xerogels

Nanostructured carbon xerogels were synthesized through sol-gel polymerization of resorcinol and formaldehyde, with Cs_2CO_3 as a catalyst. The synthesis involved varying the resorcinol/catalyst ratios to modulate gel porosity. A detailed synthesis method is provided in Chapter 9, Section 9.2.1.

3.1.5 Design of 3D geometries using Computer-Aided Design (CAD)

Detailed prototypes of 3D CAD models were developed using Solid-Works software to accurately represent the channel geometries of monoliths. The design methodology is detailed in Chapter 11, Section 11.2.1.

3.1.6 Fabrication of 3D-printed carbon monoliths

A hybrid method that combining sol-gel polymerization with advanced 3D printing technology was used to fabricate 3D-printed carbon monoliths. This innovative hybrid method is discussed in Chapter 10, Section 10.2.2.

3.1.7 Activation of 3D-printed carbon monoliths using CO₂ and H₂O

The 3D-printed carbon monoliths were activated using CO₂ and H₂O at 850 °C. The activation procedures are detailed in Chapter 11, Section 11.2.3.

3.2 Characterization techniques

The characterization of clay-based materials and 3D-printed carbon monoliths involved techniques such as CO₂ adsorption, N₂ adsorption, Hg intrusion porosimetry, SEM, XRD, FT-IR, thermogravimetric analysis, XPS, Zeta potential, helium pycnometry, cation exchange analysis, determination of acidic and basic sites, point of zero charge and stress-strain experiments. Each technique is discussed in the chapters of this thesis.

3.3 Adsorption tests

Adsorption tests were conducted in both batch and continuous operations. Experimental adsorption data were collected using a batch adsorption system, a stirred tank batch adsorber for suspended particles and a monolithic packed bed adsorber. The operating conditions included pH, temperature, ionic strength, initial concentration, stirring speed, volumetric flow rate, and the channel geometries of the 3D-printed monoliths. Detailed descriptions of each operation are provided in the corresponding chapters.

CHAPTER

**REMOVAL OF TETRACYCLINE
FROM AQUEOUS SOLUTIONS BY
ADSORPTION ON RAW Ca-
BENTONITE. EFFECT OF
OPERATING CONDITIONS AND
ADSORPTION MECHANISM**

4

4.1 Introduction

Human, industrial and agricultural activities contribute significantly to environmental pollution. Nowadays, great concern has been arisen due to the occurrence and detection of various toxic organic compounds of anthropogenic origin in water resources. These new chemicals, known as emerging pollutants or contaminants of emerging concern, have commonly used as personal care products, drugs, pesticides, hormones, among others. These compounds are continuously discharged into water resources, causing persistence and bioaccumulation, and can pose a hazardous threat to human beings and the environment (Wilkinson et al., 2017).

Tetracycline (TC) is a wide-spectrum antibiotic having high activity toward an ample variety of microorganisms. TC is also commonly employed to stimulate the growth rate and boost the feed efficiency of animals because of its low cost (Chopra and Roberts, 2001; Gao et al., 2012). TC has been detected in surface waters (rivers, lakes and seawater), groundwater, drinking water, sediments and wastewater and sludge (Xu et al., 2021). The concentrations of TC in surface waters and effluents from wastewater treatment plants fluctuated from 0.0011 to 110 µg/L and 0.001 to 3170 µg/L, respectively (Xu et al., 2021).

Diverse removal processes have been examined for eliminating TC in water solutions, inclusive of advanced oxidation processes. The heterogeneous photocatalysis of TC was achieved using TiO₂ (Maroga Mboula et al., 2012), and the results showed that TC was partially mineralized, generating by-products with low biodegradability and less toxicity than TC. Furthermore, the TC ozonation in a water solution was also investigated in the pH range of 2.2-7, and it was found that the aromatic rings and the dimethylamino group of the TC produced recalcitrant by-products during the ozonation. After 2 h, the degradation percentage of TC was 40 % (Khan et al., 2010). In a recent study, TC was photodegraded by UV irradiation and a new sulfate radical, UV/peroxymonosulfate; however, after irradiation, the solution's toxicity significantly increased due to the formation of various toxic by-products (Ao et al., 2019).

Among the alternative and promising methods for treating contaminated aqueous effluents, adsorption has attracted much consideration because of its outstanding features like simple and economical process, high removal efficiency, and without generating noxious by-products (Yu et al., 2016). Different adsorbents, varying from natural minerals to advanced nanostructured materials, have been applied in this separation method.

In several works, different carbonaceous materials were synthesized and applied for adsorbing TC. Gao et al. (2012) applied graphene oxide for adsorbing TC from water, and the results revealed that the adsorption occurred by physical and chemical interactions, and the maximum mass adsorbed of TC was 313 mg/g. Ji et al. (2009) analyzed the TC adsorption onto multiwalled carbon nanotubes (MWCNTs), and the results showed that TC was adsorbed on MWCNTs by the π - π dispersive interactions, resulting in the maximum capacity of 100 mg/g. Furthermore, Rivera-Utrilla et al. (2013) determined the adsorption capacity of granular activated carbon towards TC to be 375.4 mg/g, and the primary adsorbing mechanism was the electrostatic interactions between the TC species in solution and the carbon surface.

Among the natural adsorbents, clay minerals have several outstanding characteristics: mesoporous structure, negatively charged surface, specific surface area, hydration, swelling, high cation exchange capacity and chemical stability, which favors the adsorption of a wide variety of pollutants. Bentonite is a raw clay mainly composed of montmorillonite ($\text{Na}_{0.6}(\text{Al}_{3.4}\text{Mg}_{0.6})\text{Si}_8\text{O}_{20}(\text{OH})_4$) that belongs to the smectite group. Its trilaminar structure (2:1) is formed by one Al^{3+} octahedral sheet placed between two Si^{4+} tetrahedral sheets. The negatively charged surface of bentonite is mainly counterbalanced by Ca^{2+} , K^+ , Na^+ and Mg^{2+} , designated as exchangeable cations (Leyva-Ramos et al., 2021).

The TC adsorption on clay minerals has been studied in few works; however, the TC adsorption on bentonite has not been analyzed thoroughly, and neither has the mechanisms of TC adsorption been explained. Some studies have shown that montmorillonite exhibited a reasonable affinity towards TC. The sodium and calcium montmorillonites have been applied for removing TC (Parolo et al., 2013), and at pH =

3, the calcium montmorillonite presented a maximum mass of TC adsorbed of 315.5 mg/g. Zhao et al. (2012) determined the montmorillonite capacity for adsorbing TC to be 250 mg/g at pH = 5.5. Iron-intercalated montmorillonite was synthesized to remove TC and presented a maximum mass of TC adsorbed of 290 mg/g at pH = 5. This high capacity was due to the increment in the pore volume and specific surface area, originated by intercalating of iron-(hydr)oxide in the montmorillonite interlaminal space (Wu et al., 2016). Current studies claim that high affinity of TC can be ascribed to the TC intercalation in the interlaminal space of montmorillonite; however, detailed studies refer to the interactions between TC and bentonite, and the adsorption mechanisms at acid and neutral conditions are even scarcer.

Chapter 4 presents the TC adsorption upon various raw clay minerals, including diverse structural characteristics, and the raw bentonite (Bent) exhibited the highest adsorption capacity towards TC. The characterization of Bent and TC adsorbed onto Bent was carried out by various analytical techniques. The solution ionic strength, temperature, and pH influence in Bent capacity for adsorbing TC was also analyzed thoroughly. Furthermore, the reversibility of the TC adsorption on bentonite was examined in detail. The adsorption mechanisms of TC on bentonite in acid and neutral aqueous medium were also explained in detail.

4.2 Experimental methodology

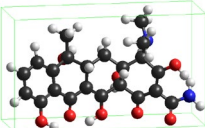
4.2.1 Materials

The calcium bentonite (Bent) was obtained from a mineral deposit in San Luis Potosi, Mexico. Virginia Vermiculite Company, Louisa, Virginia, USA, supplied vermiculite (Verm). The phlogopite (Phlo) was provided by the company RENAGO located in Oaxaca de Juarez, Oaxaca. Synerplus, Sepiolsa (Spain) and Merck supplied the kaolinite (Kaol), sepiolite (Sep) and halloysite (Hal), respectively.

The chemical structure TC is illustrated in Figure 4.1 (a), and Table 4.1 lists its physicochemical characteristics. TC can exist in four distinct species in aqueous solution, and the speciation diagram of TC is affected by the pH and is displayed in Figure 4.1 (b). This figure shows that the TC cationic species (TC⁺) predominates at

pH lesser than 3, the neutral or zwitterionic species (TC^{\pm}) prevails in a pH interval from 3 to 7, and the anionic species (TC^{-} and TC^{2-}) are predominant at pH higher than 7.

Table 4.1. Physicochemical properties of TC.

Pharmaceutical compound	Family	Molecular structure ^a	Molecular size ^a (nm)	Log D ^b	pK _a ^c
Tetracycline (TC) M.W. = 444.44	Antibiotics		X = 1.38 Y = 0.81 Z = 0.69	-1.30	3.32, 7.78, 9.58

^a Determined by Density Functional Theory (DFT) using B3LYP method.

^b Distribution coefficient at pH = 7.

^c Dissociation constants (Chopra and Roberts, 2001).

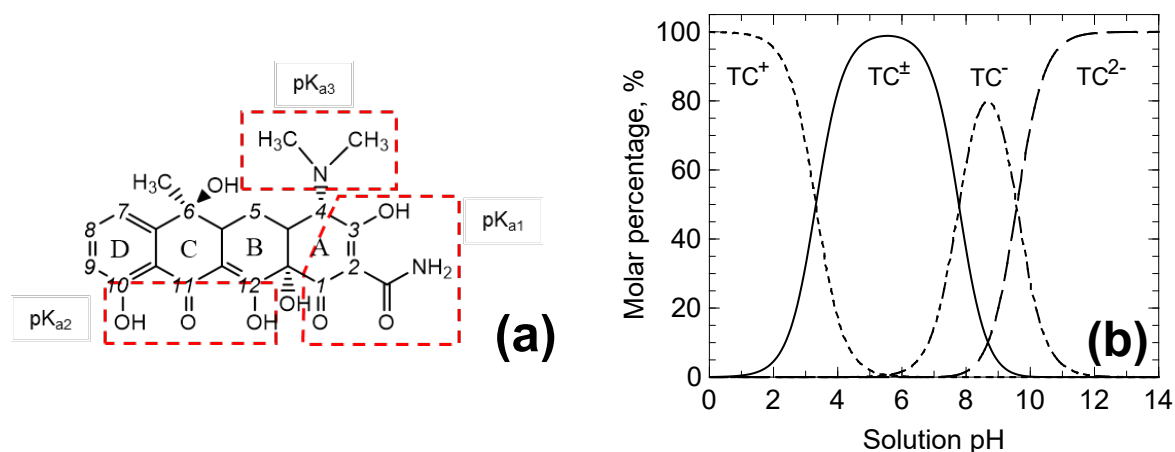


Figure 4.1. Chemical structure of TC (a) and speciation diagram of TC (b) as a function of solution pH.

4.2.2 Clay minerals preconditioning

The clay minerals were ground in an analytical mill, IKA, A 11 basic model, and sieved using -200 +400 mesh sizes, corresponding to a mean particle size of 0.056 mm. Afterward, the ground clays were rinsed various times with deionized water, separated from the washing medium by decantation, dried for 24 h at 110°C and placed in sealed containers.

4.2.3 Characterization of bentonite and bentonite with TC adsorbed

The clay mineral samples were designated as Bent, B-TC (pH 3) and B-TC (pH 7), referring to raw bentonite and bentonite saturated with TC at pH of 3 and 7, and the corresponding loading of TC was $q = 257.2$ and 153.3 mg/g, respectively. The physicochemical properties of clay mineral samples were determined by various analytical techniques. The chemical composition of Bent expressed as a weight percentage of the constituent oxides is presented in Table 4.2 (Martinez-Costa and Leyva-Ramos, 2017).

The textural characteristics were evaluated using the N₂ adsorption-desorption isotherm, appraised in an N₂ physisorption analyzer, Micromeritics, ASAP 2020 model. The Brunauer, Emmett and Teller (BET) method was employed to evaluate the specific surface area, S_{BET} (Brunauer et al., 1938). Besides, the area of the mesopores, S_{meso} , was computed by the t-plot method. The Barret-Joyner-Halenda (BJH) procedure was applied to estimate the pore size distribution and the total accumulated pore volume (Barrett et al., 1951). The total volume of the pores, V_p , and the volume of the mesopores, V_{meso} , were assessed from the pore size distribution by the computational procedures recommended by Rouquerol et al. (1998). The average pore diameter, D_p , was estimated using the following equation (Rouquerol et al., 1998):

$$D_p = \frac{4 \times V_p}{S_{BET}} \quad (4.1)$$

The clay mineral morphology was examined in a scanning electron microscope, JEOL, model JSM-6610LV. The procedure suggested by Ming and Dixon (1987) was utilized to determine the cation exchange capacity (CEC). The procedure consists of the following steps: i) Saturation of the bentonite with Na⁺ cations, ii) Exchange of Na⁺ cations by NH₄⁺ cations, and iii) Determination of Na⁺ cations released from the bentonite to the solution. The crystalline phases of a sample were identified in a Rigaku diffractometer, model DMAX 2000, under operating conditions of Cu-K α radiation ($\lambda = 0.15406$ nm), 30 mA and 30 kV. The diffractometer was programmed to carry out a scan from 4 to 45 ° (2θ) and using a step of 1.8 °/min. The coexisting phases were

identified by comparing their standards compiled by the International Center of Diffraction Data (ICDD).

The thermogravimetric analysis of the Bent, B-TC (pH 3) and B-TC (pH 7) was conducted in a Perkin Elmer analyzer, Pyris Diamond, TGA/DTA model, and the operating conditions were temperature range 25-1000°C and a heating rate of 10°C/min. The Zeta potential of Bent surface in water solution was determined in a Zetameter, Zetasizer 4 model, following the next procedure. Bent dispersions (0.01 g of particles/50 mL) were prepared in 50 mL centrifuge vials by adding Bent and the solutions of constant ionic strength (0.01 N) in the pH interval from 2 to 12, fixed by mixing appropriate aliquots of 0.01 N HCl and NaOH solutions. The vials containing the dispersions were set in a water bath at 25°C, and the pH was adjusted daily. The dispersions were mechanically stirred. After eight days, an aliquot (1 mL) was taken to quantify the Zeta potential of the Bent. Moreover, the Zeta potential of B-TC (pH 3) and (pH 7) was determined as a function of the uptake of TC adsorbed on Bent, using TC concentrations from 15 to 120 mg/L.

4.2.4 Quantification of TC concentration in water samples

A UV-Vis spectrophotometry procedure was implemented to assess the TC concentration in aqueous samples. The sample absorbance was ascertained in a Shimadzu spectrophotometer, 2600 model, set up at the specific wavelength of 357. The TC concentration was calculated using calibration curves prepared from TC standard solutions having concentrations from 0.6 to 42 mg/L and pH of 7, 5 or 3.

4.2.5 Technique for conducting the adsorption equilibrium experiments

In this work, a stock solution of TC (300 mg/L) was prepared by dissolution of a certain mass of TC (2.19 g) using a solution having a constant ionic strength of 0.01 N and pH of 3, 5, or 7. 1 L, which was made by mixing the proper volumes of 0.01 N HCl and NaOH solutions fixed with deionized water.

A batch adsorber consisting of a centrifuge vial (50 mL) was utilized to conduct the TC adsorption experiments on the clay (Figure 4.2). The TC solutions of known

initial concentration, 30-250 mg/L, were formulated by adding a given aliquot of the TC stock solution into a volumetric flask (50 mL) and then diluting using the solution with a constant ionic strength ($I = 0.01 \text{ N}$) and a particular pH. Later, 40 mL of these solutions were added to, named batch adsorbers, containing a certain mass of the clay. The solution temperature was kept constant by placing the adsorber in a thermostatic bath, and the adsorber was placed in a rotary shaker for stirring the solution for 40 min every day. The pH was determined daily and maintained constant by supplementing drops of NaOH and HCl solutions (0.01, 0.1 and 1 N). In the adsorption runs, it was noticed that the solution pH diminished when the initial pH was 7 but increased when the initial pH was 3 or 5. Thus, the solution had to be kept constant because the adsorption equilibrium depended on the solution pH. The initial volume of the solution was considered constant because the supplemented volume was invariably less than 2.0 % of the initial volume.

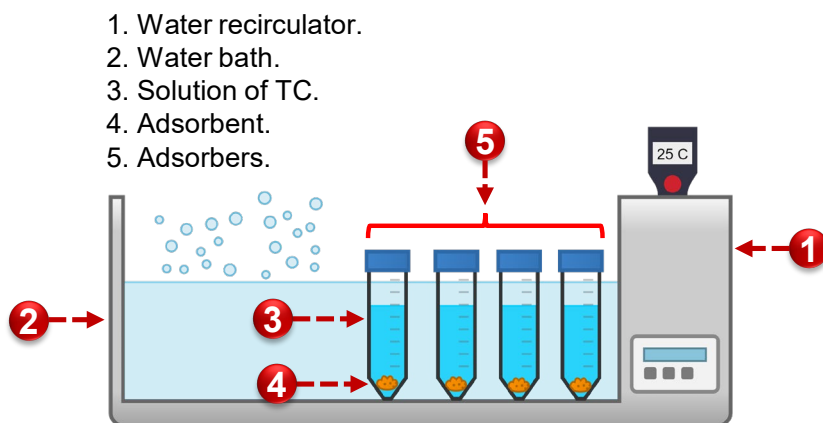


Figure 4.2. Batch adsorbers.

In preliminary runs, the solution was sampled at predetermined times, and the TC concentration in each sample was determined. Equilibrium was assumed to be reached when the TC concentrations of two consecutive samples did not change significantly. The results of the preliminary runs showed that 7 days were enough to attain equilibrium. After eight days, once equilibrium was achieved, the dispersions were centrifuged at 2500 rpm during 10 min. Subsequently, an aliquot (5 mL) was

filtered to determine the TC concentration. Then, the uptake adsorbed of TC was computed from the succeeding equation:

$$q = \frac{V}{m}(C_o - C_e) \quad (4.2)$$

where C_e and C_o are the TC equilibrium and initial concentrations, mg/L; m is the amount of clay mineral, g; q is the mass adsorbed of TC, mg/g; V is the TC solution volume, L.

4.2.6 Technique for performing the desorption equilibrium experiments

Once equilibrium was attained, according to the conditions outlined previously, the desorption experiments were carried out. The Bent equilibrated with TC was extracted from the solution and subsequently transferred to another adsorber holding a solution without TC (40 mL) with a particular ionic strength and pH. The pH was measured and adjusted daily, as described above. Upon reaching desorption equilibrium (eight days), a 5 mL aliquot was filtered to quantify the concentration of TC. The amount of TC not desorbed was assessed from the following equation:

$$q_d = q_o - \frac{V}{m}C_{ed} \quad (4.3)$$

where C_{ed} is the concentration of TC at equilibrium in the desorption experiment, q_o is the uptake of TC adsorbed starting the desorption experiment, mg/g; q_d represents the uptake of TC that did not desorb in the desorption run, mg/g.

4.2.7 Procedure for determining the amounts of cations adsorbed during adsorption of TC

The method consisted of two steps. In this first one, the Bent was allowed to equilibrate with the solution without TC. A solution (pH of 3 or 7, $I = 0.01$ N) volume was poured into a batch adsorber, and the Bent dosage was 30 mg/40 mL (pH = 3) and 50 mg/40 mL (pH = 7), soon afterward, the adsorber was partially submerged in a thermostatic bath, mechanically shaken, and adjusting the solution pH to maintain it constantly. After 8 days, the pH was determined, and the solution was sampled (1 mL) to quantify by Atomic Absorption spectrometry the exchangeable cation concentrations

(Na⁺, K⁺, Ca²⁺ and Mg²⁺) in the solution before TC adsorption. In the second step, the adsorption of TC was carried out by supplementing an aliquot of a TC solution with a specific concentration to make the initial TC concentration equal to 250 mg/L in the adsorber solution. Promptly, the pH was measured and designated as pH_{in}, and the concentrations of the exchangeable cations were corrected due to adding the aliquot, and these concentrations were designated as C_{i0}. After eight days in contact, the solution's final pH (pH_{fn}) was registered, and the final concentrations of cations, C_{if}, and TC in this solution were quantified.

The equivalents of cations adsorbed or desorbed were determined by performing an equivalents balance, similar to the mass balance represented by Equation (4.2). The overall uptake of TC adsorbed due to various mechanisms as well as the uptakes of H⁺ and exchangeable cations adsorbed were computed by the succeeding equations (Salazar-Rabago and Leyva-Ramos, 2016).

$$Q_{TC} = \frac{q_e \times 100}{EW_{TC}} \quad (4.4)$$

$$Q_{H^+} = \frac{(10^{-pH_{in}} - 10^{-pH_{fn}}) \times 1000 \times V \times 100}{m} \quad (4.5)$$

$$Q_i = \frac{(C_{i0} - C_{if}) \times 1000 \times V \times 100}{m} \quad (4.6)$$

where C_{if} and C_{i0} are the final and initial concentrations of the exchangeable cation *i*, eq/L; EW_{TC} is the equivalent weight of TC, 444.44 g/eq; Q_{TC} is the uptake of TC adsorbed on Bent, cmol(+)/kg; Q_{H⁺} and Q_{*i*} are the uptakes of H⁺ and exchangeable cation *i* adsorbed by ion exchange, cmol(+)/kg; pH_{fn} and pH_{in} are the final and initial pH values of the solution, and V represents the TC solution volume in the adsorber, L. It is essential to mention that Q_{H⁺} and Q_{*i*} would be positive if the H⁺ and exchangeable cations were adsorbed on Bent, whereas they would be negative if the H⁺ and exchangeable cations were desorbed from Bent.

The total uptake of cations (exchangeable cations and H⁺) adsorbed during the adsorption of TC on Bent was computed as follows:

$$Q_{T,Cat} = Q_{H^+} + \sum Q_i \quad (4.7)$$

4.3 Results and discussion

4.3.1 Cation exchange capacity, chemical composition, textural characteristics and morphology of bentonite

The CEC, chemical composition and textural properties of Bent are registered in Table 4.2. The CEC of Bent was determined to be 75.2 cmol(+)/kg. This CEC value is within the CEC interval for bentonite reported in the literature, 70-140 cmol(+)/kg (Borden, 2001; Wang et al., 2010). As seen in Table 4.2, the weight percentage of the constituent oxides showed that the mineral clay used in this work is calcium bentonite due to the content of CaO (3.26%).

Table 4.2. Chemical composition and textural properties of Bent and B-TC (pH 3).

Chemical composition of Bent		Textural properties and CEC		
(% weight)		Property	Bent	B-TC (pH 3)
SiO ₂	65.70	S _{BET} ^a (m ² /g)	45	13
Al ₂ O ₃	19.60	V _p ^b (cm ³ /g)	0.087	0.063
Fe ₂ O ₃	3.73	D _p (nm)	7.8	19.7
K ₂ O	2.88	S _{meso} ^c (m ² /g)	32	13
CaO	3.26	V _{meso} ^d (cm ³ /g)	0.075	0.046
MgO	3.73	CEC ^e (cmol(+)/kg)	75.2	-
Na ₂ O	0.79			

^a Specific surface area determined by the BET method.

^b Total pore volume evaluated by the BJH method.

^c Mesoporous area calculated by the “t-plot” method.

^d Mesoporous volume obtained by the BJH method.

^e CEC evaluated by the method proposed by Ming and Dixon (1987).

The D_p, S_{BET}, V_p and V_{meso} of Bent were 7.8 nm, 44.5 m²/g, 0.087 cm³/g and 0.075 cm³/g, correspondingly. These values agree with those reported for raw bentonites (Moma et al., 2018; Moraes et al., 2011). The S_{BET}, V_p and V_{meso} for B-TC (pH 3) decreased to 13 m²/g, 0.063 cm³/g and 0.046 cm³/g, correspondingly, and D_p increased from 7.8 to 19.7 nm, after the TC adsorption on Bent. The significant

decrease in S_{BET} , V_p and V_{meso} can be attributed to the filling up and blocking off the mesopores by the TC molecules adsorbed.

Figure 4.3 depicts the N_2 adsorption-desorption isotherms on Bent and B-TC (pH 3), and the two isotherms are of type IIb, characteristic of clays or aggregates of platy particles. According to the IUPAC classification, both isotherms show a hysteresis loop of type H3, characteristic of mesoporous materials (Sing, 1985). The mesoporous structure of this type of clays is due to the interparticle spaces produced by the disorderly arrangement of the clay sheets (Domínguez and Schifter, 1992). The B-TC (pH 3) displays a narrower hysteresis loop, indicating that its mesopores were obstructed after the TC adsorption on the pore surface of Bent.

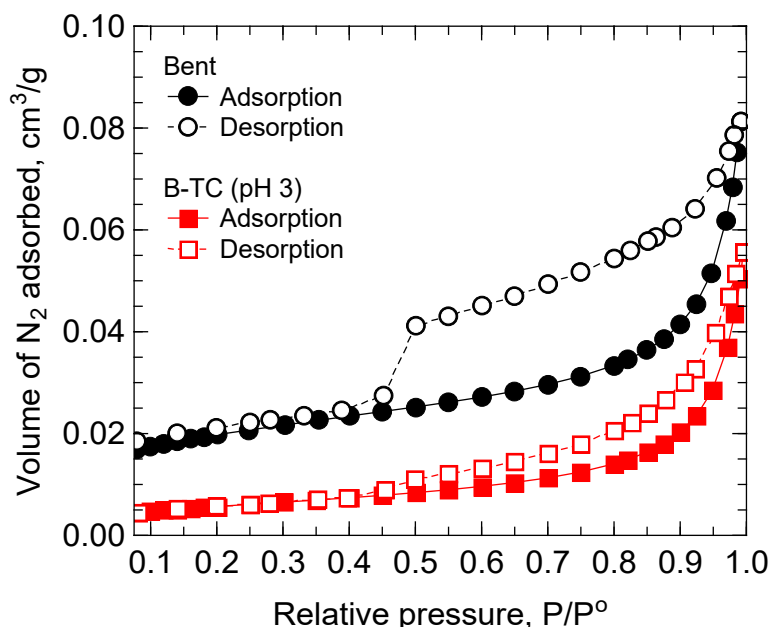


Figure 4.3. Adsorption-desorption isotherms of N_2 on Bent and B-TC (pH 3) at $-196.15\text{ }^\circ\text{C}$.

The cumulative pore volume percentage for Bent and B-TC (pH 3) are displayed in Figure 4.4. As seen in this figure, the Bent and B-TC (pH 3) are mainly composed of mesopores because the mesopore volume represents 86 and 73 % of the total pore volume, respectively. The mesopore volume of B-TC (pH 3) was reduced after adsorption of TC, suggesting that TC adsorption is mainly occurring in the mesopores. This result also explains why the D_p of B-TC (pH 3) is higher than the D_p of Bent.

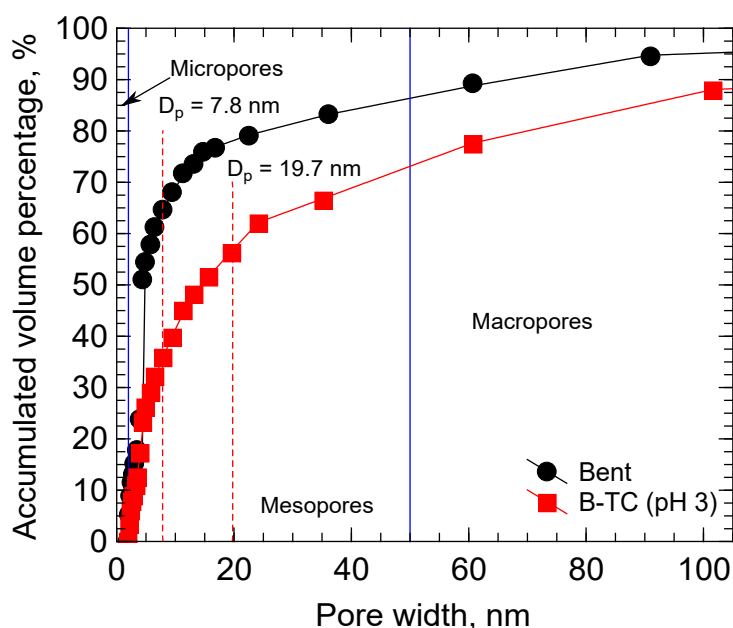


Figure 4.4. The cumulative pore volume percentage of Bent and B-TC (pH 3).

Figure 4.5 (a) shows an overall view of Bent and B-TC (pH 3) particles by SEM. Morphology of clay can be observed in detail at higher magnifications (areas selected by yellow and red dashed lines). Bent shows flatty particles stacked randomly typical of an open-textured Ca-montmorillonite, Figure 4.5 (b) and (c). The morphology changed in B-TC (pH 3), exhibiting bigger particle sizes and adsorbed TC formed dense agglomerates on the external surface of Bent and empty spaces between randomly stacked flatty particles. The SEM analysis confirmed that the adsorption of TC partially took place on the external surface of Bent particles and spaces between particles.

4.3.2 Zeta potential distribution

Figure 4.6 (a) depicts the zeta potential distribution of Bent vs. the pH. In the pH interval tested, the Bent presented a negative surface charge, exhibiting more negative zeta potential while increasing the solution pH. The negative charge of Bent is attributed to negative charge deficiency caused by isomorphous substitutions of Si^{4+} for Al^{3+} and Al^{3+} for Mg^{2+} or Fe^{2+} in the octahedral and tetrahedral sheets, correspondingly (Domínguez and Schifter, 1992).

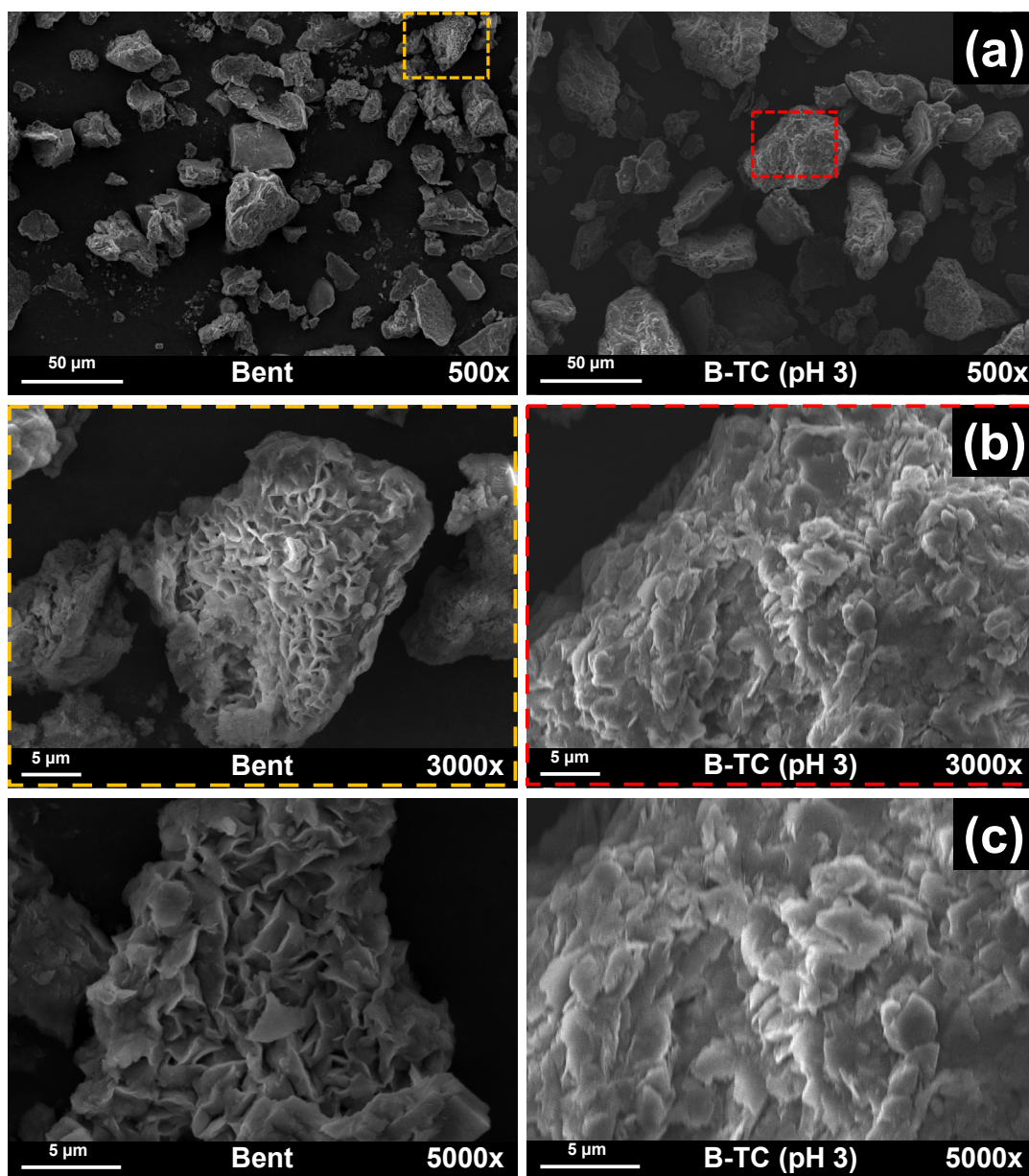


Figure 4.5. SEM images of Bent and B-TC (pH 3) recorded at 500X (a), 3000X (b) and 5000X (c).

Furthermore, Figure 4.6 (b) displays that the initial concentration of TC influences the zeta potential at pH = 3 and 7. The TC initial concentration influenced Bent surface charge because the TC adsorbed on Bent surface can balance the surface charge of Bent. Consequently, the uptake adsorbed of TC on Bent grew by

incrementing the initial concentration and was calculated as explained in Section 4.2.5. As seen in Figure 4.6 (a), at pH = 3, the negative surface charge shifted towards less negative values or even positive, while the TC initial concentration or the mass of TC adsorbed raised. In contrast, at pH = 7, there was no significant difference in surface charge of Bent for higher TC initial concentrations. Variations in surface charge can be visualized clearly by calculating the Zeta potential difference $\Delta(\text{ZP})$ as a function of the uptake of TC adsorbed (q). The $\Delta(\text{ZP})$ was calculated applying the following equation:

$$\Delta(\text{ZP}) = (\text{ZP})_{\text{B-TC}} - (\text{ZP})_{\text{Bent}} \quad (4.8)$$

where $(\text{ZP})_{\text{B-TC}}$ is the zeta potential of bentonite saturated with TC (B-TC), mV, and $(\text{ZP})_{\text{Bent}}$ is the zeta potential of Bent, mV. Figure 4.6 (b) shows the $\Delta(\text{ZP})$ vs. q , and as shown in this figure, at pH = 3, the $\Delta(\text{ZP})$ increased linearly, augmenting the mass of TC adsorbed. On the contrary, at pH = 7, the $\Delta(\text{ZP})$ showed no significant change as a function of q .

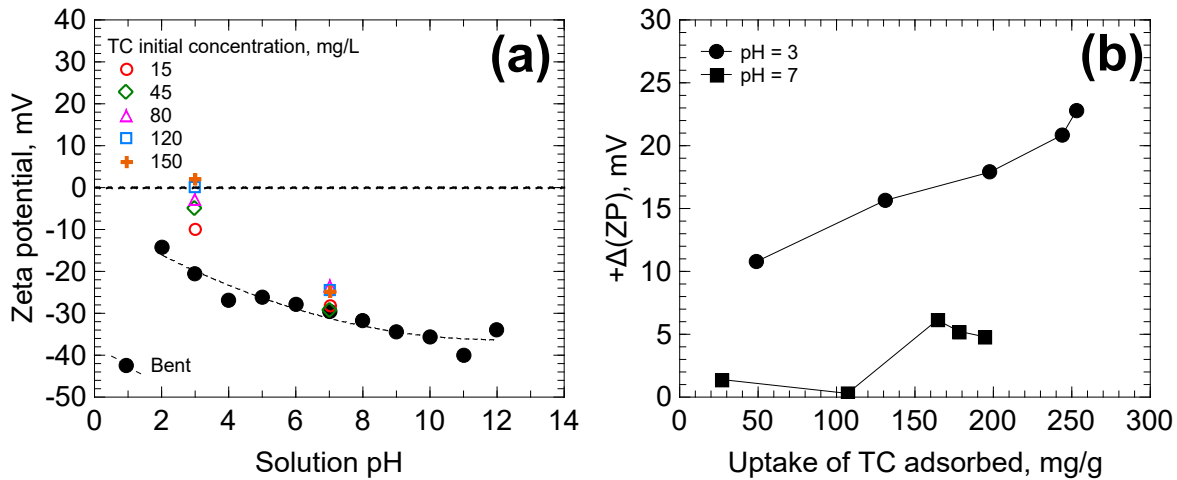


Figure 4.6. Zeta potential distribution of Bent as a function of TC initial concentration (a) and Zeta potential difference of Bent as a function of the uptake of TC adsorbed (b) at $T = 25\text{ }^{\circ}\text{C}$ and pH of 3 and 7.

The behavior of $\Delta(\text{ZP})$ at pH = 3 revealed that the adsorption mechanism of TC on Bent depends significantly on the electrostatic attractions since TC^+ is attracted to negatively charged surface and adsorbed on the cationic sites of Bent, balancing the negative charge of the surface. On the contrary, at pH = 7, the slight variation of $\Delta(\text{ZP})$

showed no contribution of electrostatic attractions in the adsorption mechanism of TC. Thus, the adsorption of the TC[±] and TC⁻ species at pH = 7 may be caused by non-electrostatic interactions, like hydrophobic interactions, formation of coordination complexes or hydrogen bonding (Flores et al., 2017; Ibrahim et al., 2018; Porubcan et al., 1978; Undabeytia et al., 1999; Yamamoto et al., 2018).

4.3.3 X-ray diffraction testing

The XRD patterns of Bent, B-TC (pH 7) and B-TC (pH 3) are shown in Figure 4.7. The principal reflections in the XRD pattern of Bent show the crystalline plane with the (001) Miller index at 5.89 ° (2θ) and the reflections at 19.72, 23.51 and 34.74 ° (2θ) which corresponded to the montmorillonite (JCPDS 13-0135) (X. Wang et al., 2015; Y. Wang et al., 2019), corroborating that Bent is mainly composed of montmorillonite. The X-ray pattern of Bent also contains quartz and feldspar reflections, constituting the secondary crystalline compounds in Bent. Besides, the possible coexistence of illite was detected at 9.8° (2θ) (Elgamouz et al., 2019).

The plane (001) related to the basal reflection was 1.50 nm in Bent. Usually, the thickness of the 2:1 laminar configuration of the montmorillonite is 0.96 nm (Moore and Hower, 1986). Therefore, the interlayer space in basal reflection (001) observed for Bent, 0.54 nm, is related to the presence of two H₂O molecules (0.25 nm) between the sheets and associated with the hydration of the interlaminal Ca²⁺ cation. The estimated basal reflection (001) for B-TC (pH 7) and B-TC (pH 3) were 1.62 and 1.89, corresponding to interlayer spaces of 0.66 and 0.93 nm, correspondingly. According to the TC molecular size (Table 4.1), the interlayer space for the B-TC (pH 3) sample is wide enough to corroborate that the TC molecules are intercalated in the interlayer space of Bent and oriented parallel over their XZ or XY cross-sectional area, or slightly tilted. This result agrees with other studies (Parolo et al., 2013; Wu et al., 2016).

In the B-TC (pH 7) sample, the interlayer space was slightly smaller than the shortest dimension (Z) of the TC molecule. However, it has been reported that the increment in interlaminal space caused by the adsorption of organic molecules can be at least 0.1 nm lesser than the smallest dimension of the adsorbed molecule (Greene-

Kelly, 1955), suggesting that the TC^{\pm} species, despite their electric charge, can be partially intercalated in the interlayer space in a tilted orientation over their XY cross-sectional area. Some authors have reported that the intercalation of nitrobenzene, pyridine and benzoic acid can be in the interlayer space of montmorillonite, even though these compounds are neutral species (Farmer and Mortland, 1966; Lu et al., 2010; Yariv et al., 1966). The TC adsorbed on Bent was confirmed only in B-TC (pH 3) due to the identification of its main reflection at about 8.5° (2θ), recalling that the B-TC (pH 3) is the sample with the highest amount of TC adsorbed.

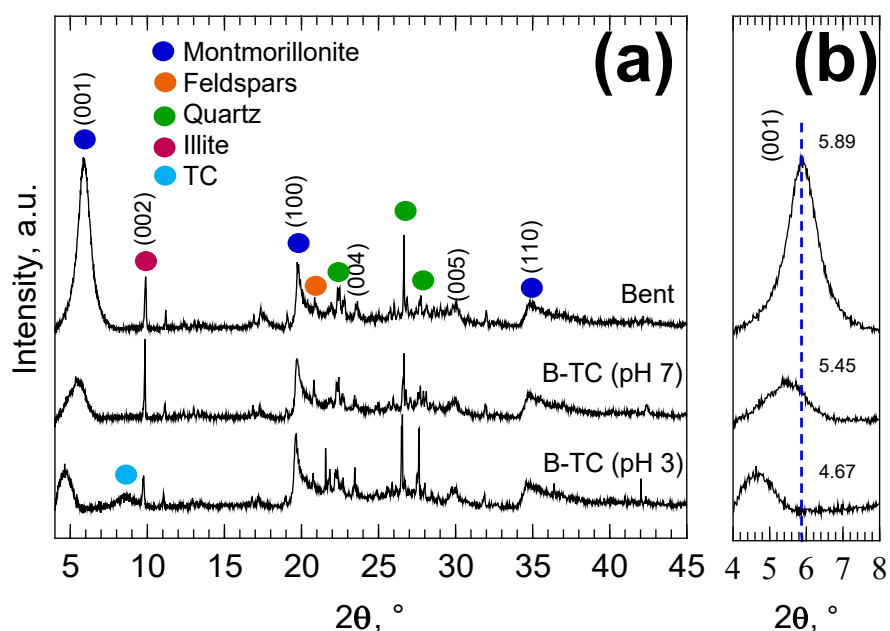


Figure 4.7. X-ray patterns obtained for Bent, B-TC (pH 3) and B-TC (pH 7) (a). Enlargement of the area depicting the (001) reflection of Bent (b).

4.3.4 Infrared spectroscopy analysis

Figure 4.8 (a) displays the infrared spectra for Bent, B-TC (pH 3), B-TC (pH 7) and TC samples in the wavenumber range of $400\text{-}4000\text{ cm}^{-1}$. The spectrum of Bent shows an absorption band at 514 cm^{-1} due to bending vibrations (δ) of the (Al-O-Si) bond, followed by a very strong band comprising the region between $1071\text{-}900\text{ cm}^{-1}$, corresponding to the stretching vibrations (ν) of the (Al-O-Al) and (Si-O-Si) bonds in Bent. The band at 3616 cm^{-1} is associated with vibrations of the structural $\nu(\text{OH})$ groups

of Bent, while the other around 3400 cm^{-1} represents the -OH groups coordinated by hydrogen bonding $\delta(\text{O-H})$. Alabarse et al. (2011) found out that the $\nu(\text{O-H})$ vibration of interlayer water is shown at 1631 cm^{-1} .

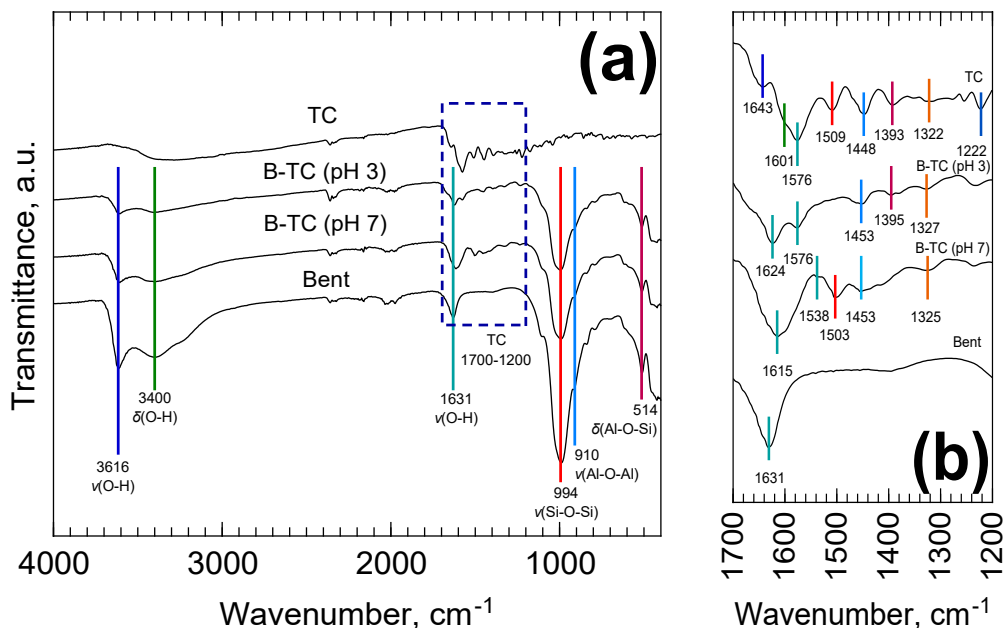


Figure 4.8. FT-IR spectra of Bent, B-TC (pH 3), B-TC (pH 7) and TC (a). The amplification of the spectra selected by the blue dashed line showing the TC bands (b).

The absorption bands of the TC spectrum are at 1643 , 1509 and 1222 cm^{-1} , Figure 4.8 (b), and designated as Amides I, II and III, corresponding to vibrations of the bonds $\nu(\text{C=O})$, $\delta(\text{N-H})$ and $\nu(\text{C-N})$ about the amide group. The vibrations of the $\nu(\text{C=O})$ bond of the A and C rings (See Figure 4.1 (a)) are displayed at 1601 and 1576 cm^{-1} , respectively. The band at 1448 cm^{-1} matches to skeletal vibrations $\nu(\text{C=C})$, while those located between 1430 and 1230 cm^{-1} are assigned to the $\nu(\text{C-C})$, $\delta(\text{C-C})$, $\nu(\text{amine, N-H})$, $\delta(\text{amine, C-N})$ and $\nu(\text{C-O})$ bonds (Kang et al., 2011).

The TC bands in the B-TC (pH 3) and B-TC (pH 7) confirmed TC adsorption on Bent. The bands of the $\delta(\text{C-N})$ (1393 cm^{-1}) and $\nu(\text{N-H})$ (1322 cm^{-1}) bonds of the dimethylamino group shifted towards longer wavenumbers in B-TC (pH 3). Besides, the $\nu(\text{O-H})$ band of interlaminar water showed a shift from 1631 to 1624 cm^{-1} . This shift is related to the interaction between the group $-\text{NH}(\text{CH}_3)_2^+$ (TC^+ species) with the

negative surface of Bent, and the coordination of the polar groups of TC⁺ with the hydration water of the clay by hydrogen bonds. B-TC (pH 7) showed a displacement of $\nu(\text{N-H})$ band from 1322 to 1325 cm⁻¹ attributed to a weak electrostatic attraction between the -NH(CH₃)₂⁺ group (TC[±] species) with the negative surface of Bent. Similarly, the $\nu(\text{C=O})$ band of the C-ring of TC moved to lower wavenumbers (1538 cm⁻¹), and its intensity decreased also. This distortion can be related to the resonance of the double bond C=O of the C ring of the TC⁻ species with the oxygen bound in C12 (See Figure 4.1 (a)), causing a high electronic density that leads to a negative charge on the resonant ring. It has been reported that this negative charge is usually stabilized by the formation of coordination complexes with highly polarizable divalent cations (Lambs et al., 1988). The interlamellar water $\nu(\text{O-H})$ band shifted from 1631 to 1615 cm⁻¹, suggesting the formation of outer-sphere coordination complexes among the TC⁻ species and the hydration sphere of the interlamellar Ca²⁺ cation. These results agree with different adsorption studies of organic compounds on montmorillonite, which is the main component of Bent (Farmer and Mortland, 1966; Lu et al., 2010; Parfitt and Mortland, 1968; Yariv et al., 1966).

4.3.5 Thermogravimetric analysis

The thermogravimetric analysis (TGA/DTG) of Bent, B-TC (pH 3) and B-TC (pH 7) samples are presented in Figure 4.9. The TGA curve of Bent, Figure 4.9 (a), displays a mass loss of around 6.1% from 25 to 200°C, associated with the water adsorbed onto the external surface and in the interlayer space of Bent. Subsequently, another mass loss of approximately 4.8% is observed between 200 and 1000°C, corresponding to dehydroxylation reactions in the octahedral sheet of Bent (Guggenheim and Koster van Groos, 2001). The overall mass loss from 25 to 1000°C was 10.9%, confirming the high thermal stability of Bent.

The TGA curves of B-TC (pH 7) and B-TC (pH 3) are shown in Figures 4.9 (b) and 4.9 (c), respectively, and a mass loss of 5.5% for B-TC (pH 7) and 3.8% for B-TC (pH 3) is observed between 25 and 200°C associated to the water adsorbed on the B-TC. In the range 200-1000°C, a mass loss of 10.2 and 13.9% is noticed for B-TC (pH

7) and B-TC (pH 3), respectively, confirming the decomposition of the TC adsorbed and dehydroxylation reactions (Cervini et al., 2016). The TC decomposition in both samples mainly occurred at 316.4°C. Assuming that the mass loss caused by dehydroxylation of the structural -OH groups of Bent (4.8%) is the same as those for B-TC (pH 7) and B-TC (pH 3); thus, the decomposition of the TC was 5.4 and 9.1%, respectively. The mass adsorbed of TC on B-TC (pH 7) and B-TC (pH 3) was $q = 153.3$ and 257.2 mg/g, respectively, then only 37.1 and 38.9% of the mass of TC adsorbed was decomposed in B-TC (pH 7) and B-TC (pH 3). This finding reveals that the TC adsorbed did not completely decompose in the temperature range used in this work. The partial decomposition of TC adsorbed is explained, recalling that part of TC intercalated in Bent interlayer space and Bent structure protected TC molecules thermally.

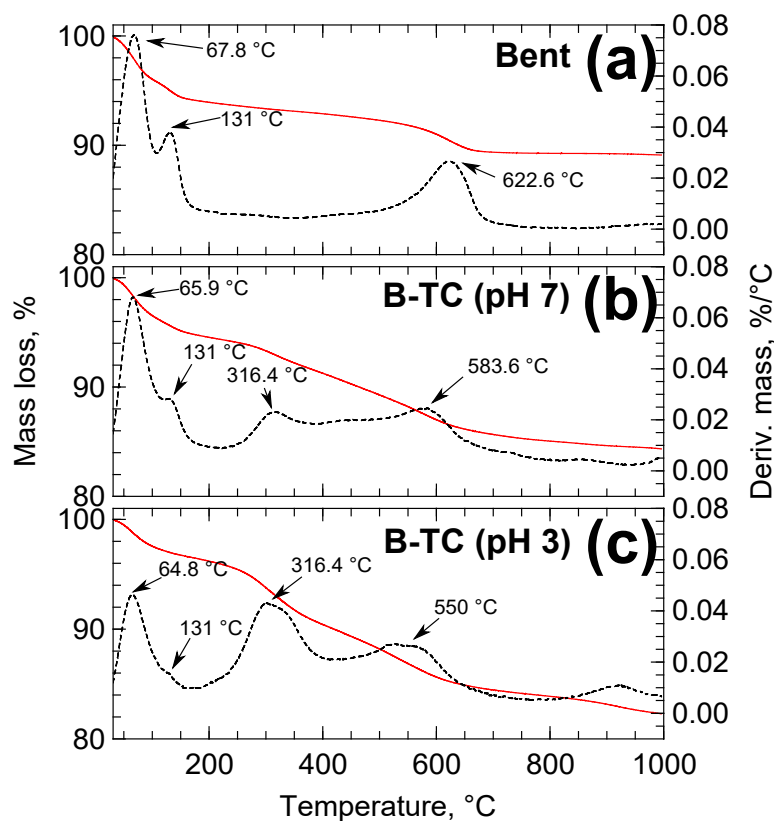


Figure 4.9. TGA (red line) and DTG (black dashed line) curves obtained for Bent (a), B-TC (pH 7) (b) and B-TC (pH 3) (c).

4.3.6 Adsorption isotherms of TC

The experimental data for the TC adsorption equilibrium onto raw clays were interpreted using the Radke-Prausnitz (R-P), Freundlich and Langmuir mathematical models expressed by the succeeding equations:

$$q = kC_e^{1/n} \quad (4.9)$$

$$q = \frac{q_m KC_e}{1 + KC_e} \quad (4.10)$$

$$q = \frac{aC_e}{1 + bC_e^\beta} \quad (4.11)$$

where k ($\text{mg}^{1-1/n} \text{L}^{1/n}/\text{g}$) is a parameter associated with adsorption capacity, q_m (mg/g) represents the maximum mass of TC adsorbed, K (L/mg) is a parameter associated with the heat of adsorption, and a (L/g), b ($\text{L}^\beta/\text{mg}^\beta$) and β are constants of the R-P isotherm.

Table 4.3 lists the average percentage deviations (%D) and the parameters for each isotherm. The parameters were assessed employing a nonlinear least-squares optimization procedure and the Rosenbrock-Newton algorithm, and %D was appraised with the succeeding relationship:

$$\%D = \left(\frac{1}{N} \sum_{i=1}^N \left| \frac{q_{i,\text{exp}} - q_{i,\text{pred}}}{q_{i,\text{exp}}} \right| \right) \times 100 \% \quad (4.12)$$

where N is the number of experimental data points; $q_{i,\text{exp}}$ is the uptake adsorbed of TC evaluated experimentally, mg/g ; $q_{i,\text{pred}}$ is the uptake adsorbed of TC computed using the adsorption isotherm, mg/g .

In 12 out of 15 cases of the experimental conditions presented in Table 4.3, the %D obtained for the Langmuir and R-P isotherms were smaller than those for the Freundlich model. Besides, 9 out of 15 cases, the parameter β of the R-P model is $\beta = 1$, so the R-P isotherm transforms into the Langmuir isotherm model. For this reason, Langmuir isotherm was chosen for predicting the experimental data.

Table 4.3. Adsorption isotherm parameters and average percentage deviation for the adsorption of TC on raw clays.

Natural clays	pH	I (N)	T (°C)	Freundlich			Langmuir			Radke-Prausnitz			
				K ($\text{mg}^{1-1/n} \text{L}^{1/n}/\text{g}$)	n	%D	q_m (mg/g)	K (L/mg)	%D	a (L/g)	b ($\text{L}^\beta/\text{mg}^\beta$)	β	%D
Sep	3	0.01	25	10.75	2.83	3.8	60.53	0.061	6.0	8.30	0.418	0.77	0.9
Verm	3	0.01	25	5.93	3.31	5.7	26.45	0.069	13.9	8.23	0.980	0.78	7.0
Phlo	3	0.01	25	0.97	1.78	9.5	21.33	0.015	5.4	0.33	0.015	1.00	5.4
Hal	3	0.01	25	7.00	2.75	4.7	39.56	0.068	16.0	46.91	6.239	0.65	5.3
Kaol	3	0.01	25	2.42	2.28	10.6	21.26	0.041	13.9	1.59	0.249	0.75	13.3
Bent	3	0.01	25	36.15	2.14	16.0	367.50	0.037	4.2	13.00	0.035	1.00	5.0
	5	0.01	25	30.28	2.12	20.3	334.52	0.032	10.7	10.81	0.034	0.99	10.7
	7	0.01	25	22.83	2.14	14.5	243.70	0.034	4.2	7.03	0.027	1.00	4.2
	3	0.05	25	40.35	2.38	20.0	344.31	0.038	3.5	12.98	0.038	1.00	3.5
	3	0.10	25	35.58	2.31	21.9	340.07	0.032	7.3	11.13	0.033	1.00	7.5
	3	0.50	25	9.38	1.44	8.9	428.14	0.011	3.4	4.51	0.011	1.00	3.5
	7	0.05	25	18.10	1.87	17.5	290.56	0.023	8.8	7.07	0.025	1.00	9.3
	7	0.10	25	17.30	1.91	18.1	264.81	0.023	9.8	6.21	0.023	1.00	9.8
	7	0.01	15	17.94	2.07	5.6	230.01	0.025	6.5	11.69	0.244	0.70	3.5
	7	0.01	35	21.33	1.87	18.3	317.34	0.027	9.2	8.61	0.027	1.00	9.2

4.3.7 Comparing the adsorption capacity of TC on various raw clays

At pH = 3 and T = 25°C, the adsorption isotherms of TC onto Sep, Bent, Phlo, Hal, Verm and Kaol are displayed in Figure 4.10 (a). Also, Figure 4.10 (b) shows an amplification of the adsorption isotherms in the uptake of TC adsorbed range from 0 to 70 mg/g. The experiments were performed at pH = 3 to favor the adsorption on acidic clays because the predominant species of TC was the cationic species (TC⁺) in the water solution. The results showed that Bent exhibited the maximum mass adsorbed of TC, 283.5 mg/g, and the capacities diminished as follows: Bent >> Sep > Hal > Verm > Kaol ≈ Phlo. For a TC equilibrium concentration of 100 mg/L, the Bent adsorption capacity towards TC was 5.40-fold higher than that for Sep and up to 22.5-fold larger than that for Phlo.

The highest capacity of Bent for adsorbing TC can be related to their structural arrangement, the swelling capacity, the degree of isomorphous substitution, and the residual charges in its structure. Verm and Phlo have a similar laminar structure like Bent; however, the Mg²⁺ and K⁺ ions are the main interlayer cations in these clays

(Domínguez and Schifter, 1992). These cations promote higher residual charges, generating strong bonds between the interlaminar ions and the clay sheets, diminishing the adsorption of TC. Even though Kaol is considered a swelling clay, it presented low TC adsorption capacity due to the large molecular size of TC. On the other hand, Sep and Hal cannot swell because of their fibrous and tubular structures, hindering that the molecules of TC can access the Sep channels or the interior of the Hal tubular structure.

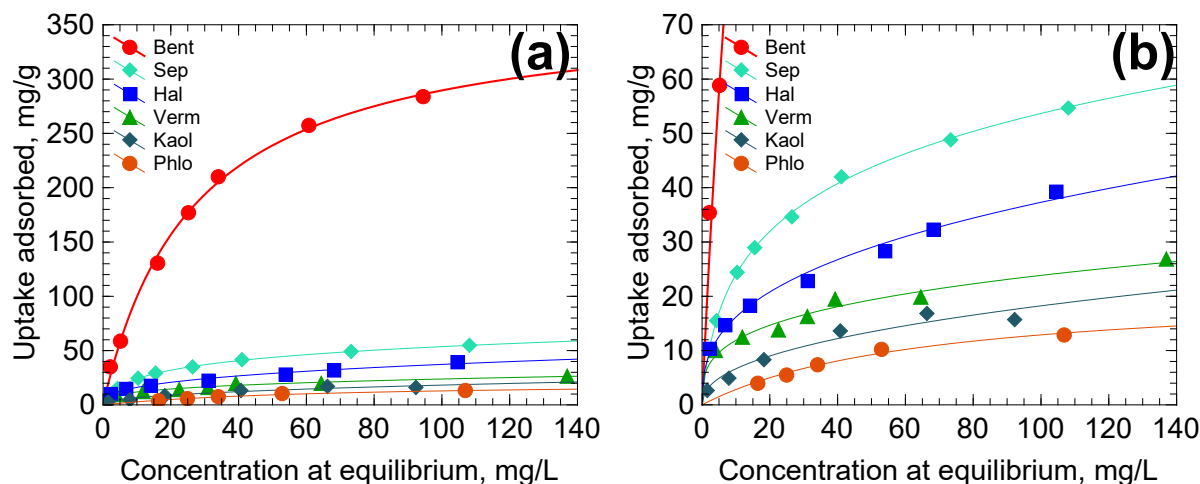


Figure 4.10. Effect of the type of raw clay on the adsorption isotherms of TC at pH = 3 and T = 25 °C (a). Amplification in the uptake of TC adsorbed range from 0 to 70 mg/g (b). The lines represent the best-fit isotherm.

Table 4.4 shows the TC mass adsorbed on different materials, and the Bent used in this work presented a maximum mass adsorbed of 283.5 mg/g, which is larger than the capacities found for other raw clays and even comparable or superior to carbon-based adsorbents. Furthermore, Bent presents outstanding advantages such as low cost and abundance, making Bent a very effective adsorbent for eliminating TC from aqueous solutions.

4.3.8 Influence of solution pH upon the capacity of bentonite for adsorbing TC

Figure 4.11 depicts the solution pH effect upon the TC adsorption onto Bent at 25 °C and pH of 3, 5 and 7. No adsorption runs were carried out at pH > 7 since it was observed that TC was partially mineralized in alkaline media. The maximum adsorption

capacity was 183.1, 263.8 and 283.5 mg/g for pH of 7, 5, and 3, correspondingly, so that the capacity for adsorbing TC notably diminishes by incrementing pH, and the highest uptake of TC adsorbed was at pH = 3. According to the results, the affinity of Bent towards the species of TC decreases as follows: $TC^+ > TC^\pm > TC^-$. At pH = 3, TC^+ is the predominant species, and Bent surface is negative so that the adsorption capacity is favored by electrostatic attractions among TC^+ and the negative surface charge of Bent. Moreover, the contribution of electrostatic attraction to the adsorption of TC^\pm and TC^- on Bent is not significant at pH = 7 because the net charge of these species is 0 and -1, respectively, and the Bent surface is negatively charged. Hence, the species TC^\pm and TCH^- would not be attracted or repelled from the surface of the clay, suggesting that the adsorption of both species on Bent is mainly due to other mechanisms.

Table 4.4. Adsorption capacities of several adsorbent materials towards TC.

Adsorbents	Maximum adsorption capacity (mg/g)	Experimental conditions	Reference
Commercial activated carbon	471.1	pH = 7-8, T = 25°C	Rivera-Utrilla et al. (2013)
Granular activated carbon	375.4	pH = 7-8, T = 25°C	Rivera-Utrilla et al. (2013)
Graphene oxide	313.0	pH = 3.6, T = 25°C	Gao et al. (2012)
Bentonite	283.5	pH = 3, T = 25°C	This work
Montmorillonite	250.0	pH = 5.5, T = 25°C	Zhao et al. (2012)
MOF graphite oxide pellets	228.0	pH = 4, T = 25°C	Yu et al. (2018)
Rectorite	140.0	pH = 4-5, T = 25°C	Chang et al. (2009)
Multi-walled carbon nanotubes	100.0	pH = 5.8, T = 25°C	Ji et al. (2009)
Nano sheet layered double hydroxide	98.04	pH = 3, T = 10°C	Soori et al. (2016)
Illite	32.0	pH = 5-6, T = 25°C	Chang et al. (2012)

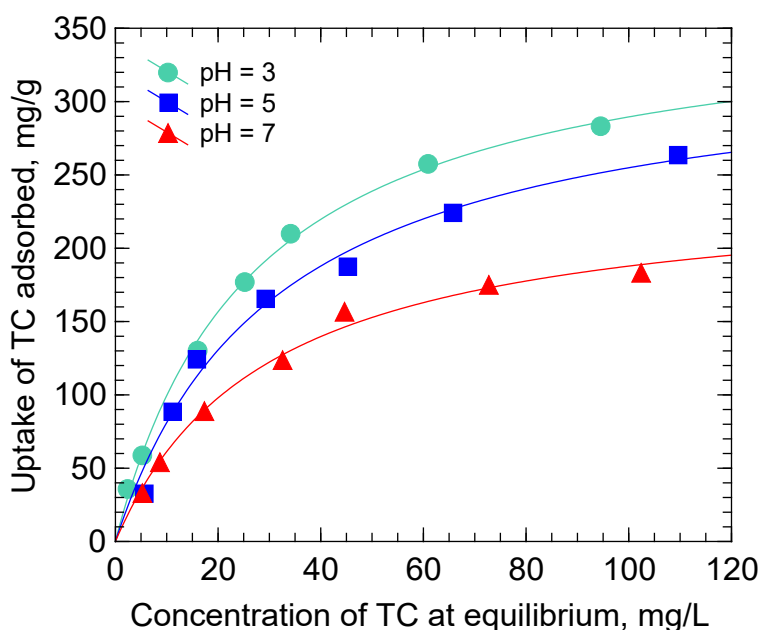


Figure 4.11. Effect of the solution pH on the adsorption isotherms of TC on Bent at $T = 25\text{ }^{\circ}\text{C}$. The lines represent the Langmuir isotherm.

4.3.9 Analysis of cations exchanged during adsorption of TC

This analysis was performed by a two-step procedure described above. The amount of each exchangeable cation (Q_i) and H^+ (Q_{H^+}) adsorbed or desorbed on the clay during the TC adsorption on Bent at pH 3 and 7 are given in Table 4.5. At pH = 3, the Q_i values were negative, indicating that the exchangeable cations were desorbed from the Bent to the solution, and the opposite occurred with the H^+ . Li et al. (2010) noted similar trends for the adsorption of TC on smectite. At pH = 3, the TC^+ and H^+ competed for the same adsorption sites, and this tendency was found by Zhao et al. (2012) for the TC adsorption onto montmorillonite. The total uptake of exchangeable cations and H^+ , $Q_{\text{T,Cat}}$, was $-57.39\text{ cmol}(+)/\text{kg}$, almost the same as the uptake of TC, Q_{TC} , of $57.9\text{ cmol}(+)/\text{kg}$, which is lower than the CEC of Bent ($75.2\text{ cmol}(+)/\text{kg}$). Thus, the adsorption of TC^+ and H^+ on TC was essentially due to the cation exchange of the exchangeable cations. Wang et al. (2010) reported similar results for the ciprofloxacin adsorption on montmorillonite.

Table 4.5. Exchangeable cations and H⁺ concentration at the beginning and the end of the adsorption of TC on Bent and uptake of TC adsorbed on Bent.

Species	B-TC (pH = 3)			B-TC (pH = 7)		
	Q _{TC} = 57.9 cmol(+)/kg			Q _{TC} = 35.18 cmol(+)/kg		
	C _{io} ×10 ⁵ (eq/L)	C _{if} ×10 ⁵ (eq/L)	Q _i (cmol(+)/kg)	C _{io} ×10 ⁵ (eq/L)	C _{if} ×10 ⁵ (eq/L)	Q _i (cmol(+)/kg)
Mg ²⁺	9.93	13.98	-5.35	6.87	1.07	4.66
Ca ²⁺	25.15	41.77	-21.93	16.99	4.89	9.72
K ⁺	8.12	12.10	-5.25	8.52	6.04	2.00
Na ⁺	937.9	1025	-115.1	934.9	1013.9	-63.41
H ⁺	100	31.62	90.27	0.010	0.012	-0.0025
Q _{T,Cat}			-57.39			-47.03
TC	57.50	13.7		53.90	10.1	

At pH = 7, the uptakes of the Mg²⁺, Ca²⁺ and K⁺ cations were positive, confirming that these cations were adsorbed on the surface of Bent. In contrast, the uptakes of Na⁺ and H⁺ (Q_{H⁺}) were negative, showing that both cations were desorbed from the Bent surface; however, Q_{H⁺} was insignificant. The value of Q_{T,Cat} was -47.03 cmol(+)/kg, while the uptake of TC adsorbed was 35.18 cmol(+)/kg. According to the speciation diagram (Figure 4.1 (b)), at pH = 7, the species of TC present in water solution were the anionic species TC⁻ (16.6%) and the zwitterionic species TC[±] (83.6%), but the cationic group -NH(CH₃)₂⁺ of TC⁻ and TC[±] can interact with the negatively charged Bent surface (Parolo et al., 2013). Furthermore, at pH > 6, the species of TC present in the solution can be affected by the concentration of Mg²⁺ and Ca²⁺. The reduction of the Mg²⁺ and Ca²⁺ concentrations in the solution can also be ascribed to forming outer-sphere coordination complexes between the TC⁻ and Ca²⁺ and Mg²⁺ such as Ca(TCH)₂ and CaTC(TCH)⁻ (Lambs et al., 1988; Parolo et al., 2013). Other works have described the occurrence of these complexes in the adsorbing mechanism of TC on montmorillonite (Parolo et al., 2013; Zhao et al., 2012).

4.3.10 Variation of the adsorption capacity of bentonite with the ionic strength

The importance of the solution ionic strength (0.01, 0.05, and 0.1 N) in the adsorption of TC on Bent at pH = 7 and 3 and 25°C is illustrated in Figure 4.12. As noticed in Figure 4.12 (a), the mass of TC adsorbed diminishes by incrementing the solution ionic. Incrementing the ionic strength from 0.01 to 0.1 N resulted in an 11.4% reduction of the uptake of TC adsorbed at an equilibrium concentration of 60 mg/L. Additional experiments at a higher ionic strength of 0.5 N revealed that the adsorption diminished 34.74% from 0.01 N to 0.5 N. At pH = 7, the mass of TC adsorbed did not show a significant change by rising the solution ionic strength (See Figure 4.12 (b)).

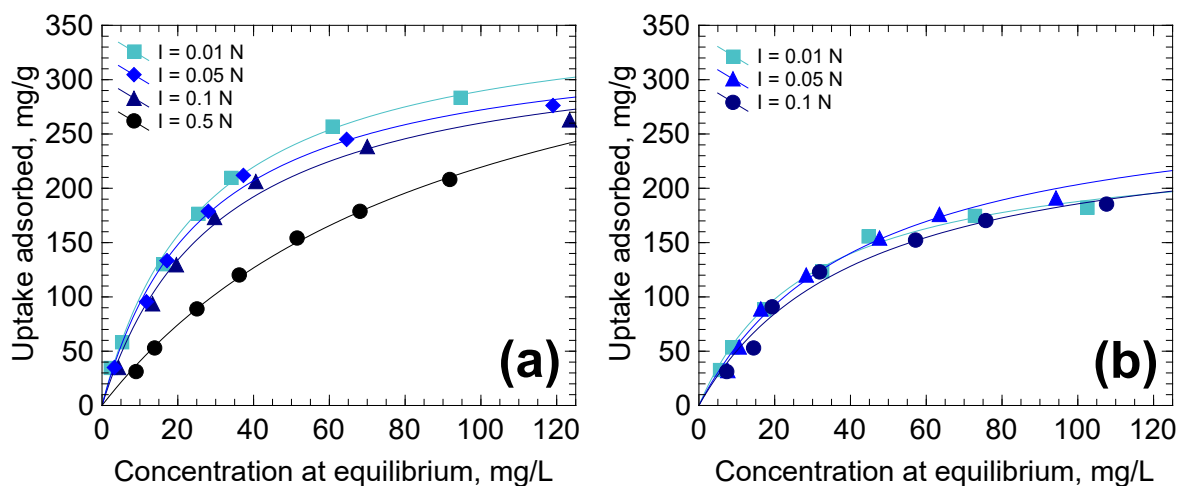


Figure 4.12. Effect of the solution ionic strength on the adsorption isotherms of TC on Bent at T = 25 °C and pH = 3 (a) and pH = 7 (b). The lines represent the Langmuir isotherm.

These studies showed a competition among the TC⁺ species and Na⁺ ions in solution for the available adsorption sites and further confirmed that electrostatic attractions and cation exchange have an essential role in the uptake of adsorbed of TC on Bent at pH = 3. There is no crucial decrease in the mass adsorbed at lower ionic strength since the concentration of Na⁺ cations cannot compete significantly for adsorption sites. In contrast, at a higher Na⁺ concentration, the TC adsorption diminishes. At pH = 7, the Bent adsorption capacity does not depend on the

concentration of Na⁺ ions, confirming the presence of weak electrostatic interactions in the adsorption mechanism of the TC[±] species.

4.3.11 Variation of the bentonite adsorption capacity with temperature

The influence of temperature upon the capacity of Bent for adsorbing TC is presented in Figure 4.13. The Bent adsorption capacity towards TC raises incrementing the temperature; for an equilibrium concentration of 100 mg/L, the uptake adsorbed of TC was 231.8, 187.8, and 164.7 mg/g at 35, 25, and 15 °C, sequentially, indicating a decrease in adsorption capacity of about 1.40 times, while the temperature reduces from 35 to 15°C.

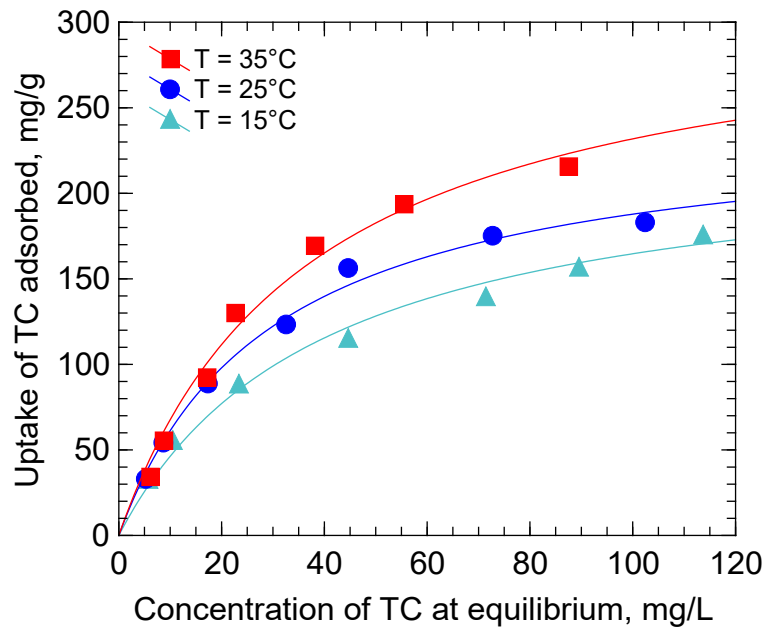


Figure 4.13. Effect of the temperature on the adsorption isotherms of TC on Bent at pH = 7. The lines represent the Langmuir isotherm.

The isosteric heat of adsorption was appraised with the succeeding relationship:

$$(\Delta H_{\text{ads}})_q = \frac{R \ln \left(\frac{C_{e1}}{C_{e2}} \right)}{\frac{1}{T_1} - \frac{1}{T_2}} \quad (4.13)$$

where C_{e1} and C_{e2} denote the concentrations of TC at the temperatures T_1 and T_2 , correspondingly, both at the same mass of TC adsorbed, mg/L; T is the solution temperature, K; R is the ideal gas constant, 8.314 J/mol K; $(\Delta H_{ads})_q$ stands for the isosteric heat of adsorption of TC onto Bent for a given mass of TC adsorbed, J/mol.

For a mass of TC adsorbed of 172.8 mg/g, the TC equilibrium concentrations were $C_{e1} = 38.2$ mg/L ($T_1 = 308.15$ K) and $C_{e2} = 113.4$ mg/L ($T_2 = 288.15$ K). The $(\Delta H_{ads})_q$ was 40.3 kJ/mol, indicating that TC adsorption on Bent is endothermic. Chemical adsorption is characterized by having high heat of adsorption similar to those for chemical reactions (> 40 kJ/mol) (Leyva-Ramos, 2010). The results demonstrate that adsorption of TC on Bent at pH = 7 occurs by physical and chemical interactions.

4.3.12 Desorption of TC adsorbed on bentonite

The reversibility of TC adsorbed on Bent was analyzed by conducting adsorption runs at pH = 3 and subsequently desorbing at pH = 3 and 7. At pH = 3, the experimental data for adsorption equilibrium data are shown in Figure 4.14, denoted by the letter A and followed by the experiment number. Likewise, the experimental data for desorption equilibrium are represented as D3 and D7, where 3 and 7 are related to the desorption pH and preceded by the desorption experiment number.

The adsorption process could be considered reversible when the desorption equilibrium data were on the adsorption isotherm. As shown in Figure 4.14, the desorption equilibrium data for pH = 3 is over the adsorption isotherm at pH = 3. On the other hand, the desorption equilibrium data for pH = 7 were relatively close to the adsorption isotherm (pH of 7).

The desorption percentage, %Des, was computed from the succeeding equation:

$$\%Des = \frac{q_o - q_d}{q_o - q_{d,rev}} \times 100 \% \quad (4.14)$$

where q_o and q_{ed} are the uptakes of TC adsorbed at the start, and the termination of the desorption experiment and the uptake of TC adsorbed at the desorption equilibrium supposing that the adsorption is reversible is denoted as $q_{d,rev}$. The adsorption could

be considered reversible if the %Des was equal to 100%. Contrarily, the adsorption would be irreversible when %Des was less than 100%. The $q_{d,rev}$ was computed by solving the Langmuir isotherm and Equation (4.3) representing the desorption mass balance.

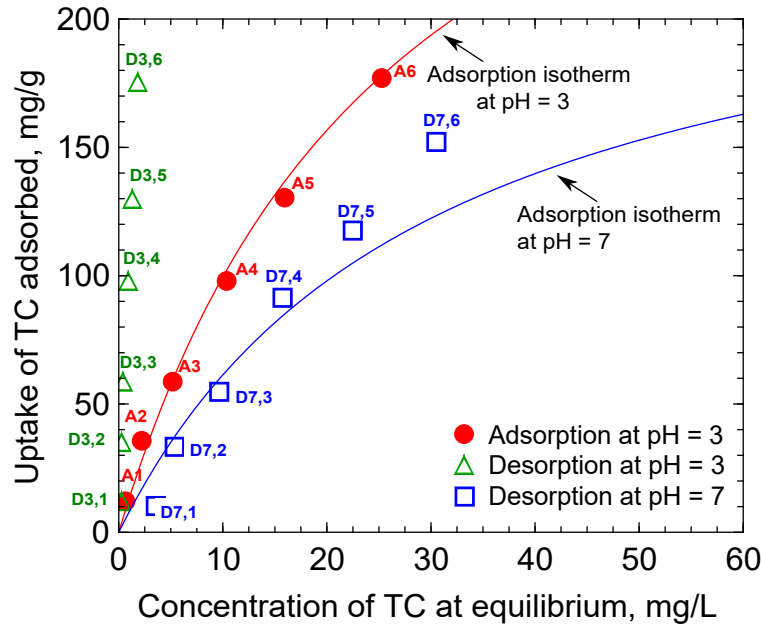


Figure 4.14. Adsorption isotherm of TC on Bent at pH = 3 and T = 25 °C; and desorption isotherm of TC at pH of 3 and 7. The lines represent the Langmuir isotherm.

Table 4.6 lists the q_o , q_d , $q_{d,rev}$ and %Des, and the %Des values vary from 72.0 to 100% and 8.50 to 27.4% for pH of 7 and 3, respectively. At pH = 3, the average %Des was 11.99%, revealing that the adsorption was essentially irreversible and mainly due to chemical adsorption. Moreover, at pH = 7, the adsorption was reversible for concentrations at equilibrium lower than 10 mg/L because the %Des values were very close to 100%. Nevertheless, for concentrations bigger than 10 mg/L, %Des varied between 70 and 90%, indicating that desorption was irreversible. The partial desorption of the TC by raising the solution pH corroborated that the chemical and physical mechanisms were involved in the TC adsorption at pH = 7.

Table 4.6. Desorption percentages of TC from Bent at T = 25 °C.

Exp. No.	q _o (mg/g)	Desorption at pH = 7			Desorption at pH = 3		
		q _d (mg/g)	q _{d,rev} (mg/g)	%Des	q _d (mg/g)	q _{d,rev} (mg/g)	%Des
1	11.98	10.57	11.39	~100.0	11.88	11.62	27.4
2	35.44	33.35	33.56	~100.0	35.33	34.64	10.0
3	58.78	55.10	55.34	~100.0	58.64	56.84	7.1
4	98.11	91.86	91.02	88.1	97.75	94.39	9.7
5	130.6	117.8	115.3	84.0	129.9	122.9	9.3
6	176.97	152.64	143.2	72.0	175.56	160.3	8.5

4.3.13 Adsorption mechanisms of TC on bentonite

The adsorption of TC on Bent depends on the solution pH because of the changes experienced by the chemical groups of the TC molecule and the surface charge of Bent. At pH = 3, where the TC⁺ species predominates, adsorption occurs onto Bent external surface and in the interlaminar space, and it is governed by electrostatic attractions, followed by the cationic exchange between interlaminar cations, particularly Ca²⁺, and the TC⁺ species (Figure 4.15 (a)). Also, there is interaction through hydrogen bonding between the polar groups of the adsorbed TC molecule and the hydrated water of the exchangeable cations, which were not released from the interlayer space of Bent. At pH = 7, the coexisting species TC[±] and TC⁻ can be adsorbed by physical and chemical mechanisms. In the first mechanism, adsorption occurs onto the Bent external surface and in the interlaminar space and is promoted by weak physical interactions between the -NH(CH₃)₂⁺ group of the TC[±] species and the negative charge of Bent. Herein, TC[±] orients as closely as possible to the cationic sites of Bent. The second mechanism involves forming outer-sphere coordination complexes between the TC⁻ species and the internal sphere of hydration of the interlaminar Ca²⁺ ion. At this point, the ionization of the phenolic-diketone group causes a high electron density, allowing that the positive charge of the Ca²⁺ ions can be partially shared with the anionic TC⁻ species. Through electronic delocalization on the chelating ring, the coordination complex stabilizes the electronic density, avoiding the repulsive forces and

allowing the adsorption via forming cationic bonding between the TC⁻ species and the cationic sites of Bent Figure 4.15 (b).

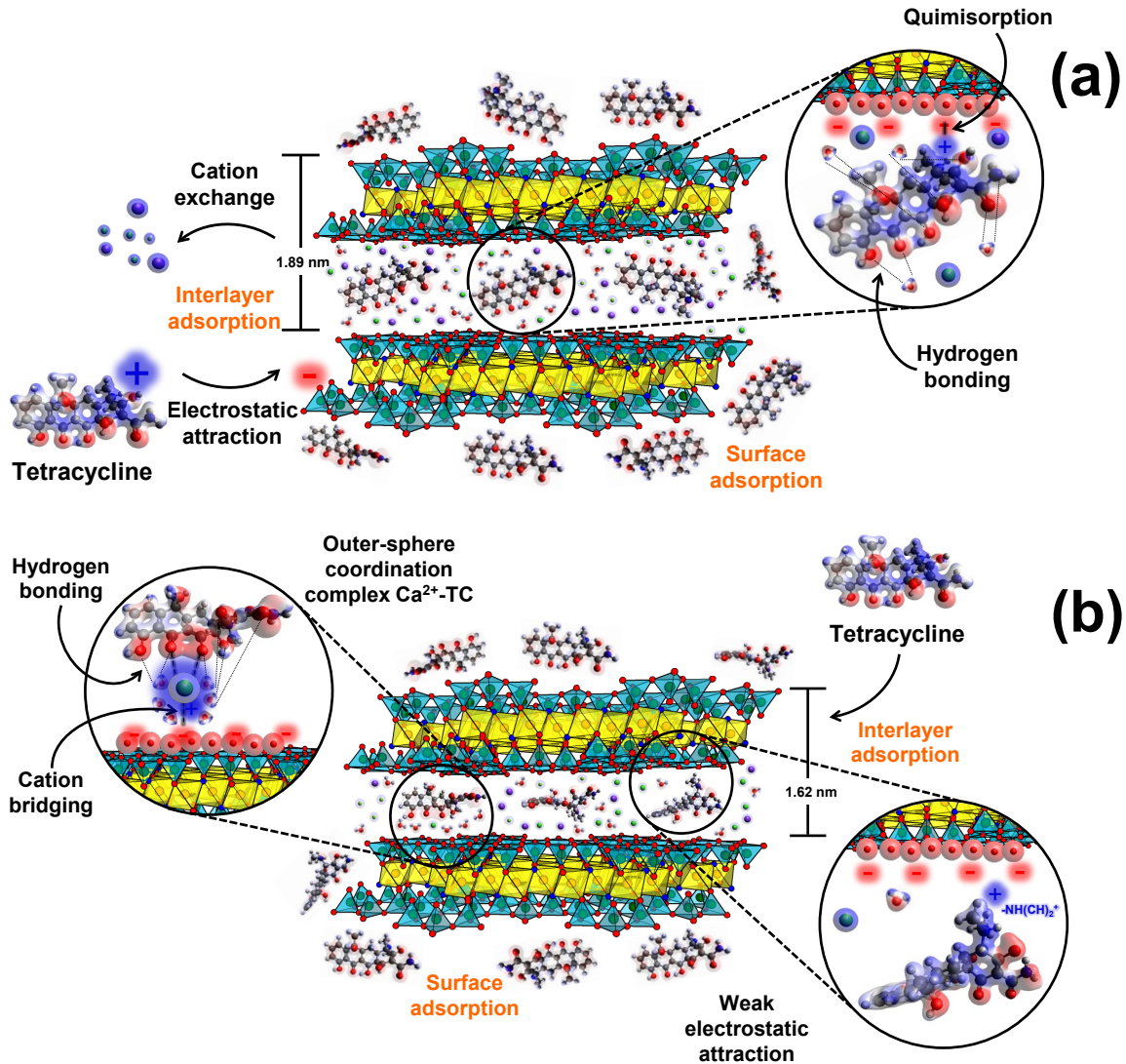


Figure 4.15. Adsorption mechanisms of TC on Bent at pH = 3 (a) and pH = 7 (b).

4.4 Conclusions

The capacity of the raw clays for adsorbing TC from water is strongly influenced by its structural arrangement, swelling capability, nature of interlayer cations, and the TC molecular size. Bent showed the highest adsorption capacity, while the uptakes of TC adsorbed on Sep, Hal, Verm, Kaol, and Phlo fluctuated from 10 to 60 mg/g. The

uptake of TC adsorbed on Bent was significantly influenced by the solution pH. At $T = 25^{\circ}\text{C}$ and pH of 3, the maximum mass adsorbed of TC was 283.5 mg/g, where TC^+ is the dominant species. The effect of the ionic strength revealed the presence of electrostatic and non-electrostatic mechanisms. The TC adsorption on Bent is endothermic, and the desorption of TC is partially reversible, proving that physical and chemical mechanisms can explain the TC adsorption.

The characterization of TC adsorbed on Bent revealed that adsorption occurred onto both the external surface and in the interlayer space of Bent. At $\text{pH} = 3$, the adsorption of TC^+ is governed by cation exchange and electrostatic attractions, and basal space (001) was 1.89 nm, indicating a parallel and inclined orientation of the TC^+ species in the interlayer space. Otherwise, at $\text{pH} = 7$, the adsorption of TC^{\pm} species was carried out by weak electrostatic attractions, whereas the TC^- species was adsorbed by outer-sphere coordination complexes of the type $\text{Ca}^{2+}\text{-TC}$. Likewise, the basal reflection (001) was 1.62 nm, confirming the partial intercalation of the TC^{\pm} and TC^- species within the interlaminar space of Bent.

REFERENCES

- Aboussabek, A., Aziam, R., El Qdhy, S., Boukarma, L., Zerbet, M., Sinan, F., & Chiban, M. (2024). Synthesis and characterization of hybrid clay@Fe₃O₄ for acid blue113 sequestration using a fixed-bed adsorption column. *International Journal of Environmental Science and Technology*, 21(4), 4171–4186. <https://doi.org/10.1007/s13762-023-05287-9>
- Abuzneid, Y. S., Alzeerelhouseini, H. I. A., Rabi, D., Hilail, I., Rjoob, H., Rabee, A., Amro, N., Qafisheh, Q., & Kharraz, M. (2022). Carbamazepine induced stevens-johnson syndrome that developed into toxic epidermal necrolysis: Review of the literature. *Case Reports in Dermatological Medicine*, 2022, 1–4. <https://doi.org/10.1155/2022/6128688>
- Ahmed, M. J., & Hameed, B. H. (2018). Removal of emerging pharmaceutical contaminants by adsorption in a fixed-bed column: A review. *Ecotoxicology and Environmental Safety*, 149, 257–266. <https://doi.org/10.1016/j.ecoenv.2017.12.012>
- Ahmed, S. F., Mofijur, M., Nuzhat, S., Chowdhury, A. T., Rafa, N., Uddin, Md. A., Inayat, A., Mahlia, T. M. I., Ong, H. C., Chia, W. Y., & Show, P. L. (2021). Recent developments in physical, biological, chemical, and hybrid treatment techniques for removing emerging contaminants from wastewater. *Journal of Hazardous Materials*, 416, 125912. <https://doi.org/10.1016/j.jhazmat.2021.125912>
- Ahuja, S. (2021). Current status of pharmaceutical contamination in water. In: S. Ahuja (Ed.), *Handbook of Water Purity and Quality* (pp. 255–270). <https://doi.org/10.1016/B978-0-12-821057-4.00008-2>
- Alabarse, F. G., Conceição, R. V., Balzaretti, N. M., Schenato, F., & Xavier, A. M. (2011). In-situ FTIR analyses of bentonite under high-pressure. *Applied Clay Science*, 51(1–2), 202–208. <https://doi.org/10.1016/j.clay.2010.11.017>
- Alegre, C., Sebastián, D., & Lázaro, M. J. (2019). Carbon xerogels electrochemical oxidation and correlation with their physico-chemical properties. *Carbon*, 144, 382–394. <https://doi.org/10.1016/j.carbon.2018.12.065>

- Ali, S. N. F., El-Shafey, E. I., Al-Busafi, S., & Al-Lawati, H. A. J. (2019). Adsorption of chlorpheniramine and ibuprofen on surface functionalized activated carbons from deionized water and spiked hospital wastewater. *Journal of Environmental Chemical Engineering*, 7(1), 102860. <https://doi.org/10.1016/j.jece.2018.102860>
- Allahkarami, E., Dehghan Monfared, A., Silva, L. F. O., & Dotto, G. L. (2022). Application of Pb–Fe spinel-activated carbon for phenol removal from aqueous solutions: Fixed-bed adsorption studies. *Environmental Science and Pollution Research*, 30(9), 23870–23886. <https://doi.org/10.1007/s11356-022-23891-z>
- Al-rimawi, F., Daana, M., Khamis, M., Karaman, R., Khoury, H., & Qurie, M. (2019). Removal of selected pharmaceuticals from aqueous solutions using natural jordanian zeolite. *Arabian Journal for Science and Engineering*, 44(1), 209–215. <https://doi.org/10.1007/s13369-018-3406-9>
- Amarasiri, M., Sano, D., & Suzuki, S. (2020). Understanding human health risks caused by antibiotic resistant bacteria (ARB) and antibiotic resistance genes (ARG) in water environments: Current knowledge and questions to be answered. *Critical Reviews in Environmental Science and Technology*, 50(19), 2016–2059. <https://doi.org/10.1080/10643389.2019.1692611>
- Andrade, C. (2018). Major congenital malformations associated with exposure to antiepileptic drugs during pregnancy. *Journal of Clinical Psychopharmacology*, 79(4). <https://doi.org/10.4088/JCP.18f12449>
- Anim, A. K., Thompson, K., Duodu, G. O., Tscharke, B., Birch, G., Goonetilleke, A., Ayoko, G. A., & Mueller, J. F. (2020). Pharmaceuticals, personal care products, food additive and pesticides in surface waters from three Australian east coast estuaries (Sydney, Yarra and Brisbane). *Marine Pollution Bulletin*, 153, 111014. <https://doi.org/10.1016/j.marpolbul.2020.111014>
- Antonelli, R., Malpass, G. R. P., da Silva, M. G. C., & Vieira, M. G. A. (2020). Adsorption of ciprofloxacin onto thermally modified bentonite clay: Experimental design, characterization, and adsorbent regeneration. *Journal of Environmental Chemical Engineering*, 8(6), 104553. <https://doi.org/10.1016/j.jece.2020.104553>

- Ao, S., Okoye, P. U., Rokhum, S. L., & Khanday, W. A. (2024). Sheet-like graphitized glucose-based mesoporous carbon for aqueous adsorption of tetracycline antibiotic. *Diamond and Related Materials*, 141, 110718. <https://doi.org/10.1016/j.diamond.2023.110718>
- Ao, X., Sun, W., Li, S., Yang, C., Li, C., & Lu, Z. (2019). Degradation of tetracycline by medium pressure UV-activated peroxymonosulfate process: Influencing factors, degradation pathways, and toxicity evaluation. *Chemical Engineering Journal*, 361, 1053–1062. <https://doi.org/10.1016/j.cej.2018.12.133>
- Apiratikul, R., & Chu, K. H. (2021). Improved fixed bed models for correlating asymmetric adsorption breakthrough curves. *Journal of Water Process Engineering*, 40, 101810. <https://doi.org/10.1016/j.jwpe.2020.101810>
- Appelo, C. A. J., & Wersin, P. (2007). Multicomponent diffusion modeling in clay systems with application to the diffusion of tritium, iodide, and sodium in opalinus clay. *Environmental Science and Technology*, 41(14), 5002–5007. <https://doi.org/10.1021/es0629256>
- Arenillas, A., & Fernández, R. (2022). Geles y espumas de carbono. *Tendencias Actuales en los Materiales de Carbono*, 1–6.
- Arenillas, A., Menéndez, J. A., Reichenauer, G., Celzard, A., Fierro, V., Maldonado Hodar, F. J., Bailón-García, E., & Job, N. (2019). *Organic and carbon gels. From laboratory synthesis to applications*. Springer International Publishing.
- Aryee, A. A., Mpatani, F. M., Dovi, E., Li, Q., Wang, J., Han, R., Li, Z., & Qu, L. (2021). A novel antibacterial biocomposite based on magnetic peanut husk for the removal of trimethoprim in solution: Adsorption and mechanism study. *Journal of Cleaner Production*, 329, 129722. <https://doi.org/10.1016/j.jclepro.2021.129722>
- Avila, P., Montes, M., & Miró, E. E. (2005). Monolithic reactors for environmental applications. *Chemical Engineering Journal*, 109(1–3), 11–36. <https://doi.org/10.1016/j.cej.2005.02.025>
- Azizi-Lalabadi, M., & Pirsahab, M. (2021). Investigation of steroid hormone residues in fish: A systematic review. *Process Safety and Environmental Protection*, 152, 14–24. <https://doi.org/10.1016/j.psep.2021.05.020>

- Babić, B. M., Milonjić, S. K., Polovina, M. J., & Kaludierović, B. V. (1999). Point of zero charge and intrinsic equilibrium constants of activated carbon cloth. *Carbon*, 37(3), 477–481. [https://doi.org/10.1016/S0008-6223\(98\)00216-4](https://doi.org/10.1016/S0008-6223(98)00216-4)
- Babić, B., Kaluđerović, B., Vračar, Lj., & Krstajić, N. (2004). Characterization of carbon cryogel synthesized by sol–gel polycondensation and freeze-drying. *Carbon*, 42(12–13), 2617–2624. <https://doi.org/10.1016/j.carbon.2004.05.046>
- Bagnis, S., Boxall, A., Gachanja, A., Fitzsimons, M., Murigi, M., Snape, J., Tappin, A., Wilkinson, J., & Comber, S. (2020). Characterization of the Nairobi River catchment impact zone and occurrence of pharmaceuticals: Implications for an impact zone inclusive environmental risk assessment. *Science of the Total Environment*, 703, 134925. <https://doi.org/10.1016/j.scitotenv.2019.134925>
- Bailón-García, E., Carrasco-Marín, F., Pérez-Cadenas, A. F., & Maldonado-Hódar, F. J. (2014). Microspheres of carbon xerogel: An alternative Pt-support for the selective hydrogenation of citral. *Applied Catalysis A: General*, 482, 318–326. <https://doi.org/10.1016/j.apcata.2014.06.011>
- Bailón-García, E., Drwal, E., Grzybek, T., Henriques, C., & Ribeiro, M. F. (2020). Catalysts based on carbon xerogels with high catalytic activity for the reduction of NO_x at low temperatures. *Catalysis Today*, 356, 301–311. <https://doi.org/10.1016/j.cattod.2020.03.004>
- Bakos, L. P., Mensah, J., László, K., Igricz, T., & Szilágyi, I. M. (2018). Preparation and characterization of a nitrogen-doped mesoporous carbon aerogel and its polymer precursor. *Journal of Thermal Analysis and Calorimetry*, 134(2), 933–939. <https://doi.org/10.1007/s10973-018-7318-4>
- Barrett, E. P., Joyner, L. G., & Halenda, P. P. (1951). The determination of pore volume and area distributions in porous substances. I. Computations from nitrogen isotherms. *Journal of the American Chemical Society*, 73(1), 373–380. <https://doi.org/10.1021/ja01145a126>
- Barry, D. W., & Pattishall, K. H. (1983). Trimethoprim alone: Clinical uses. In: George H. Hitchings (Ed.), *Inhibition of Folate Metabolism in Chemotherapy. The origins*

- and Uses of Co-trimoxazole* (pp. 261–291). https://doi.org/10.1007/978-3-642-81890-5_13
- Bavasso, I., Montanaro, D., & Petrucci, E. (2022). Ozone-based electrochemical advanced oxidation processes. *Current Opinion in Electrochemistry*, 34, 101017. <https://doi.org/10.1016/j.coelec.2022.101017>
- Bazarin, G., Módenes, A. N., Espinoza-Quiñones, F. R., Borba, C. E., Trigueros, D. E. G., & Dall'Oglio, I. C. (2024). High removal performance of reactive blue 5G dye from industrial dyeing wastewater using biochar in a fixed-bed adsorption system: Approaches and insights based on modeling, isotherms, and thermodynamics study. *Journal of Environmental Chemical Engineering*, 12(1), 111761. <https://doi.org/10.1016/j.jece.2023.111761>
- Beckwée, E. J., Wittevrongel, G. R., & Claessens, B. (2022). Comparing column dynamics in the liquid and vapor phase adsorption of biobutanol on an activated carbon monolith. *Adsorption*, 28(5–6), 209–218. <https://doi.org/10.1007/s10450-022-00362-y>
- Bedoui, K., Bekri-Abbes, I., & Srasra, E. (2008). Removal of cadmium (II) from aqueous solution using pure smectite and Lewatite S 100: The effect of time and metal concentration. *Desalination*, 223(1–3), 269–273. <https://doi.org/10.1016/J.DESAL.2007.02.078>
- Bekçi, Z., Seki, Y., & Yurdakoç, M. (2006). Equilibrium studies for trimethoprim adsorption on montmorillonite KSF. *Journal of Hazardous Materials*, 133(1–3), 233–242. <https://doi.org/10.1016/j.jhazmat.2005.10.029>
- Berges, J., Moles, S., Ormad, M. P., Mosteo, R., & Gómez, J. (2021). Antibiotics removal from aquatic environments: Adsorption of enrofloxacin, trimethoprim, sulfadiazine, and amoxicillin on vegetal powdered activated carbon. *Environmental Science and Pollution Research*, 28(7), 8442–8452. <https://doi.org/10.1007/s11356-020-10972-0>
- Berninger, J. P., Du, B., Connors, K. A., Eytcheson, S. A., Kolkmeier, M. A., Prosser, K. N., Valenti, T. W., Chambliss, C. K., & Brooks, B. W. (2011). Effects of the

- antihistamine diphenhydramine on selected aquatic organisms. *Environmental Toxicology and Chemistry*, 30(9), 2065–2072. <https://doi.org/10.1002/etc.590>
- Bexfield, L. M., Toccalino, P. L., Belitz, K., Foreman, W. T., & Furlong, E. T. (2019). Hormones and pharmaceuticals in groundwater used as a source of drinking water across the united states. *Environmental Science and Technology*, 53(6), 2950–2960. <https://doi.org/10.1021/acs.est.8b05592>
- Biel-Maeso, M., Baena-Nogueras, R. M., Corada-Fernández, C., & Lara-Martín, P. A. (2018). Occurrence, distribution and environmental risk of pharmaceutically active compounds (PhACs) in coastal and ocean waters from the Gulf of Cadiz (SW Spain). *Science of the Total Environment*, 612, 649–659. <https://doi.org/10.1016/j.scitotenv.2017.08.279>
- Boehm, H. P. (1966). Chemical identification of surface groups. *Advances in Catalysis*, 16(C), 179–274. [https://doi.org/10.1016/S0360-0564\(08\)60354-5](https://doi.org/10.1016/S0360-0564(08)60354-5)
- Borden, D. (2001). Baseline studies of the clay minerals society source clays: Cation exchange capacity measurements by the ammonia-electrode method. *Clays and Clay Minerals*, 49(5), 444–445. <https://doi.org/10.1346/CCMN.2001.0490510>
- Bosco, S. M. D., Jimenez, R. S., Vignado, C., Fontana, J., Geraldo, B., Figueiredo, F. C. A., Mandelli, D., & Carvalho, W. A. (2006). Removal of Mn(II) and Cd(II) from wastewaters by natural and modified clays. *Adsorption*, 12(2), 133–146. <https://doi.org/10.1007/s10450-006-0375-1>
- Brain, R. A., Johnson, D. J., Richards, S. M., Sanderson, H., Sibley, P. K., & Solomon, K. R. (2004). Effects of 25 pharmaceutical compounds to Lemna gibba using a seven-day static-renewal test. *Environmental Toxicology and Chemistry*, 23(2), 371. <https://doi.org/10.1897/02-576>
- Brigatti, M. F., Galán, E., & Theng, B. K. G. (2013). Structure and mineralogy of clay minerals. In: F. Bergaya & G. Lagaly (Eds.), *Handbook of Clay Science* ed. 5 (pp. 21–81). <https://doi.org/10.1016/B978-0-08-098258-8.00002-X>
- Brogden, R. N., Carmine, A. A., Heel, R. C., Speight, T. M., & Avery, G. S. (1982). Trimethoprim: A review of its antibacterial activity, pharmacokinetics and

- therapeutic use in urinary tract infections. *Drugs*, 23(6), 405–430. <https://doi.org/10.2165/00003495-198223060-00001>
- Brunauer, S., Emmett, P. H., & Teller, E. (1938). Adsorption of gases in multimolecular layers. *Journal of the American Chemical Society*, 60(2), 309–319. <https://doi.org/10.1021/ja01269a023>
- Bui, T. X., Pham, V. H., Le, S. T., & Choi, H. (2013). Adsorption of pharmaceuticals onto trimethylsilylated mesoporous SBA-15. *Journal of Hazardous Materials*, 254–255, 345–353. <https://doi.org/10.1016/j.jhazmat.2013.04.003>
- Çalışkan Salihi, E., Cantürk Talman, R. Y., & Göktürk, S. (2023). Preparation and characterization of surfactant loaded clays as drug adsorbents. *Journal of Dispersions Science and Technology*, 44(1), 165–173. <https://doi.org/10.1080/01932691.2021.1931289>
- Çalışkan Salihi, E., Cantürk Talman, R. Y., & Göktürk, S. (2023). Preparation and characterization of surfactant loaded clays as drug adsorbents. *Journal of Dispersions Science and Technology*, 44(1), 165–173. <https://doi.org/10.1080/01932691.2021.1931289>
- Cantarella, M., Carroccio, S. C., Dattilo, S., Avolio, R., Castaldo, R., Puglisi, C., & Privitera, V. (2019). Molecularly imprinted polymer for selective adsorption of diclofenac from contaminated water. *Chemical Engineering Journal*, 367, 180–188. <https://doi.org/10.1016/j.cej.2019.02.146>
- Carabineiro, S. A. C., Thavorn-amornsri, T., Pereira, M. F. R., Serp, P., & Figueiredo, J. L. (2012). Comparison between activated carbon, carbon xerogel and carbon nanotubes for the adsorption of the antibiotic ciprofloxacin. *Catalysis Today*, 186(1), 29–34. <https://doi.org/10.1016/j.cattod.2011.08.020>
- Carmland, M., Jensen, T. S., & Finnerup, N. B. (2022). Anticonvulsants in the management of chronic pain. In: M. E. Lynch, K. D. Craig & P. W. Peng (Eds.), *Clinical Pain Management: A Practical Guide* ed. 2 (pp. 181–187). Wiley. <https://doi.org/10.1002/9781119701170.ch17>
- Carrales-Alvarado, D. H., Leyva-Ramos, R., Bailón-García, E., Carrasco-Marín, F., & Villela-Martinez, D. E. (2022). Synthesis, characterization, and application of

- pristine and clay-templated carbon xerogel microspheres for removing diclofenac and heavy metals from water solution. *Environmental Science and Pollution Research*, 30(12), 34684–34697. <https://doi.org/10.1007/s11356-022-24615-z>
- Carrales-Alvarado, D. H., Leyva-Ramos, R., Martínez-Costa, J. I., & Ocampo-Pérez, R. (2018). Competitive adsorption of dimetridazole and metronidazole antibiotics on carbon materials from aqueous solution. *Water, Air, & Soil Pollution*, 229(4), 108–123. <https://doi.org/10.1007/s11270-018-3730-4>
- Carrales-Alvarado, D. H., Leyva-Ramos, R., Rodríguez-Ramos, I., Mendoza-Mendoza, E., & Moral-Rodríguez, A. E. (2020). Adsorption capacity of different types of carbon nanotubes towards metronidazole and dimetridazole antibiotics from aqueous solutions: effect of morphology and surface chemistry. *Environmental Science and Pollution Research*, 27(14), 17123–17137. <https://doi.org/10.1007/s11356-020-08110-x>
- Carrales-Alvarado, D. H., Rodríguez-Ramos, I., Leyva-Ramos, R., Mendoza-Mendoza, E., & Villela-Martínez, D. E. (2020). Effect of surface area and physical–chemical properties of graphite and graphene-based materials on their adsorption capacity towards metronidazole and trimethoprim antibiotics in aqueous solution. *Chemical Engineering Journal*, 402, 126155. <https://doi.org/10.1016/j.cej.2020.126155>
- Castelo-Quibén, J., Bailón-García, E., Pérez-Fernández, F. J., Carrasco-Marín, F., & Pérez-Cadenas, A. F. (2019). Mesoporous carbon nanospheres with improved conductivity for electro-catalytic reduction of O₂ and CO₂. *Carbon*, 155, 88–99. <https://doi.org/10.1016/j.carbon.2019.08.007>
- Cavazos-Cuello, L. A., Dávila-Guzmán, N. E., Botello-González, J., Ocampo-Pérez, R., Leura-Vicencio, A. K., & Salazar Rábago, J. J. (2023). Mechanistic evaluation in the removal of chlorpheniramine and ciprofloxacin on activated carbons. *Environmental Research*, 238, 117196. <https://doi.org/10.1016/j.envres.2023.117196>
- Čelić, M., Gros, M., Farré, M., Barceló, D., & Petrović, M. (2019). Pharmaceuticals as chemical markers of wastewater contamination in the vulnerable area of the Ebro

- Delta (Spain). *Science of the Total Environment*, 652, 952–963. <https://doi.org/10.1016/j.scitotenv.2018.10.290>
- Cervini, P., Machado, L. C. M., Ferreira, A. P. G., Ambrozini, B., & Cavalheiro, yder T. G. (2016). Thermal decomposition of tetracycline and chlortetracycline. *Journal of Analytical and Applied Pyrolysis*, 118, 317–324. <https://doi.org/10.1016/j.jaap.2016.02.015>
- Chaari, I., Fakhfakh, E., Medhioub, M., & Jamoussi, F. (2019). Comparative study on adsorption of cationic and anionic dyes by smectite rich natural clays. *Journal of Molecular Structure*, 1179, 672–677. <https://doi.org/10.1016/j.molstruc.2018.11.039>
- Chai, J.-B., Au, P.-I., Mubarak, N. M., Khalid, M., Ng, W. P.-Q., Jagadish, P., Walvekar, R., & Abdullah, E. C. (2020). Adsorption of heavy metal from industrial wastewater onto low-cost Malaysian kaolin clay-based adsorbent. *Environmental Science and Pollution Research*, 27(12), 13949–13962. <https://doi.org/10.1007/s11356-020-07755-y>
- Challis, J. K., Cuscito, L. D., Joudan, S., Luong, K. H., Knapp, C. W., Hanson, M. L., & Wong, C. S. (2018). Inputs, source apportionment, and transboundary transport of pesticides and other polar organic contaminants along the lower Red River, Manitoba, Canada. *Science of the Total Environment*, 635, 803–816. <https://doi.org/10.1016/j.scitotenv.2018.04.128>
- Chang, P.-H., Jean, J.-S., Jiang, W.-T., & Li, Z. (2009). Mechanism of tetracycline sorption on rectorite. *Colloids and Surfaces A: Physicochemical and Engineering Aspects*, 339(1–3), 94–99. <https://doi.org/10.1016/j.colsurfa.2009.02.002>
- Chang, P.-H., Li, Z., Jean, J.-S., Jiang, W.-T., Wang, C.-J., & Lin, K.-H. (2012). Adsorption of tetracycline on 2:1 layered non-swelling clay mineral illite. *Applied Clay Science*, 67–68, 158–163. <https://doi.org/10.1016/j.clay.2011.11.004>
- Chang, Y. S., Au, P. I., Mubarak, N. M., Khalid, M., Jagadish, P., Walvekar, R., & Abdullah, E. C. (2020). Adsorption of Cu(II) and Ni(II) ions from wastewater onto bentonite and bentonite/GO composite. *Environmental Science and Pollution Research*, 27(26), 33270–33296. <https://doi.org/10.1007/s11356-020-09423-7>

- Chaparro-Garnica, C. Y., Bailón-García, E., Davó-Quiñonero, A., Da Costa, P., Lozano-Castelló, D., & Bueno-López, A. (2021a). High performance tunable catalysts prepared by using 3D printing. *Materials*, 14(17), 5017. <https://doi.org/10.3390/ma14175017>
- Chaparro-Garnica, C. Y., Bailón-García, E., Davó-Quiñonero, A., Lozano-Castelló, D., & Bueno-López, A. (2022). Sponge-like carbon monoliths: Porosity control of 3D-printed carbon supports and its influence on the catalytic performance. *Chemical Engineering Journal*, 432, 134218. <https://doi.org/10.1016/j.cej.2021.134218>
- Chaparro-Garnica, C. Y., Bailón-García, E., Lozano-Castelló, D., & Bueno-López, A. (2021b). Design and fabrication of integral carbon monoliths combining 3D printing and sol-gel polymerization: Effects of the channel morphology on the CO-PROX reaction. *Catalysis Science & Technology*, 11(19), 6490–6497. <https://doi.org/10.1039/D1CY01104A>
- Chaturvedi, P., Shukla, P., Giri, B. S., Chowdhary, P., Chandra, R., Gupta, P., & Pandey, A. (2021). Prevalence and hazardous impact of pharmaceutical and personal care products and antibiotics in environment: A review on emerging contaminants. *Environmental Research*, 194, 110664. <https://doi.org/10.1016/j.envres.2020.110664>
- Chaubey, A. K., Patel, M., Pittman, C. U., & Mohan, D. (2023). Acetaminophen and trimethoprim batch and fixed-bed sorption on MgO/Al₂O₃-modified rice husk biochar. *Colloids and Surfaces A: Physicochemical and Engineering Aspects*, 677, 132263. <https://doi.org/10.1016/j.colsurfa.2023.132263>
- Chen, W.-H., Huang, J.-R., Lin, C.-H., & Huang, C.-P. (2020). Catalytic degradation of chlorpheniramine over GO-Fe₃O₄ in the presence of H₂O₂ in water: The synergistic effect of adsorption. *Science of the Total Environment*, 736, 139468. <https://doi.org/10.1016/j.scitotenv.2020.139468>
- Cheng, G., Li, X., Li, X., Chen, J., Liu, Y., Zhao, G., & Zhu, G. (2022). Surface imprinted polymer on a metal-organic framework for rapid and highly selective adsorption of sulfamethoxazole in environmental samples. *Journal of Hazardous Materials*, 423, 127087. <https://doi.org/10.1016/j.jhazmat.2021.127087>

- Chernova, E., Zhakovskaya, Z., & Berezina, N. (2021). Occurrence of pharmaceuticals in the Eastern Gulf of Finland (Russia). *Environmental Science and Pollution Research*, 28(48), 68871–68884. <https://doi.org/10.1007/s11356-021-15250-1>
- Chopra, I., & Roberts, M. (2001). Tetracycline antibiotics: Mode of action, applications, molecular biology, and epidemiology of bacterial resistance. *Microbiology and Molecular Biology Reviews*, 65(2), 232–260. <https://doi.org/10.1128/MMBR.65.2.232-260.2001>
- Cooney, D. O. (1998). *Adsorption design for wastewater treatment*. CRC Press
- Crain, F. T., & Gottlieb, S. (1935). A study of the mechanism of the effect of chlorine on the biochemical oxygen demand. *Transactions of the Kansas Academy of Science (1903-)*, 38, 145. <https://doi.org/10.2307/3624825>
- Cunningham, V. L., Perino, C., D'Aco, V. J., Hartmann, A., & Bechter, R. (2010). Human health risk assessment of carbamazepine in surface waters of North America and Europe. *Regulatory Toxicology and Pharmacology*, 56(3), 343–351. <https://doi.org/10.1016/j.yrtph.2009.10.006>
- da Cunha, R., do Carmo Batista, W. V. F., de Oliveira, H. L., dos Santos, A. C., dos Reis, P. M., Borges, K. B., Martelli, P. B., Furtado, C. A., & de Fátima Gorgulho, H. (2021). Carbon Xerogel/TiO₂ composites as photocatalysts for acetaminophen degradation. *Journal of Photochemistry and Photobiology A: Chemistry*, 412, 113248. <https://doi.org/10.1016/j.jphotochem.2021.113248>
- da Silva Santos, N., Oliveira, R., Lisboa, C. A., Mona e Pinto, J., Sousa-Moura, D., Camargo, N. S., Perillo, V., Oliveira, M., Grisolia, C. K., & Domingues, I. (2018). Chronic effects of carbamazepine on zebrafish: Behavioral, reproductive and biochemical endpoints. *Ecotoxicology and Environmental Safety*, 164, 297–304. <https://doi.org/10.1016/j.ecoenv.2018.08.015>
- Dai, J., Meng, X., Zhang, Y., & Huang, Y. (2020). Effects of modification and magnetization of rice straw derived biochar on adsorption of tetracycline from water. *Bioresource Technology*, 311, 123455. <https://doi.org/10.1016/j.biortech.2020.123455>

- Dargahi, A., Moradi, M., Marafat, R., Vosoughi, M., Mokhtari, S. A., Hasani, K., & Asl, S. M. (2021). Applications of advanced oxidation processes (electro-Fenton and sono-electro-Fenton) for degradation of diazinon insecticide from aqueous solutions: optimization and modeling using RSM-CCD, influencing factors, evaluation of toxicity, and degradation pathway. *Biomass Conversion and Biorefinery*, 13, 10615–10632. <https://doi.org/10.1007/s13399-021-01753-x>
- De Oliveira, T., Fernandez, E., Fougère, L., Destandau, E., Boussafir, M., Sohmiya, M., Sugahara, Y., & Guégan, R. (2018). Competitive association of antibiotics with a clay mineral and organoclay derivatives as a control of their lifetimes in the environment. *ACS Omega*, 3(11), 15332–15342. <https://doi.org/10.1021/acsomega.8b02049>
- De Oliveira, T., Guégan, R., Thiebault, T., Milbeau, C. Le, Muller, F., Teixeira, V., Giovanela, M., & Boussafir, M. (2017). Adsorption of diclofenac onto organoclays: Effects of surfactant and environmental (pH and temperature) conditions. *Journal of Hazardous Materials*, 323, 558–566. <https://doi.org/10.1016/j.jhazmat.2016.05.001>
- de Paiva, L. B., Morales, A. R., & Valenzuela Díaz, F. R. (2008). Organoclays: properties, preparation and applications. *Applied Clay Science*, 42(1–2), 8–24. <https://doi.org/10.1016/j.clay.2008.02.006>
- del Mar Orta, M., Martín, J., Medina-Carrasco, S., Santos, J. L., Aparicio, I., & Alonso, E. (2019). Adsorption of propranolol onto montmorillonite: Kinetic, isotherm and pH studies. *Applied Clay Science*, 173, 107–114. <https://doi.org/10.1016/j.clay.2019.03.015>
- Dhar, A. K., Himu, H. A., Bhattacharjee, M., Mostufa, Md. G., & Parvin, F. (2023). Insights on applications of bentonite clays for the removal of dyes and heavy metals from wastewater: A review. *Environmental Science and Pollution Research*, 30(3), 5440–5474. <https://doi.org/10.1007/s11356-022-24277-x>
- Ding, J., Gao, Q., Cui, B., Zhao, Q., Zhao, G., Qiu, S., Bu, L., & Zhou, S. (2021). Solar-assisted electrooxidation process for enhanced degradation of bisphenol A:

- Performance and mechanism. *Separation and Purification Technology*, 277, 119467. <https://doi.org/10.1016/j.seppur.2021.119467>
- Domínguez, J. M., & Schifter, I. (1992). *Las arcillas: El barro noble*. Fondo de Cultura Económica, México.
- Dwivedi, C. P., Sahu, J. N., Mohanty, C. R., Mohan, B. R., & Meikap, B. C. (2008). Column performance of granular activated carbon packed bed for Pb(II) removal. *Journal of Hazardous Materials*, 156(1–3), 596–603. <https://doi.org/10.1016/j.jhazmat.2007.12.097>
- Ebele, A. J., Oluseyi, T., Drage, D. S., Harrad, S., & Abou-Elwafa Abdallah, M. (2020). Occurrence, seasonal variation and human exposure to pharmaceuticals and personal care products in surface water, groundwater and drinking water in Lagos State, Nigeria. *Emerging Contaminants*, 6, 124–132. <https://doi.org/10.1016/j.emcon.2020.02.004>
- Eckert, M., Suthar, H., & Drillet, J.-F. (2022). Influence of resorcinol to sodium carbonate ratio on carbon xerogel properties for aluminium ion battery. *Materials*, 15(7), 2597. <https://doi.org/10.3390/ma15072597>
- Elgamouz, A., Tijani, N., Shehadi, I., Hasan, K., & Al-Farooq Kawam, M. (2019). Characterization of the firing behaviour of an illite-kaolinite clay mineral and its potential use as membrane support. *Heliyon*, 5(8), e02281. <https://doi.org/10.1016/j.heliyon.2019.e02281>
- Elmouwahidi, A., Bailón-García, E., Pérez-Cadenas, A. F., Celzard, A., Fierro, V., & Carrasco-Marín, F. (2021). Carbon microspheres with tailored texture and surface chemistry as electrode materials for supercapacitors. *ACS Sustainable Chemistry and Engineering*, 9(1), 541–551. <https://doi.org/10.1021/acssuschemeng.0c08024>
- Emmerich, K. (2013). Full characterization of smectites. In: F. Bergaya & G. Lagaly (Eds.), *Handbook of Clay Science* ed. 5 (pp. 381–404). <https://doi.org/10.1016/B978-0-08-098259-5.00015-9>
- Eskenazi, D., Kreit, P., Pirard, J.-P., Job, N., & Compère, P. (2018). Toward a continuous synthesis of porous carbon xerogel beads. *AIChE Journal*, 64(3), 1049–1058. <https://doi.org/10.1002/aic.16056>

- Espinosa-Iglesias, D., Valverde-Sarmiento, C., Pérez-Cadenas, A. F., Bautista-Toledo, M. I., Maldonado-Hódar, F. J., & Carrasco-Marín, F. (2015). Mesoporous carbon-xerogels films obtained by microwave assisted carbonization. *Materials Letters*, 141, 135–137. <https://doi.org/10.1016/j.matlet.2014.11.052>
- Es-sahbany, H., Hsissou, R., El Hachimi, M. L., Allaoui, M., Nkhili, S., & Elyoubi, M. S. (2021). Investigation of the adsorption of heavy metals (Cu, Co, Ni and Pb) in treatment synthetic wastewater using natural clay as a potential adsorbent (Sale-Morocco). *Materials Today Proceedings*, 45, 7290–7298. <https://doi.org/10.1016/j.matpr.2020.12.1100>
- Fairén-Jiménez, D., Carrasco-Marín, F., & Moreno-Castilla, C. (2008). Inter- and intra-primary-particle structure of monolithic carbon aerogels obtained with varying solvents. *Langmuir*, 24(6), 2820–2825. <https://doi.org/10.1021/la703386q>
- Farkas, M. H., Berry, J. O., & Aga, D. S. (2007). Chlortetracycline Detoxification in Maize via Induction of Glutathione S -Transferases after Antibiotic Exposure. *Environmental Science & Technology*, 41(4), 1450–1456. <https://doi.org/10.1021/es061651j>
- Farmer, V. C., & Mortland, M. M. (1966). An infrared study of the co-ordination of pyridine and water to exchangeable cations in montmorillonite and saponite. *Journal of the Chemical Society A: Inorganic, Physical, Theoretical*, 344. <https://doi.org/10.1039/J19660000344>
- Fernández, R., Ruiz, A. I., García-Delgado, C., González-Santamaría, D. E., Antón-Herrero, R., Yunta, F., Poyo, C., Hernández, A., Eymar, E., & Cuevas, J. (2018). Stevensite-based geofilter for the retention of tetracycline from water. *Science of the Total Environment*, 645, 146–155. <https://doi.org/10.1016/j.scitotenv.2018.07.120>
- Fernández-Andrade, K. J., González-Vargas, M. C., Rodríguez-Rico, I. L., Ruiz-Reyes, E., Quiroz-Fernández, L. S., Baquerizo-Crespo, R. J., & Rodríguez-Díaz, J. M. (2022). Evaluation of mass transfer in packed column for competitive adsorption of Tartrazine and brilliant blue FCF: A statistical analysis. *Results in Engineering*, 14, 100449. <https://doi.org/10.1016/j.rineng.2022.100449>

- Flores, F. M., Undabeytia-López, T., Morillo-González, E., & Torres-Sánchez, R. M. (2017). Pyrimethanil adsorption on montmorillonite and organo-montmorillonite. Kinetic and equilibrium study. *Scientific Research Abstracts*, 7, 264. <http://hdl.handle.net/10261/160789>
- França, D. B., Trigueiro, P., Silva Filho, E. C., Fonseca, M. G., & Jaber, M. (2020). Monitoring diclofenac adsorption by organophilic alkyipyridinium bentonites. *Chemosphere*, 242, 125109. <https://doi.org/10.1016/j.chemosphere.2019.125109>
- Furian, A. F., Figuera, M. R., Royes, L. F. F., & Oliveira, M. S. (2022). Recent advances in assessing the effects of mycotoxins using animal models. *Current Opinion in Food Science*, 47, 100874. <https://doi.org/10.1016/j.cofs.2022.100874>
- Furusawa, T., & Smith, J. M. (1973). Fluid-particle and intraparticle mass transport rates in slurries. *Industrial & Engineering Chemistry Fundamentals*, 12(2), 197–203. <https://doi.org/10.1021/i160046a009>
- Gaikwad, M. M., Kakunuri, M., & Sharma, C. S. (2019). Enhanced catalytic graphitization of resorcinol formaldehyde derived carbon xerogel to improve its anodic performance for lithium ion battery. *Materials Today Communications*, 20, 100569. <https://doi.org/10.1016/j.mtcomm.2019.100569>
- Gao, Y., Li, Y., Zhang, L., Huang, H., Hu, J., Shah, S. M., & Su, X. (2012). Adsorption and removal of tetracycline antibiotics from aqueous solution by graphene oxide. *Journal of Colloid and Interface Science*, 368(1), 540–546. <https://doi.org/10.1016/j.jcis.2011.11.015>
- García-Reyes, C. B., Salazar-Rábago, J. J., Polo, M. S., & Ramos, V. C. (2022). Synthesis and use of silica xerogels doped with iron as a photocatalyst to pharmaceuticals degradation in water. *Catalysts*, 12(11), 1341. <https://doi.org/10.3390/catal12111341>
- García-Reyes, C. B., Salazar-Rábago, J. J., Sánchez-Polo, M., Loredó-Cancino, M., & Leyva-Ramos, R. (2021). Ciprofloxacin, ranitidine, and chlorphenamine removal from aqueous solution by adsorption. Mechanistic and regeneration analysis. *Environmental Technology & Innovation*, 24, 102060. <https://doi.org/10.1016/j.eti.2021.102060>

- Garikoé, I., & Guel, B. (2022). Solid-state synthesis of organoclays: Physicochemical properties and application for bisphenol a removal from aqueous solutions. In: W. Oueslati (Ed.), *Nanoclay - Recent Advances, New Perspectives and Applications*. <https://doi.org/10.5772/intechopen.107503>
- Ghanbari, F., Hassani, A., Waclawek, S., Wang, Z., Matyszczyk, G., Lin, K.-Y. A., & Dolatabadi, M. (2021). Insights into paracetamol degradation in aqueous solutions by ultrasound-assisted heterogeneous electro-Fenton process: Key operating parameters, mineralization and toxicity assessment. *Separation and Purification Technology*, 266, 118533. <https://doi.org/10.1016/j.seppur.2021.118533>
- Ghate, E., Ganjidoust, H., & Ayati, B. (2021). The thermodynamics, kinetics, and isotherms of sulfamethoxazole adsorption using magnetic activated carbon nanocomposite and its reusability potential. *Nanotechnology for Environmental Engineering*, 6(2), 32. <https://doi.org/10.1007/s41204-021-00127-y>
- Gizli, N., Çok, S. S., & Koç, F. (2022). Aerogel, xerogel, and cryogel: Synthesis, surface chemistry, and properties—Practical environmental applications and the future developments. In: D. Giannakoudakis, L. Meili & I. Anastopoulos (Eds.), *Advanced Materials for Sustainable Environmental Remediation* (pp. 195–229). Elsevier. <https://doi.org/10.1016/B978-0-323-90485-8.00021-7>
- Glaze, W. H., Kang, J.-W., & Chapin, D. H. (1987). The chemistry of water treatment processes involving ozone, hydrogen peroxide and ultraviolet radiation. *Ozone: Science & Engineering*, 9(4), 335–352. <https://doi.org/10.1080/01919518708552148>
- Gogoi, A., Mazumder, P., Tyagi, V. K., Tushara Chaminda, G. G., An, A. K., & Kumar, M. (2018). Occurrence and fate of emerging contaminants in water environment: A review. *Groundwater for Sustainable Development*, 6, 169–180. <https://doi.org/10.1016/j.gsd.2017.12.009>
- Gorini, F., Chiappa, E., Gargani, L., & Picano, E. (2014). Potential effects of environmental chemical contamination in congenital heart disease. *Pediatric Cardiology*, 35(4), 559–568. <https://doi.org/10.1007/s00246-014-0870-1>

- Govender, S., & Friedrich, H. (2017). Monoliths: A review of the basics, preparation methods and their relevance to oxidation. *Catalysts*, 7(2), 62. <https://doi.org/10.3390/catal7020062>
- Greene-Kelly, R. (1955). Sorption of aromatic organic compounds by montmorillonite. Part 1.—Orientation studies. *Transactions of the Faraday Society*, 51(0), 412–424. <https://doi.org/10.1039/TF9555100412>
- Gregg, S. J., & Sing, K. S. W. (1982). Adsorption, Surface Area and Porosity. *Journal of The Electrochemical Society*, 114(11). <https://doi.org/10.1149/1.2426447>
- Grenni, P., Patrolecco, L., Rauseo, J., Spataro, F., Di Lenola, M., Aimola, G., Zacchini, M., Pietrini, F., Di Baccio, D., Stanton, I. C., Gaze, W. H., & Barra Caracciolo, A. (2019). Sulfamethoxazole persistence in a river water ecosystem and its effects on the natural microbial community and Lemna minor plant. *Microchemical Journal*, 149, 103999. <https://doi.org/10.1016/j.microc.2019.103999>
- Guggenheim, S., & Koster van Groos, A. F. (2001). Baseline studies of the clay minerals society source clays: Thermal analysis. *Clays and Clay Minerals*, 49(5), 433–443. <https://doi.org/10.1346/CCMN.2001.0490509>
- Gulen, B., & Demircivi, P. (2020). Adsorption properties of flouroquinolone type antibiotic ciprofloxacin into 2:1 dioctahedral clay structure: Box-Behnken experimental design. *Journal of Molecular Structure*, 1206, 127659. <https://doi.org/10.1016/j.molstruc.2019.127659>
- Guo, F., Chen, Z., Huang, X., Cao, L., Cheng, X., Shi, W., & Chen, L. (2021). Cu₃P nanoparticles decorated hollow tubular carbon nitride as a superior photocatalyst for photodegradation of tetracycline under visible light. *Separation and Purification Technology*, 275, 119223. <https://doi.org/10.1016/j.seppur.2021.119223>
- Guo, K., Wu, Z., Chen, C., & Fang, J. (2022). UV/Chlorine process: An efficient advanced oxidation process with multiple radicals and functions in water treatment. *Accounts of Chemical Research*, 55(3), 286–297. <https://doi.org/10.1021/acs.accounts.1c00269>
- Guo, S., Gao, M., Shen, T., Xiang, Y., & Cao, G. (2019). Effective adsorption of sulfamethoxazole by novel Organo-Vts and their mechanistic insights.

- Microporous and Mesoporous Materials*, 286, 36–44. <https://doi.org/10.1016/j.micromeso.2019.05.032>
- Guruge, K. S., Goswami, P., Tanoue, R., Nomiya, K., Wijesekara, R. G. S., & Dharmaratne, T. S. (2019). First nationwide investigation and environmental risk assessment of 72 pharmaceuticals and personal care products from Sri Lankan surface waterways. *Science of the Total Environment*, 690, 683–695. <https://doi.org/10.1016/j.scitotenv.2019.07.042>
- Habibi, A., Belaroui, L. S., Bengueddach, A., López Galindo, A., Sainz Díaz, C. I., & Peña, A. (2018). Adsorption of metronidazole and spiramycin by an Algerian palygorskite. Effect of modification with tin. *Microporous and Mesoporous Materials*, 268, 293–302. <https://doi.org/10.1016/j.micromeso.2018.04.020>
- Halling-Sørensen, B. (2000). Algal toxicity of antibacterial agents used in intensive farming. *Chemosphere*, 40(7), 731–739. [https://doi.org/10.1016/S0045-6535\(99\)00445-2](https://doi.org/10.1016/S0045-6535(99)00445-2)
- Hameed, A., Hameed, B. H., Almomani, F. A., Usman, M., Ba-Abbad, M. M., & Khraisheh, M. (2024). Dynamic simulation of lead(II) metal adsorption from water on activated carbons in a packed-bed column. *Biomass Conversion and Biorefinery*, 14(7), 8283–8292. <https://doi.org/10.1007/s13399-022-03079-8>
- Hanh, P. T. H., Phoungthong, K., Chantrapromma, S., Choto, P., Thanomsilp, C., Siriwat, P., Wisittipanit, N., & Suwunwong, T. (2023). Adsorption of tetracycline by magnetic mesoporous silica derived from bottom ash—biomass power plant. *Sustainability*, 15(6), 4727. <https://doi.org/10.3390/su15064727>
- Haye, E., Job, N., Wang, Y., Penninckx, S., Stergiopoulos, V., Tumanov, N., Cardinal, M., Busby, Y., Colomer, J.-F., Su, B.-L., Pireaux, J.-J., & Houssiau, L. (2020). ZnO/Carbon xerogel photocatalysts by low-pressure plasma treatment, the role of the carbon substrate and its plasma functionalization. *Journal of Colloid and Interface Science*, 570, 312–321. <https://doi.org/10.1016/j.jcis.2020.03.015>
- Hejna, M., Kapuścińska, D., & Aksmann, A. (2022). Pharmaceuticals in the aquatic environment: A review on eco-toxicology and the remediation potential of algae.

-
- International Journal of Environmental Research and Public Health*, 19(13), 7717. <https://doi.org/10.3390/ijerph19137717>
- Hernández, D., Quiñones, L., Lazo, L., Charnay, C., Velázquez, M., Altshuler, E., & Rivera, A. (2023). Removal of an emergent contaminant by a palygorskite from Pontezuela/Cuban region. *Journal of Porous Materials*, 30(4), 1149–1161. <https://doi.org/10.1007/s10934-022-01400-4>
- Hernández-Tenorio, R., González-Juárez, E., Guzmán-Mar, J. L., Hinojosa-Reyes, L., & Hernández-Ramírez, A. (2022). Review of occurrence of pharmaceuticals worldwide for estimating concentration ranges in aquatic environments at the end of the last decade. *Journal of Hazardous Materials Advances*, 8, 100172. <https://doi.org/10.1016/j.hazadv.2022.100172>
- Ho, A. M.-C., Weinshilboum, R. M., Frye, M. A., & Biernacka, J. M. (2021). Genetics and antiepileptic mood stabilizer treatment response in bipolar disorder: What do we know? *Pharmacogenomics*, 22(14), 913–925. <https://doi.org/10.2217/pgs-2021-0041>
- Homem, V., & Santos, L. (2011). Degradation and removal methods of antibiotics from aqueous matrices – A review. *Journal of Environmental Management*, 92(10), 2304–2347. <https://doi.org/10.1016/j.jenvman.2011.05.023>
- Hossain, A., Nakamichi, S., Habibullah-Al-Mamun, M., Tani, K., Masunaga, S., & Matsuda, H. (2018). Occurrence and ecological risk of pharmaceuticals in river surface water of Bangladesh. *Environmental Research*, 165, 258–266. <https://doi.org/10.1016/j.envres.2018.04.030>
- Hossain, Md. M., Mok, Y. S., Nguyen, V. T., Sosiawati, T., Lee, B., Kim, Y. J., Lee, J. H., & Heo, I. (2022). Plasma-catalytic oxidation of volatile organic compounds with honeycomb catalyst for industrial application. *Chemical Engineering Research and Design*, 177, 406–417. <https://doi.org/10.1016/j.cherd.2021.11.010>
- Hosseini, S., Moghaddas, H., Masoudi Soltani, S., & Kheawhom, S. (2020). Technological applications of honeycomb monoliths in environmental processes: A review. *Process Safety and Environmental Protection*, 133, 286–300. <https://doi.org/10.1016/j.psep.2019.11.020>

- Hou, J., Bao, W., Zhang, J., Yu, J., Chen, L., Di, G., Zhou, Q., & Li, X. (2023). Characteristics and mechanisms of sulfamethoxazole adsorption onto modified biochars with hierarchical pore structures: Batch, predictions using artificial neural network and fixed bed column studies. *Journal of Water Process Engineering*, 54, 103975. <https://doi.org/10.1016/j.jwpe.2023.103975>
- Houeto, P., Carton, A., Guerbet, M., Mauclaire, A.-C., Gatignol, C., Lechat, P., & Masset, D. (2012). Assessment of the health risks related to the presence of drug residues in water for human consumption: Application to carbamazepine. *Regulatory Toxicology and Pharmacology*, 62(1), 41–48. <https://doi.org/10.1016/j.yrtph.2011.11.012>
- Hsu, L.-C., Liu, Y.-T., Syu, C.-H., Huang, M.-H., Tzou, Y.-M., & Teah, H. Y. (2018). Adsorption of tetracycline on Fe (hydr)oxides: effects of pH and metal cation (Cu^{2+} , Zn^{2+} and Al^{3+}) addition in various molar ratios. *Royal Society Open Science*, 5(3), 171941. <https://doi.org/10.1098/rsos.171941>
- Huang, Z., Fang, X., Wang, S., Zhou, N., & Fan, S. (2023). Effects of KMnO_4 pre- and post-treatments on biochar properties and its adsorption of tetracycline. *Journal of Molecular Liquids*, 373, 121257. <https://doi.org/10.1016/j.molliq.2023.121257>
- Hussain, S., & Ali, S. (2021). Removal of heavy metal by ion exchange using bentonite clay. *Journal of Ecological Engineering*, 22(1), 104–111. <https://doi.org/10.12911/22998993/128865>
- Ibarra Torres, C. E., Serrano Quezada, T. E., Kharissova, O. V., Kharisov, B. I., & Gómez de la Fuente, Ma. I. (2021). Carbon-based aerogels and xerogels: Synthesis, properties, oil sorption capacities, and DFT simulations. *Journal of Environmental Chemical Engineering*, 9(1), 104886. <https://doi.org/10.1016/j.jece.2020.104886>
- Ibrahim, Z., Koubaissy, B., Mohsen, Y., Hamieh, T., Daou, T. J., Nouali, H., Foddis, M.-L., & Toufaily, J. (2018). Adsorption of pyridine onto activated montmorillonite clays: Effect factors, adsorption behavior and mechanism study. *American Journal of Analytical Chemistry*, 09(10), 464–481. <https://doi.org/10.4236/ajac.2018.910035>

- Imanipoor, J., Mohammadi, M., & Dinari, M. (2021). Evaluating the performance of L-methionine modified montmorillonite K10 and 3-aminopropyltriethoxysilane functionalized magnesium phyllosilicate organoclays for adsorptive removal of azithromycin from water. *Separation and Purification Technology*, 275, 119256. <https://doi.org/10.1016/j.seppur.2021.119256>
- Inreiter, N., Huemer, B., Springer, B., Humer, F., & Allerberger, F. (2016). Antibiotics in Austrian drinking water resources, survey 2014. *Die Bodenkultur: Journal of Land Management, Food and Environment*, 67(1), 35–43. <https://doi.org/10.1515/boku-2016-0004>
- Isidori, M., Parrella, A., Pistillo, P., & Temussi, F. (2009). Effects of ranitidine and its photoderivatives in the aquatic environment. *Environment International*, 35(5), 821–825. <https://doi.org/10.1016/j.envint.2008.12.002>
- Issaka, E., AMU-Darko, J. N.-O., Yakubu, S., Fapohunda, F. O., Ali, N., & Bilal, M. (2022). Advanced catalytic ozonation for degradation of pharmaceutical pollutants—A review. *Chemosphere*, 289, 133208. <https://doi.org/10.1016/j.chemosphere.2021.133208>
- Jandyal, A., Chaturvedi, I., Wazir, I., Raina, A., & Ul Haq, M. I. (2022). 3D printing – A review of processes, materials and applications in industry 4.0. *Sustainable Operations and Computers*, 3, 33–42. <https://doi.org/10.1016/j.susoc.2021.09.004>
- Jayaseelan, S. S., Radhakrishnan, S., Saravanakumar, B., Seo, M.-K., Khil, M.-S., Kim, H.-Y., & Kim, B.-S. (2018). Mesoporous 3D NiCo₂O₄/MWCNT nanocomposite aerogels prepared by a supercritical CO₂ drying method for high performance hybrid supercapacitor electrodes. *Colloids and Surfaces A: Physicochemical Engineering Aspects*, 538, 451–459. <https://doi.org/10.1016/j.colsurfa.2017.11.037>
- Jentink, J., Dolk, H., Loane, M. A., Morris, J. K., Wellesley, D., Garne, E., & de Jong-van den Berg, L. (2010). Intrauterine exposure to carbamazepine and specific congenital malformations: Systematic review and case-control study. *BMJ*, 341(dec02 1), c6581–c6581. <https://doi.org/10.1136/bmj.c6581>

- Ji, L., Chen, W., Duan, L., & Zhu, D. (2009). Mechanisms for strong adsorption of tetracycline to carbon nanotubes: A comparative study using activated carbon and graphite as adsorbents. *Environmental Science & Technology*, 43(7), 2322–2327. <https://doi.org/10.1021/es803268b>
- Jia, D.-A., Zhou, D.-M., Wang, Y.-J., Zhu, H.-W., & Chen, J.-L. (2008). Adsorption and cosorption of Cu(II) and tetracycline on two soils with different characteristics. *Geoderma*, 146(1–2), 224–230. <https://doi.org/10.1016/j.geoderma.2008.05.023>
- Jjemba, P. K. (2006). Excretion and ecotoxicity of pharmaceutical and personal care products in the environment. *Ecotoxicology and Environmental Safety*, 63(1), 113–130. <https://doi.org/10.1016/j.ecoenv.2004.11.011>
- Job, N., Théry, A., Pirard, R., Marien, J., Kocon, L., Rouzaud, J.-N., Béguin, F., & Pirard, J.-P. (2005). Carbon aerogels, cryogels and xerogels: Influence of the drying method on the textural properties of porous carbon materials. *Carbon*, 43(12), 2481–2494. <https://doi.org/10.1016/j.carbon.2005.04.031>
- Jones, K. L., Lacro, R. V., Johnson, K. A., & Adams, J. (1989). Pattern of malformations in the children of women treated with carbamazepine during pregnancy. *The New England Journal of Medicine*, 320(25), 1661–1666. <https://doi.org/10.1056/NEJM198906223202505>
- Kairigo, P., Ngumba, E., Sundberg, L.-R., Gachanja, A., & Tuhkanen, T. (2020). Occurrence of antibiotics and risk of antibiotic resistance evolution in selected Kenyan wastewaters, surface waters and sediments. *Science of the Total Environment*, 720, 137580. <https://doi.org/10.1016/j.scitotenv.2020.137580>
- Kang, J., Liu, H., Zheng, Y.-M., Qu, J., & Chen, J. P. (2011). Application of nuclear magnetic resonance spectroscopy, Fourier transform infrared spectroscopy, UV–Visible spectroscopy and kinetic modeling for elucidation of adsorption chemistry in uptake of tetracycline by zeolite beta. *Journal of Colloid and Interface Science*, 354(1), 261–267. <https://doi.org/10.1016/j.jcis.2010.10.065>
- Karimi, K. J., Ngumba, E., Ahmad, A., Duse, A. G., Olago, D., Ndwigah, S. N., Mwanthi, M. A., Ayah, R., & Dulo, S. (2023). Contamination of groundwater with sulfamethoxazole and antibiotic resistant *Escherichia coli* in informal settlements

- in Kisumu, Kenya. *PLOS Water*, 2(4), e0000076. <https://doi.org/10.1371/journal.pwat.0000076>
- Kausar, A., Naeem, K., Hussain, T., Nazli, Z.-H., Bhatti, H. N., Jubeen, F., Nazir, A., & Iqbal, M. (2019). Preparation and characterization of chitosan/clay composite for direct Rose FRN dye removal from aqueous media: Comparison of linear and non-linear regression methods. *Journal of Materials Research and Technology*, 8(1), 1161–1174. <https://doi.org/10.1016/j.jmrt.2018.07.020>
- Kavitha, V. (2022). Global prevalence and visible light mediated photodegradation of pharmaceuticals and personal care products (PPCPs)-a review. *Results in Engineering*, 14, 100469. <https://doi.org/10.1016/j.rineng.2022.100469>
- Khan, H. K., Rehman, M. Y. A., & Malik, R. N. (2020). Fate and toxicity of pharmaceuticals in water environment: An insight on their occurrence in South Asia. *Journal of Environmental Management*, 271, 111030. <https://doi.org/10.1016/j.jenvman.2020.111030>
- Kibuye, F. A., Gall, H. E., Elkin, K. R., Ayers, B., Veith, T. L., Miller, M., Jacob, S., Hayden, K. R., Watson, J. E., & Elliott, H. A. (2019). Fate of pharmaceuticals in a spray-irrigation system: From wastewater to groundwater. *Science of the Total Environment*, 654, 197–208. <https://doi.org/10.1016/j.scitotenv.2018.10.442>
- Klavarioti, M., Mantzavinos, D., & Kassinos, D. (2009). Removal of residual pharmaceuticals from aqueous systems by advanced oxidation processes. *Environment International*, 35(2), 402–417. <https://doi.org/10.1016/j.envint.2008.07.009>
- Kondor, A. C., Jakab, G., Vancsik, A., Filep, T., Szeberényi, J., Szabó, L., Maász, G., Ferincz, Á., Dobosy, P., & Szalai, Z. (2020). Occurrence of pharmaceuticals in the Danube and drinking water wells: Efficiency of riverbank filtration. *Environmental Pollution*, 265, 114893. <https://doi.org/10.1016/j.envpol.2020.114893>
- Korus, A., Gutierrez, J.-P., Szlęk, A., Jagiello, J., & Hornung, A. (2022). Pore development during CO₂ and H₂O activation associated with the catalytic role of inherent inorganics in sewage sludge char and its performance during the

- reforming of volatiles. *Chemical Engineering Journal*, 446, 137298. <https://doi.org/10.1016/j.cej.2022.137298>
- Kovacev, N., Li, S., Zeraati-Rezaei, S., Hemida, H., Tsolakis, A., & Essa, K. (2021). Effects of the internal structures of monolith ceramic substrates on thermal and hydraulic properties: Additive manufacturing, numerical modelling and experimental testing. *The International Journal of Advanced Manufacturing Technology*, 112(3–4), 1115–1132. <https://doi.org/10.1007/s00170-020-06493-2>
- Kovalakova, P., Cizmas, L., McDonald, T. J., Marsalek, B., Feng, M., & Sharma, V. K. (2020). Occurrence and toxicity of antibiotics in the aquatic environment: A review. *Chemosphere*, 251, 126351. <https://doi.org/10.1016/j.chemosphere.2020.126351>
- Krakkó, D., Heieren, B. T., Illés, Á., Kvamme, K., Dóbbé, S., & Zárny, G. (2022). (V)UV degradation of the antibiotic tetracycline: Kinetics, transformation products and pathway. *Process Safety and Environmental Protection*, 163, 395–404. <https://doi.org/10.1016/j.psep.2022.05.027>
- Kristofco, L. A., & Brooks, B. W. (2017). Global scanning of antihistamines in the environment: Analysis of occurrence and hazards in aquatic systems. *Science of the Total Environment*, 592, 477–487. <https://doi.org/10.1016/j.scitotenv.2017.03.120>
- Kulik, K., Lenart-Boroń, A., & Wyrzykowska, K. (2023). Impact of antibiotic pollution on the bacterial population within surface water with special focus on mountain rivers. *Water*, 15(5), 975. <https://doi.org/10.3390/w15050975>
- Kutuzova, A., Dontsova, T., & Kwapinski, W. (2021). Application of TiO₂-Based photocatalysts to antibiotics degradation: Cases of sulfamethoxazole, trimethoprim and ciprofloxacin. *Catalysts*, 11(6), 728. <https://doi.org/10.3390/catal11060728>
- Kwan, P., & Brodie, M. J. (2001). Effectiveness of first antiepileptic drug. *Epilepsia*, 42(10), 1255–1260. <https://doi.org/10.1046/j.1528-1157.2001.04501.x>
- Lagaly, G., Ogawa, M., & Dékány, I. (2013). Clay mineral–organic interactions. F. Bergaya & G. Lagaly (Eds.), *Handbook of Clay Science* ed. 5 (pp. 435–505). <https://doi.org/10.1016/B978-0-08-098258-8.00015-8>

- Lambs, L., Decock-Le Reverend, B., Kozlowski, H., & Berthon, G. (1988). Metal ion-tetracycline interactions in biological fluids. 9. Circular dichroism spectra of calcium and magnesium complexes with tetracycline, oxytetracycline, doxycycline, and chlortetracycline and discussion of their binding modes. *Inorganic Chemistry*, 27(17), 3001–3012. <https://doi.org/10.1021/ic00290a022>
- Legrini, O., Oliveros, E., & Braun, A. M. (1993). Photochemical processes for water treatment. *Chemical Reviews*, 93(2), 671–698. <https://doi.org/10.1021/cr00018a003>
- Lei, M., Zhang, L., Lei, J., Zong, L., Li, J., Wu, Z., & Wang, Z. (2015). Overview of emerging contaminants and associated human health effects. *BioMed Research International*, 2015, 1–12. <https://doi.org/10.1155/2015/404796>
- Leichtweis, J., Vieira, Y., Welter, N., Silvestri, S., Dotto, G. L., & Carissimi, E. (2022). A review of the occurrence, disposal, determination, toxicity and remediation technologies of the tetracycline antibiotic. *Process Safety and Environmental Protection*, 160, 25–40. <https://doi.org/10.1016/j.psep.2022.01.085>
- Leon y Leon, C. A., Solar, J. M., Calemma, V., & Radovic, L. R. (1992). Evidence for the protonation of basal plane sites on carbon. *Carbon*, 30(5), 797–811. [https://doi.org/10.1016/0008-6223\(92\)90164-R](https://doi.org/10.1016/0008-6223(92)90164-R)
- Letsinger, S., & Kay, P. (2019). Comparison of prioritisation schemes for human pharmaceuticals in the aquatic environment. *Environmental Science and Pollution Research*, 26(4), 3479–3491. <https://doi.org/10.1007/s11356-018-3834-9>
- Leyva-Ramos, R. (2010). Fundamentos de adsorción en sistemas líquido-sólido. In: M. I. Litter, A. M. Sancha & A. M. Ingallinella (Eds.), *IBEROANSEN. Tecnologías económicas para el abatimiento de arsénico en aguas* (pp. 43–50), CYTED.
- Leyva-Ramos, R., & Geankopolis, C. J. (1985). Model simulation and analysis of surface diffusion of liquids in porous solids. *Chemical Engineering Science*, 40(5), 799–807. [https://doi.org/10.1016/0009-2509\(85\)85032-6](https://doi.org/10.1016/0009-2509(85)85032-6)
- Leyva-Ramos, R., & Geankopolis, C. J. (1994). Diffusion in liquid-filled pores of activated carbon. I. Pore volume diffusion. *The Canadian Journal of Chemical Engineering*, 72(2), 262–271. <https://doi.org/10.1002/cjce.5450720213>

-
- Leyva-Ramos, R., Jacobo-Azuara, A., & Martínez-Costa, J. I. (2021). Organoclays. fundamentals and applications for removing toxic pollutants from water solution. In: J. C. Moreno-Piraján, L. Giraldo-Gutierrez & F. Gómez-Granados (Eds.), *Porous Materials: Theory and Its Application for Environmental Remediation* (pp. 341–363). https://doi.org/10.1007/978-3-030-65991-2_13
- Leyva-Ramos, R., Ocampo-Perez, R., & Mendoza-Barron, J. (2012). External mass transfer and hindered diffusion of organic compounds in the adsorption on activated carbon cloth. *Chemical Engineering Journal*, 183, 141–151. <https://doi.org/10.1016/j.cej.2011.12.046>
- Leyva-Ramos, R., Ocampo-Pérez, R., Bautista-Toledo, I., Rivera-Utrilla, J., Medellín-Castillo, N. A., & Aguilar-Madera, C. A. (2020). The adsorption kinetics of sodium dodecylbenzenesulfonate on activated carbon. Branched-pore diffusional model revisited and comparison with other diffusional models. *Chemical Engineering Communications*, 207(5), 705–721. <https://doi.org/10.1080/00986445.2019.1615898>
- Leyva-Ramos, R., Salazar-Rábago, J. J., & Ocampo-Pérez, R. (2021). A novel intraparticle mass transfer model for the biosorption rate of methylene blue on white pine (*Pinus durangensis*) sawdust. Diffusion-permeation. *Chemical Engineering Research and Design*, 172, 43–52. <https://doi.org/10.1016/j.cherd.2021.05.029>
- Li, C.-M., Chen, C.-H., & Chen, W.-H. (2017). Different influences of nanopore dimension and pH between chlorpheniramine adsorptions on graphene oxide-iron oxide suspension and particle. *Chemical Engineering Journal*, 307, 447–455. <https://doi.org/10.1016/j.cej.2016.08.107>
- Li, F., Xie, L., Sun, G., Kong, Q., Su, F., Cao, Y., Wei, J., Ahmad, A., Guo, X., & Chen, C.-M. (2019). Resorcinol-formaldehyde based carbon aerogel: Preparation, structure and applications in energy storage devices. *Microporous and Mesoporous Materials*, 279, 293–315. <https://doi.org/10.1016/j.micromeso.2018.12.007>

- Li, M., Yang, K., Huang, X., Liu, S., Jia, Y., Gu, P., & Miao, H. (2022). Efficient degradation of trimethoprim by catalytic ozonation coupled with Mn/FeOx-functionalized ceramic membrane: Synergic catalytic effect and enhanced anti-fouling performance. *Journal of Colloid and Interface Science*, 616, 440–452. <https://doi.org/10.1016/j.jcis.2022.02.061>
- Li, S., Wang, Z., Zhao, X., Yang, X., Liang, G., & Xie, X. (2019). Insight into enhanced carbamazepine photodegradation over biochar-based magnetic photocatalyst Fe₃O₄/BiOBr/BC under visible LED light irradiation. *Chemical Engineering Journal*, 360, 600–611. <https://doi.org/10.1016/j.cej.2018.12.002>
- Li, Z., Chang, P.-H., Jean, J.-S., Jiang, W.-T., & Hong, H. (2011). Mechanism of chlorpheniramine adsorption on Ca-montmorillonite. *Colloids and Surfaces A: Physicochemical and Engineering Aspects*, 385(1–3), 213–218. <https://doi.org/10.1016/j.colsurfa.2011.06.013>
- Li, Z., Chang, P.-H., Jean, J.-S., Jiang, W.-T., & Wang, C.-J. (2010). Interaction between tetracycline and smectite in aqueous solution. *Journal of Colloid and Interface Science*, 341(2), 311–319. <https://doi.org/10.1016/j.jcis.2009.09.054>
- Li, Z., Jiang, H., Wang, X., Wang, C., & Wei, X. (2023). Effect of pH on adsorption of tetracycline antibiotics on graphene oxide. *International Journal of Environmental Research and Public Health*, 20(3), 2448. <https://doi.org/10.3390/ijerph20032448>
- Li, Z.-H., Zlabek, V., Grabic, R., Velisek, J., Machova, J., & Randak, T. (2010). Enzymatic alterations and RNA/DNA ratio in intestine of rainbow trout, *Oncorhynchus mykiss*, induced by chronic exposure to carbamazepine. *Ecotoxicology*, 19(5), 872–878. <https://doi.org/10.1007/s10646-010-0468-1>
- Li, Z.-H., Zlabek, V., Velisek, J., Grabic, R., Machova, J., Kolarova, J., Li, P., & Randak, T. (2011). Acute toxicity of carbamazepine to juvenile rainbow trout (*Oncorhynchus mykiss*): Effects on antioxidant responses, hematological parameters and hepatic EROD. *Ecotoxicology and Environmental Safety*, 74(3), 319–327. <https://doi.org/10.1016/j.ecoenv.2010.09.008>
- Lim, J.-W., Choi, Y., Yoon, H.-S., Park, Y.-K., Yim, J.-H., & Jeon, J.-K. (2010). Extrusion of honeycomb monoliths employed with activated carbon-LDPE hybrid materials.

-
- Journal of Industrial and Engineering Chemistry*, 16(1), 51–56. <https://doi.org/10.1016/j.jiec.2010.01.022>
- Lin, A. Y.-C., Yu, T.-H., & Lateef, S. K. (2009). Removal of pharmaceuticals in secondary wastewater treatment processes in Taiwan. *Journal of Hazardous Materials*, 167(1–3), 1163–1169. <https://doi.org/10.1016/j.jhazmat.2009.01.108>
- Lin, C.-H., Li, C.-M., Chen, C.-H., & Chen, W.-H. (2019). Removal of chlorpheniramine and variations of nitrosamine formation potentials in municipal wastewaters by adsorption onto the GO-Fe₃O₄. *Environmental Science and Pollution Research*, 26(20), 20701–20711. <https://doi.org/10.1007/s11356-019-05278-9>
- Lin, X., Xu, J., Keller, A. A., He, L., Gu, Y., Zheng, W., Sun, D., Lu, Z., Huang, J., Huang, X., & Li, G. (2020). Occurrence and risk assessment of emerging contaminants in a water reclamation and ecological reuse project. *Science of the Total Environment*, 744, 140977. <https://doi.org/10.1016/j.scitotenv.2020.140977>
- Liu, H., Wang, P., Zhang, B., Li, H., Li, J., Li, Y., & Chen, Z. (2021). Morphology controlled carbon aerogel with enhanced thermal insulation and mechanical properties: a simple route for the regulated synthesis. *Journal of Non-Crystalline Solids*, 564, 120828. <https://doi.org/10.1016/j.jnoncrysol.2021.120828>
- Liu, P., Wang, Q., Zheng, C., & He, C. (2017). Sorption of sulfadiazine, norfloxacin, metronidazole, and tetracycline by granular activated carbon: Kinetics, mechanisms, and isotherms. *Water, Air, & Soil Pollution*, 228(4), 129. <https://doi.org/10.1007/s11270-017-3320-x>
- Liu, S., Wu, P., Yu, L., Li, L., Gong, B., Zhu, N., Dang, Z., & Yang, C. (2017). Preparation and characterization of organo-vermiculite based on phosphatidylcholine and adsorption of two typical antibiotics. *Applied Clay Science*, 137, 160–167. <https://doi.org/10.1016/j.clay.2016.12.002>
- Liu, W., Zhao, C., Wang, S., Niu, L., Wang, Y., Liang, S., & Cui, Z. (2018). Adsorption of cadmium ions from aqueous solutions using nano-montmorillonite: Kinetics, isotherm and mechanism evaluations. *Research on Chemical Intermediates*, 44(3), 1441–1458. <https://doi.org/10.1007/s11164-017-3178-y>

- Liu, Y., He, X., Fu, Y., & Dionysiou, D. D. (2016). Degradation kinetics and mechanism of oxytetracycline by hydroxyl radical-based advanced oxidation processes. *Chemical Engineering Journal*, 284, 1317–1327. <https://doi.org/10.1016/j.cej.2015.09.034>
- Liu, Y.-J., Liu, H.-S., Hu, C.-Y., & Lo, S.-L. (2019). Simultaneous aqueous chlorination of amine-containing pharmaceuticals. *Water Research*, 155, 56–65. <https://doi.org/10.1016/j.watres.2019.01.061>
- Lofrano, G., Sacco, O., Venditto, V., Carotenuto, M., Libralato, G., Guida, M., Meric, S., & Vaiano, V. (2020). Occurrence and potential risks of emerging contaminants in water. In: O. Sacco & V. Vaiano (Eds.), *Visible Light Active Structured Photocatalysts for the Removal of Emerging Contaminants: Science and Engineering* (pp. 1–25). <https://doi.org/10.1016/B978-0-12-818334-2.00001-8>
- López-Pacheco, I. Y., Silva-Núñez, A., Salinas-Salazar, C., Arévalo-Gallegos, A., Lizarazo-Holguin, L. A., Barceló, D., Iqbal, H. M. N., & Parra-Saldívar, R. (2019). Anthropogenic contaminants of high concern: Existence in water resources and their adverse effects. *Science of the Total Environment*, 690, 1068–1088. <https://doi.org/10.1016/j.scitotenv.2019.07.052>
- Lowell, S., Shields, J. E., Thomas, M. A., & Thommes, M. (2004). *Characterization of porous solids and powders: Surface area, pore size and density*. Springer Netherlands.
- Lu, C., Huang, Y. H., Hong, J. S., Wu, Y. J., Li, J., & Cheng, J. P. (2018). The effects of melamine on the formation of carbon xerogel derived from resorcinol and formaldehyde and its performance for supercapacitor. *Journal of Colloid and Interface Science*, 524, 209–218. <https://doi.org/10.1016/j.jcis.2018.04.006>
- Lu, L., Cai, J., & Frost, R. L. (2010). Near infrared spectroscopy of benzoic acid adsorbed on montmorillonite. *Spectroscopy Letters*, 43(4), 266–274. <https://doi.org/10.1080/00387010903329417>
- Lützhøft, H.-C. H., Halling-Sørensen, B., & Jørgensen, S. E. (1999). Algal toxicity of antibacterial agents applied in Danish fish farming. *Archives of Environmental*

- Contamination and Toxicology*, 36(1), 1–6.
<https://doi.org/10.1007/s002449900435>
- Lv, G., Liu, L., Li, Z., Liao, L., & Liu, M. (2012). Probing the interactions between chlorpheniramine and 2:1 phyllosilicates. *Journal of Colloid and Interface Science*, 374(1), 218–225. <https://doi.org/10.1016/j.jcis.2012.01.029>
- Lv, J., Wang, L., Song, Y., & Li, Y. (2015). N-nitrosodimethylamine formation from ozonation of chlorpheniramine: Influencing factors and transformation mechanism. *Journal of Hazardous Materials*, 299, 584–594. <https://doi.org/10.1016/j.jhazmat.2015.07.062>
- Ma, J., Qi, J., Yao, C., Cui, B., Zhang, T., & Li, D. (2012). A novel bentonite-based adsorbent for anionic pollutant removal from water. *Chemical Engineering Journal*, 200–202, 97–103. <https://doi.org/10.1016/j.cej.2012.06.014>
- Madikizela, L. M., & Ncube, S. (2021). Occurrence and ecotoxicological risk assessment of non-steroidal anti-inflammatory drugs in South African aquatic environment: What is known and the missing information? *Chemosphere*, 280, 130688. <https://doi.org/10.1016/j.chemosphere.2021.130688>
- Maggio, A. A., Jalil, M. E. R., Villarroel-Rocha, J., Sapag, K., & Baschini, M. T. (2022). Fe- and SiFe-pillared clays from a mineralogical waste as adsorbents of ciprofloxacin from water. *Applied Clay Science*, 220, 106458. <https://doi.org/10.1016/j.clay.2022.106458>
- Malato, S., Fernández-Ibáñez, P., Maldonado, M. I., Blanco, J., & Gernjak, W. (2009). Decontamination and disinfection of water by solar photocatalysis: Recent overview and trends. *Catalysis Today*, 147(1), 1–59. <https://doi.org/10.1016/j.cattod.2009.06.018>
- Malvar, J. L., Martín, J., Orta, M. del M., Medina-Carrasco, S., Santos, J. L., Aparicio, I., & Alonso, E. (2020). Simultaneous and individual adsorption of ibuprofen metabolites by a modified montmorillonite. *Applied Clay Science*, 189, 105529. <https://doi.org/10.1016/j.clay.2020.105529>
- Maroga Mboula, V., Héquet, V., Gru, Y., Colin, R., & Andrès, Y. (2012). Assessment of the efficiency of photocatalysis on tetracycline biodegradation. *Journal of*

-
- Hazardous Materials*, 209–210, 355–364.
<https://doi.org/10.1016/j.jhazmat.2012.01.032>
- Marsh, A., Heath, A., Patureau, P., Evernden, M., & Walker, P. (2018). Alkali activation behaviour of un-calcined montmorillonite and illite clay minerals. *Applied Clay Science*, 166, 250–261. <https://doi.org/10.1016/j.clay.2018.09.011>
- Martín, J., Orta, M. del M., Medina-Carrasco, S., Santos, J. L., Aparicio, I., & Alonso, E. (2019). Evaluation of a modified mica and montmorillonite for the adsorption of ibuprofen from aqueous media. *Applied Clay Science*, 171, 29–37. <https://doi.org/10.1016/j.clay.2019.02.002>
- Martinez-Costa, J. I., & Leyva-Ramos, R. (2017). Effect of surfactant loading and type upon the sorption capacity of organobentonite towards pyrogallol. *Colloids and Surfaces A: Physicochemical and Engineering Aspects*, 520, 676–685. <https://doi.org/10.1016/j.colsurfa.2017.02.033>
- Martinez-Costa, J. I., Leyva-Ramos, R., & Padilla-Ortega, E. (2018). Sorption of diclofenac from aqueous solution on an organobentonite and adsorption of cadmium on organobentonite saturated with diclofenac. *Clays and Clay Minerals*, 66(6), 515–528. <https://doi.org/10.1346/CCMN.2018.064119>
- Martínez-Costa, J. I., Leyva-Ramos, R., Padilla-Ortega, E., Aragón-Piña, A., & Carrales-Alvarado, D. H. (2018). Antagonistic, synergistic and non-interactive competitive sorption of sulfamethoxazole-trimethoprim and sulfamethoxazole cadmium (II) on a hybrid clay nanosorbent. *Science of the Total Environment*, 640–641, 1241–1250. <https://doi.org/10.1016/j.scitotenv.2018.05.399>
- Martínez-Huitle, C. A., & Ferro, S. (2006). Electrochemical oxidation of organic pollutants for the wastewater treatment: Direct and indirect processes. *Chemical Society Reviews*, 35(12), 1324–1340. <https://doi.org/10.1039/B517632H>
- Mathews, A. P. (1975). *Mathematical modelling of multicomponent adsorption in batch reactors*. Tesis doctoral. The University of Michigan. <https://www.proquest.com/openview/b07ce35904b6c7f1c073efc2b41f2538/1?pq-origsite=gscholar&cbl=18750&diss=y>

- McKay, G., & Al-Duri, B. (1991). Extended empirical Freundlich isotherm for binary systems: a modified procedure to obtain the correlative constants. *Chemical Engineering and Processing: Process Intensification*, 29(3), 133–138. [https://doi.org/10.1016/0255-2701\(91\)85012-D](https://doi.org/10.1016/0255-2701(91)85012-D)
- Medina, O. E., Galeano-Caro, D., Castelo-Quibén, J., Ocampo-Pérez, R., Perez-Cadenas, A. F., Carrasco-Marín, F., Franco, C. A., & Corteés, F. B. (2021). Monolithic carbon xerogels-metal composites for crude oil removal from oil in-saltwater emulsions and subsequent regeneration through oxidation process: Composites synthesis, adsorption studies, and oil decomposition experiments. *Microporous and Mesoporous Materials*, 319, 111039. <https://doi.org/10.1016/j.micromeso.2021.111039>
- Mhamdi, M., Elaloui, E., & Trabelsi-Ayadi, M. (2014). Kinetics of cadmium adsorption by smectite of Oued Tfal (Gafsa Basin). *Desalination and Water Treatment*, 52(22–24), 4245–4256. <https://doi.org/10.1080/19443994.2013.810371>
- Micallef, J., Soeiro, T., & Jonville-Béra, A.-P. (2020). Non-steroidal anti-inflammatory drugs, pharmacology, and COVID-19 infection. *Therapies*, 75(4), 355–362. <https://doi.org/10.1016/j.therap.2020.05.003>
- Milić, N., Milanović, M., Letić, N. G., Sekulić, M. T., Radonić, J., Mihajlović, I., & Miloradov, M. V. (2013). Occurrence of antibiotics as emerging contaminant substances in aquatic environment. *International Journal of Environmental Health Research*, 23(4), 296–310. <https://doi.org/10.1080/09603123.2012.733934>
- Ming, D. W. & Dixon, J. B. (1987). Quantitative determination of clinoptilolite in soils by a cation-exchange capacity method. *Clays and Clay Minerals*, 35(6), 463–468. <https://doi.org/10.1346/CCMN.1987.0350607>
- Mishra, R. K., Mentha, S. S., Misra, Y., & Dwivedi, N. (2023). Emerging pollutants of severe environmental concern in water and wastewater: A comprehensive review on current developments and future research. *Water-Energy Nexus*, 6, 74–95. <https://doi.org/10.1016/j.wen.2023.08.002>

- Moma, J., Baloyi, J., & Ntho, T. (2018). Synthesis and characterization of an efficient and stable Al/Fe pillared clay catalyst for the catalytic wet air oxidation of phenol. *RSC Advances*, 8(53), 30115–30124. <https://doi.org/10.1039/C8RA05825C>
- Moore, D. M. & Hower, J. (1986). Ordered interstratification of dehydrated and hydrated Na-smectite. *Clays and Clay Minerals*, 34(4), 379–384. <https://doi.org/10.1346/CCMN.1986.0340404>
- Moraes, D. S., Angélica, R. S., Costa, C. E. F., Rocha Filho, G. N., & Zamian, J. R. (2011). Bentonite functionalized with propyl sulfonic acid groups used as catalyst in esterification reactions. *Applied Clay Science*, 51(3), 209–213. <https://doi.org/10.1016/j.clay.2010.11.018>
- Morales-Torres, S., Maldonado-Hódar, F. J., Pérez-Cadenas, A. F., & Carrasco-Marín, F. (2012). Structural characterization of carbon xerogels: From film to monolith. *Microporous and Mesoporous Materials*, 153, 24–29. <https://doi.org/10.1016/j.micromeso.2011.12.022>
- Morales-Torres, S., Maldonado-Hódar, F. J., Pérez-Cadenas, A. F., & Carrasco-Marín, F. (2010). Textural and mechanical characteristics of carbon aerogels synthesized by polymerization of resorcinol and formaldehyde using alkali carbonates as basification agents. *Physical Chemistry Chemical Physics*, 12(35), 10365. <https://doi.org/10.1039/C003396K>
- Moral-Rodríguez, A. I., Leyva-Ramos, R., Carrasco-Marín, F., Bautista-Toledo, M. I., & Pérez-Cadenas, A. F. (2020). Adsorption of diclofenac from aqueous solution onto carbon xerogels: Effect of synthesis conditions and presence of bacteria. *Water, Air, & Soil Pollution*, 231(1), 17. <https://doi.org/10.1007/s11270-019-4385-5>
- Moral-Rodríguez, A. I., Leyva-Ramos, R., Ocampo-Pérez, R., Mendoza-Barron, J., Serratos-Alvarez, I. N., & Salazar-Rabago, J. J. (2016). Removal of ronidazole and sulfamethoxazole from water solutions by adsorption on granular activated carbon: Equilibrium and intraparticle diffusion mechanisms. *Adsorption*, 22(1), 89–103. <https://doi.org/10.1007/s10450-016-9758-0>

- Moreno-Castilla, C., & Pérez-Cadenas, A. (2010). Carbon-based honeycomb monoliths for environmental gas-phase applications. *Materials*, 3(2), 1203–1227. <https://doi.org/10.3390/ma3021203>
- Naghavi, M., Abajobir, A. A., Abbafati, C., Abbas, K. M., Abd-Allah, F., Abera, S. F., Aboyans, V., Adetokunboh, O., Afshin, A., Agrawal, A., Ahmadi, A., Ahmed, M. B., Aichour, A. N., Aichour, M. T. E., Aichour, I., Aiyar, S., Alahdab, F., Al-Aly, Z., Alam, K., ... Murray, C. J. L. (2017). Global, regional, and national age-sex specific mortality for 264 causes of death, 1980–2016: A systematic analysis for the Global Burden of Disease Study 2016. *The Lancet*, 390(10100), 1151–1210. [https://doi.org/10.1016/S0140-6736\(17\)32152-9](https://doi.org/10.1016/S0140-6736(17)32152-9)
- Nantaba, F., Wasswa, J., Kylin, H., Palm, W. U., Bouwman, H., & Kümmerer, K. (2020). Occurrence, distribution, and ecotoxicological risk assessment of selected pharmaceutical compounds in water from Lake Victoria, Uganda. *Chemosphere*, 239, 124642. <https://doi.org/10.1016/j.chemosphere.2019.124642>
- Ngigi, A. N., Magu, M. M., & Muendo, B. M. (2020). Occurrence of antibiotics residues in hospital wastewater, wastewater treatment plant, and in surface water in Nairobi County, Kenya. *Environmental Monitoring and Assessment*, 192(1), 18. <https://doi.org/10.1007/s10661-019-7952-8>
- Nguyen, D. B., Shirjana, S., Hossain, Md. M., Heo, I., & Mok, Y. S. (2020). Effective generation of atmospheric pressure plasma in a sandwich-type honeycomb monolith reactor by humidity control. *Chemical Engineering Journal*, 401, 125970. <https://doi.org/10.1016/j.cej.2020.125970>
- Nguyen, T. L., Pham, T. H., Viet, N. M., Thang, P. Q., Rajagopal, R., Sathya, R., Jung, S. H., & Kim, T. (2022). Improved photodegradation of antibiotics pollutants in wastewaters by advanced oxidation process based on Ni-doped TiO₂. *Chemosphere*, 302, 134837. <https://doi.org/10.1016/j.chemosphere.2022.134837>
- Nightingale, E. R. (1959). Phenomenological theory of ion solvation. Effective radio of hydrated ions. *The Journal of Physical Chemistry*, 63(9), 1381–1387. <https://doi.org/10.1021/J150579A011>

-
- Nkoom, M., Lu, G., Liu, J., Yang, H., & Dong, H. (2019). Bioconcentration of the antiepileptic drug carbamazepine and its physiological and biochemical effects on *Daphnia magna*. *Ecotoxicology and Environmental Safety*, 172, 11–18. <https://doi.org/10.1016/j.ecoenv.2019.01.061>
- Noh, J. S., & Schwarz, J. A. (1989). Estimation of the point of zero charge of simple oxides by mass titration. *Journal of Colloid and Interface Science*, 130(1), 157–164. [https://doi.org/10.1016/0021-9797\(89\)90086-6](https://doi.org/10.1016/0021-9797(89)90086-6)
- Obradović, M., Daković, A., Smiljanić, D., Ožegović, M., Marković, M., Rottinghaus, G. E., & Krstić, J. (2022). Ibuprofen and diclofenac sodium adsorption onto functionalized minerals: Equilibrium, kinetic and thermodynamic studies. *Microporous and Mesoporous Materials*, 335, 111795. <https://doi.org/10.1016/j.micromeso.2022.111795>
- Ocampo-Pérez, R., Leyva-Ramos, R., & Padilla-Ortega, E. (2011a). Equilibrium and kinetic adsorption of organic compounds onto organobentonite: Application of a surface diffusion model. *Adsorption Science & Technology*, 29(10), 1007–1024. <https://doi.org/10.1260/0263-6174.29.10.1007>
- Ocampo-Perez, R., Leyva-Ramos, R., Mendoza-Barron, J., & Guerrero-Coronado, R. M. (2011b). Adsorption rate of phenol from aqueous solution onto organobentonite: Surface diffusion and kinetic models. *Journal of Colloid and Interface Science*, 364(1), 195–204. <https://doi.org/10.1016/j.jcis.2011.08.032>
- Okay, O., & Lozinsky, V. I. (2014). Synthesis and structure–property relationships of cryogels. In: O. Okay (Ed.), *Polymeric Cryogels. Macroporous Gels with Remarkable Properties* 263 (pp. 103–157). Springer Cham. https://doi.org/10.1007/978-3-319-05846-7_3
- Orolínovaá, Z., Mockovčiaková, A., & Škvarla, J. (2010). Sorption of cadmium (II) from aqueous solution by magnetic clay composite. *Desalination and Water Treatment*, 24(1–3), 284–292. <https://doi.org/10.5004/dwt.2010.1644>
- Ortiz-Ramos, U., Leyva-Ramos, R., Mendoza-Mendoza, E., & Aragón-Piña, A. (2022). Removal of tetracycline from aqueous solutions by adsorption on raw Ca-

- bentonite. Effect of operating conditions and adsorption mechanism. *Chemical Engineering Journal*, 432. <https://doi.org/10.1016/j.cej.2021.134428>
- Padilla-Ortega, E., Leyva-Ramos, R., & Flores-Cano, J. V. (2013). Binary adsorption of heavy metals from aqueous solution onto natural clays. *Chemical Engineering Journal*, 225, 535–546. <https://doi.org/10.1016/j.cej.2013.04.011>
- Padilla-Ortega, E., Leyva-Ramos, R., & Mendoza-Barron, J. (2014). Role of electrostatic interactions in the adsorption of cadmium(II) from aqueous solution onto vermiculite. *Applied Clay Science*, 88–89, 10–17. <https://doi.org/10.1016/j.clay.2013.12.012>
- Padilla-Ortega, E., Medellín-Castillo, N., & Robledo-Cabrera, A. (2020). Comparative study of the effect of structural arrangement of clays in the thermal activation: Evaluation of their adsorption capacity to remove Cd(II). *Journal of Environmental Chemical Engineering*, 8(4), 103850. <https://doi.org/10.1016/j.jece.2020.103850>
- Panwar, S., Upadhyay, G. K., & Purohit, L. P. (2022). Gd-doped ZnO:TiO₂ heterogenous nanocomposites for advance oxidation process. *Materials Research Bulletin*, 145, 111534. <https://doi.org/10.1016/j.materresbull.2021.111534>
- Parfitt, R. L., & Mortland, M. M. (1968). Ketone adsorption on montmorillonite. *Soil Science Society of America Journal*, 32(3), 355–363. <https://doi.org/10.2136/sssaj1968.03615995003200030027x>
- Parida, V. K., Saidulu, D., Majumder, A., Srivastava, A., Gupta, B., & Gupta, A. K. (2021). Emerging contaminants in wastewater: A critical review on occurrence, existing legislations, risk assessment, and sustainable treatment alternatives. *Journal of Environmental Chemical Engineering*, 9(5), 105966. <https://doi.org/10.1016/j.jece.2021.105966>
- Parikh, S. K., & Silberstein, S. D. (2019). Current status of antiepileptic drugs as preventive migraine therapy. *Current Treatment Options in Neurology*, 21(4), 16. <https://doi.org/10.1007/s11940-019-0558-1>
- Park, S., & Lee, W. (2018). Removal of selected pharmaceuticals and personal care products in reclaimed water during simulated managed aquifer recharge. *Science*

- of the Total Environment*, 640–641, 671–677.
<https://doi.org/10.1016/j.scitotenv.2018.05.221>
- Parolo, M. E., Avena, M. J., Savini, M. C., Baschini, M. T., & Nicotra, V. (2013). Adsorption and circular dichroism of tetracycline on sodium and calcium-montmorillonites. *Colloids and Surfaces A: Physicochemical and Engineering Aspects*, 417, 57–64. <https://doi.org/10.1016/j.colsurfa.2012.10.060>
- Parra-Marfil, A., Aguilar-Madera, C. G., Pérez-Cadenas, A. F., Carrasco-Marín, F., Gutiérrez-Reina, S. O., Bueno-López, A., Ocampo-Pérez, R., & Bailón-García, E. (2024). Auto-pressurized multi-stage tesla-valve type microreactors in carbon monoliths obtained through 3D printing: Impact of design on fluid dynamics and catalytic activity. *Advanced Functional Materials*. <https://doi.org/10.1002/adfm.202403659>
- Parsa, M., Qi, Y., Di Nuzzo, J. J., Moussakhani, Y., Tirto, A., & Chaffee, A. L. (2023). Regenerable carbon honeycomb monoliths directly prepared from brown coal: A novel carbon product. *Chemical Engineering Journal*, 471, 144699. <https://doi.org/10.1016/j.cej.2023.144699>
- Patel, H. (2019). Fixed-bed column adsorption study: A comprehensive review. *Applied Water Science*, 9(3), 45. <https://doi.org/10.1007/s13201-019-0927-7>
- Patel, H. (2022). Comparison of batch and fixed bed column adsorption: A critical review. *International Journal of Environmental Science and Technology*, 19(10), 10409–10426. <https://doi.org/10.1007/s13762-021-03492-y>
- Pearlman, D. S. (1976). Antihistamines: Pharmacology and Clinical Use. *Drugs*, 12(4), 258–273. <https://doi.org/10.2165/00003495-197612040-00002>
- Pekala, R. W. (1989). Organic aerogels from the polycondensation of resorcinol with formaldehyde. *Journal of Materials Science*, 24(9), 3221–3227. <https://doi.org/10.1007/BF01139044>
- Pérez-Cadenas, M., Moreno-Castilla, C., Carrasco-Marín, F., & Pérez-Cadenas, A. F. (2009). Surface chemistry, porous texture, and morphology of n-doped carbon xerogels. *Langmuir*, 25(1), 466–470. <https://doi.org/10.1021/la8027786>

- Perrich, J. R. (1981). *Activated carbon adsorption for wastewater treatment*. CRC Press.
- Phong Vo, H. N., Le, G. K., Hong Nguyen, T. M., Bui, X. T., Nguyen, K. H., Rene, E. R., Vo, T. D. H., Thanh Cao, N. D., & Mohan, R. (2019). Acetaminophen micropollutant: Historical and current occurrences, toxicity, removal strategies and transformation pathways in different environments. *Chemosphere*, 236, 124391. <https://doi.org/10.1016/j.chemosphere.2019.124391>
- Pisani, L. (2011). Simple expression for the tortuosity of porous media. *Transport in Porous Media*, 88(2), 193–203. <https://doi.org/10.1007/s11242-011-9734-9>
- Pohl, J., Ahrens, L., Carlsson, G., Golovko, O., Norrgren, L., Weiss, J., & Örn, S. (2019). Embryotoxicity of ozonated diclofenac, carbamazepine, and oxazepam in zebrafish (*Danio rerio*). *Chemosphere*, 225, 191–199. <https://doi.org/10.1016/j.chemosphere.2019.03.034>
- Porubcan, L. S., Serna, C. J., White, J. L., & Hem, S. L. (1978). Mechanism of adsorption of clindamycin and tetracycline by montmorillonite. *Journal of Pharmaceutical Sciences*, 67(8), 1081–1087. <https://doi.org/10.1002/jps.2600670815>
- Prasannamedha, G., Kumar, P. S., Mehala, R., Sharumitha, T. J., & Surendhar, D. (2021). Enhanced adsorptive removal of sulfamethoxazole from water using biochar derived from hydrothermal carbonization of sugarcane bagasse. *Journal of Hazardous Materials*, 407, 124825. <https://doi.org/10.1016/j.jhazmat.2020.124825>
- Praveena, B. A., Lokesh, N., Buradi, A., Santhosh, N., Praveena, B. L., & Vignesh, R. (2022). A comprehensive review of emerging additive manufacturing (3D printing technology): Methods, materials, applications, challenges, trends and future potential. *Materials Today Proceedings*, 52, 1309–1313. <https://doi.org/10.1016/j.matpr.2021.11.059>
- Prokić, D., Vukčević, M., Mitrović, A., Maletić, M., Kalijadis, A., Janković-Častvan, I., & Đurkić, T. (2022). Adsorption of estrone, 17 β -estradiol, and 17 α -ethinylestradiol from water onto modified multi-walled carbon nanotubes, carbon cryogel, and

- carbonized hydrothermal carbon. *Environmental Science and Pollution Research*, 29(3), 4431–4445. <https://doi.org/10.1007/s11356-021-15970-4>
- Ptaszkowska-Koniarz, M., Goscianska, J., & Pietrzak, R. (2018). Synthesis of carbon xerogels modified with amine groups and copper for efficient adsorption of caffeine. *Chemical Engineering Journal*, 345, 13–21. <https://doi.org/10.1016/j.cej.2018.03.132>
- Pulicharla, R., Hegde, K., Brar, S. K., & Surampalli, R. Y. (2017). Tetracyclines metal complexation: Significance and fate of mutual existence in the environment. *Environmental Pollution*, 221, 1–14. <https://doi.org/10.1016/j.envpol.2016.12.017>
- Qtaitat, M. A. (2004). Study of the interaction of trimethoprim–montmorillonite by infrared spectroscopy. *Spectrochimica Acta Part A: Molecular and Biomolecular Spectroscopy*, 60(3), 673–678. [https://doi.org/10.1016/S1386-1425\(03\)00277-4](https://doi.org/10.1016/S1386-1425(03)00277-4)
- Querejeta, N., Rubiera, F., & Pevida, C. (2022). Experimental study on the kinetics of CO₂ and H₂O adsorption on honeycomb carbon monoliths under cement flue gas conditions. *ACS Sustainable Chemistry & Engineering*, 10(6), 2107–2124. <https://doi.org/10.1021/acssuschemeng.1c07213>
- Quinn, B., Gagne, F., & Blaise, C. (2009). Evaluation of the acute, chronic and teratogenic effects of a mixture of eleven pharmaceuticals on the cnidarian, *Hydra attenuata*. *Science of the Total Environment*, 407(3), 1072–1079. <https://doi.org/10.1016/j.scitotenv.2008.10.022>
- Ramanayaka, S., Sarkar, B., Cooray, A. T., Ok, Y. S., & Vithanage, M. (2020). Halloysite nanoclay supported adsorptive removal of oxytetracycline antibiotic from aqueous media. *Journal of Hazardous Materials*, 384, 121301. <https://doi.org/10.1016/j.jhazmat.2019.121301>
- Ramírez-Morales, D., Masís-Mora, M., Montiel-Mora, J. R., Cambronero-Heinrichs, J. C., Briceño-Guevara, S., Rojas-Sánchez, C. E., Méndez-Rivera, M., Arias-Mora, V., Tormo-Budowski, R., Brenes-Alfaro, L., & Rodríguez-Rodríguez, C. E. (2020). Occurrence of pharmaceuticals, hazard assessment and ecotoxicological evaluation of wastewater treatment plants in Costa Rica. *Science of the Total Environment*, 746, 141200. <https://doi.org/10.1016/j.scitotenv.2020.141200>

- Ramírez-Valencia, L. D., Bailón-García, E., Moral-Rodríguez, A. I., Carrasco-Marín, F., & Pérez-Cadenas, A. F. (2023). Carbon gels–green graphene composites as metal-free bifunctional electro-fenton catalysts. *Gels*, 9(8), 665. <https://doi.org/10.3390/gels9080665>
- Rastogi, A., Tiwari, M. K., & Ghangrekar, M. M. (2021). A review on environmental occurrence, toxicity and microbial degradation of Non-Steroidal Anti-Inflammatory Drugs (NSAIDs). *Journal of Environmental Management*, 300, 113694. <https://doi.org/10.1016/j.jenvman.2021.113694>
- Rathi, B. S., & Kumar, P. S. (2021). Application of adsorption process for effective removal of emerging contaminants from water and wastewater. *Environmental Pollution*, 280, 116995. <https://doi.org/10.1016/j.envpol.2021.116995>
- Rauf, N., Tahir, S. S., Kang, J.-H., & Chang, Y.-S. (2012). Equilibrium, thermodynamics and kinetics studies for the removal of alpha and beta endosulfan by adsorption onto bentonite clay. *Chemical Engineering Journal*, 192, 369–376. <https://doi.org/10.1016/j.cej.2012.03.047>
- Riva, F., Zuccato, E., Davoli, E., Fattore, E., & Castiglioni, S. (2019). Risk assessment of a mixture of emerging contaminants in surface water in a highly urbanized area in Italy. *Journal of Hazardous Materials*, 361, 103–110. <https://doi.org/10.1016/j.jhazmat.2018.07.099>
- Rivera-Utrilla, J., Gómez-Pacheco, C. V., Sánchez-Polo, M., López-Peñalver, J. J., & Ocampo-Pérez, R. (2013). Tetracycline removal from water by adsorption/bioadsorption on activated carbons and sludge-derived adsorbents. *Journal of Environmental Management*, 131, 16–24. <https://doi.org/10.1016/j.jenvman.2013.09.024>
- Roberts, J., Kumar, A., Du, J., Hepplewhite, C., Ellis, D. J., Christy, A. G., & Beavis, S. G. (2016). Pharmaceuticals and personal care products (PPCPs) in Australia's largest inland sewage treatment plant, and its contribution to a major Australian river during high and low flow. *Science of the Total Environment*, 541, 1625–1637. <https://doi.org/10.1016/j.scitotenv.2015.03.145>

- Rodríguez-López, L., Santás-Miguel, V., Cela-Dablanca, R., Núñez-Delgado, A., Álvarez-Rodríguez, E., Pérez-Rodríguez, P., & Arias-Estévez, M. (2022). Ciprofloxacin and trimethoprim adsorption/desorption in agricultural soils. *International Journal of Environmental Research and Public Health*, 19(14), 8426. <https://doi.org/10.3390/ijerph19148426>
- Rodríguez-Reinoso, F., Molina-Sabio, M., & González, M. T. (1995). The use of steam and CO₂ as activating agents in the preparation of activated carbons. *Carbon*, 33(1), 15–23. [https://doi.org/10.1016/0008-6223\(94\)00100-E](https://doi.org/10.1016/0008-6223(94)00100-E)
- Rouquerol, J., Rouquerol, F., & Sing, K. (1998). *Adsorption by powders and porous solids. Principles, methodology and applications*. Academic press.
- Rout, P. R., Zhang, T. C., Bhunia, P., & Surampalli, R. Y. (2021). Treatment technologies for emerging contaminants in wastewater treatment plants: A review. *Science of the Total Environment*, 753, 141990. <https://doi.org/10.1016/j.scitotenv.2020.141990>
- Rumore, M. M. (1984). Clinical pharmacokinetics of chlorpheniramine. *Drug Intelligence & Clinical Pharmacy*, 18(9), 701–707. <https://doi.org/10.1177/106002808401800905>
- Sahin, O. I., Saygi-Yalcin, B., & Saloglu, D. (2020). Adsorption of ibuprofen from wastewater using activated carbon and graphene oxide embedded chitosan-PVA: Equilibrium, kinetics, and thermodynamic and optimization with central composite design. *Desalination and Water Treatment*, 179, 396–417. <https://doi.org/10.5004/dwt.2020.25027>
- Saitoh, T., & Shibayama, T. (2016). Removal and degradation of β -lactam antibiotics in water using didodecyldimethylammonium bromide-modified montmorillonite organoclay. *Journal of Hazardous Materials*, 317, 677–685. <https://doi.org/10.1016/j.jhazmat.2016.06.003>
- Salazar-Rabago, J. J., & Leyva-Ramos, R. (2016). Novel biosorbent with high adsorption capacity prepared by chemical modification of white pine (*Pinus durangensis*) sawdust. Adsorption of Pb(II) from aqueous solutions. *Journal of*

-
- Environmental Management*, 169, 303–312.
<https://doi.org/10.1016/j.jenvman.2015.12.040>
- Sam, D. K., Sam, E. K., Durairaj, A., Lv, X., Zhou, Z., & Liu, J. (2020). Synthesis of biomass-based carbon aerogels in energy and sustainability. *Carbohydrate Research*, 491, 107986. <https://doi.org/10.1016/j.carres.2020.107986>
- Sanz-Prat, A., Greskowiak, J., Burke, V., Rivera Villarreyes, C. A., Krause, J., Monninkhoff, B., Sperlich, A., Schimmelpfennig, S., Duennbier, U., & Massmann, G. (2020). A model-based analysis of the reactive transport behaviour of 37 trace organic compounds during field-scale bank filtration. *Water Research*, 173, 115523. <https://doi.org/10.1016/j.watres.2020.115523>
- Sarker, P., Lei, X., Taylor, K., Holmes, W., Yan, H., Cao, D., Zappi, M. E., & Gang, D. D. (2023). Evaluation of the adsorption of sulfamethoxazole (SMX) within aqueous influents onto customized ordered mesoporous carbon (OMC) adsorbents: Performance and elucidation of key adsorption mechanisms. *Chemical Engineering Journal*, 454, 140082. <https://doi.org/10.1016/j.cej.2022.140082>
- Sathishkumar, P., Meena, R. A. A., Palanisami, T., Ashokkumar, V., Palvannan, T., & Gu, F. L. (2020). Occurrence, interactive effects and ecological risk of diclofenac in environmental compartments and biota - A review. *Science of the Total Environment*, 698, 134057. <https://doi.org/10.1016/j.scitotenv.2019.134057>
- Schaefer, T. S., & Zito, P. M. (2023). Antiemetic Histamine H1 Receptor Blockers. In: National Library of Medicine.
- Schay, G. J., Fejes, F. P., & Szethmary, J. M. (1957). Adsorption of gases and gas mixtures. *Acta Chimica Academiae Scientiarum Hungaricane*, 12, 299–308.
- Segovia-Sandoval, S. J., Padilla-Ortega, E., Carrasco-Marín, F., Berber-Mendoza, M. S., & Ocampo-Pérez, R. (2019). Simultaneous removal of metronidazole and Pb(II) from aqueous solution onto bifunctional activated carbons. *Environmental Science and Pollution Research*, 26(25), 25916–25931. <https://doi.org/10.1007/s11356-019-05857-w>
- Segovia-Sandoval, S. J., Pastrana-Martínez, L. M., Ocampo-Pérez, R., Morales-Torres, S., Berber-Mendoza, M. S., & Carrasco-Marín, F. (2020). Synthesis and

- characterization of carbon xerogel/graphene hybrids as adsorbents for metronidazole pharmaceutical removal: Effect of operating parameters. *Separation and Purification Technology*, 237, 116341. <https://doi.org/10.1016/j.seppur.2019.116341>
- Sen Gupta, S., & Bhattacharyya, K. G. (2008). Immobilization of Pb(II), Cd(II) and Ni(II) ions on kaolinite and montmorillonite surfaces from aqueous medium. *Journal of Environmental Management*, 87(1), 46–58. <https://doi.org/10.1016/j.jenvman.2007.01.048>
- Serwecińska, L. (2020). Antimicrobials and antibiotic-resistant bacteria: A Risk to the environment and to public health. *Water*, 12(12), 3313. <https://doi.org/10.3390/w12123313>
- Shah, K. J., Pan, S.-Y., Shukla, A. D., Shah, D. O., & Chiang, P.-C. (2018). Mechanism of organic pollutants sorption from aqueous solution by cationic tunable organoclays. *Journal of Colloid and Interface Science*, 529, 90–99. <https://doi.org/10.1016/j.jcis.2018.05.094>
- Shahid, M. K., Kashif, A., Fuwad, A., & Choi, Y. (2021). Current advances in treatment technologies for removal of emerging contaminants from water – A critical review. *Coordination Chemistry Reviews*, 442, 213993. <https://doi.org/10.1016/j.ccr.2021.213993>
- Sharma, A., Thakur, K. K., Mehta, P., & Pathania, D. (2018). Efficient adsorption of chlorpheniramine and hexavalent chromium (Cr(VI)) from water system using agronomic waste material. *Sustainable Chemistry and Pharmacy*, 9, 1–11. <https://doi.org/10.1016/j.scp.2018.04.002>
- Sharma, B. M., Bečanová, J., Scheringer, M., Sharma, A., Bharat, G. K., Whitehead, P. G., Klánová, J., & Nizzetto, L. (2019). Health and ecological risk assessment of emerging contaminants (pharmaceuticals, personal care products, and artificial sweeteners) in surface and groundwater (drinking water) in the Ganges River Basin, India. *Science of the Total Environment*, 646, 1459–1467. <https://doi.org/10.1016/j.scitotenv.2018.07.235>

-
- Shen, L., & Chen, Z. (2007). Critical review of the impact of tortuosity on diffusion. *Chemical Engineering Science*, 62(14), 3748–3755. <https://doi.org/10.1016/j.ces.2007.03.041>
- Shen, T., & Gao, M. (2019). Gemini surfactant modified organo-clays for removal of organic pollutants from water: A review. *Chemical Engineering Journal*, 375, 121910. <https://doi.org/10.1016/j.cej.2019.121910>
- Shouman, M. A., & Fathy, N. A. (2018). Microporous nanohybrids of carbon xerogels and multi-walled carbon nanotubes for removal of rhodamine B dye. *Journal of Water Process Engineering*, 23, 165–173. <https://doi.org/10.1016/j.jwpe.2018.03.014>
- Silva, A., Martinho, S., Stawiński, W., Węgrzyn, A., Figueiredo, S., Santos, L. H. M. L. M., & Freitas, O. (2018). Application of vermiculite-derived sustainable adsorbents for removal of venlafaxine. *Environmental Science and Pollution Research*, 25(17), 17066–17076. <https://doi.org/10.1007/s11356-018-1869-6>
- Sing, K. S. W. (1985). Reporting physisorption data for gas/solid systems with special reference to the determination of surface area and porosity (Recommendations 1984). *Pure and Applied Chemistry*, 57(4), 603–619. <https://doi.org/10.1351/pac198557040603>
- Solgi, M., Steiger, B. G. K., & Wilson, L. D. (2023). A fixed-bed column with an agro-waste biomass composite for controlled separation of sulfate from aqueous media. *Separations*, 10(4), 262. <https://doi.org/10.3390/separations10040262>
- Soori, M. M., Ghahramani, E., Kazemian, H., Al-Musawi, T. J., & Zarrabi, M. (2016). Intercalation of tetracycline in nano sheet layered double hydroxide: An insight into UV/VIS spectra analysis. *Journal of the Taiwan Institute of Chemical Engineers*, 63, 271–285. <https://doi.org/10.1016/j.jtice.2016.03.015>
- Sophia A., C., & Lima, E. C. (2018). Removal of emerging contaminants from the environment by adsorption. *Ecotoxicology and Environmental Safety*, 150, 1–17. <https://doi.org/10.1016/j.ecoenv.2017.12.026>
- Sudo, Y., Misic, D. M., & Suzuki, M. (1978). Concentration dependence of effective surface diffusion coefficient in aqueous phase adsorption on activated carbon.

- Chemical Engineering Science*, 33(9), 1287–1290. [https://doi.org/10.1016/0009-2509\(78\)85097-0](https://doi.org/10.1016/0009-2509(78)85097-0)
- Sukatis, F. F., Looi, L. J., Lim, H. N., Abdul Rahman, M. B., Mohd Zaki, M. R., & Aris, A. Z. (2024). Fixed-bed adsorption studies of endocrine-disrupting compounds from water by using novel calcium-based metal-organic frameworks. *Environmental Pollution*, 341, 122980. <https://doi.org/10.1016/j.envpol.2023.122980>
- Sun, Y., Yue, Q., Gao, B., Wang, B., Li, Q., Huang, L., & Xu, X. (2012). Comparison of activated carbons from *Arundo donax* Linn with $H_4P_2O_7$ activation by conventional and microwave heating methods. *Chemical Engineering Journal*, 192, 308–314. <https://doi.org/10.1016/j.cej.2012.04.007>
- Sutcliffe, A. G., Jones, R. B., & Woodruff, G. (1998). Eye malformations associated with treatment with carbamazepine during pregnancy. *Ophthalmic Genetics*, 19(2), 59–62. <https://doi.org/10.1076/opge.19.2.59.2321>
- Taheran, M., Naghdi, M., Brar, S. K., Verma, M., & Surampalli, R. Y. (2018). Emerging contaminants: Here today, there tomorrow! *Environmental Nanotechnology, Monitoring & Management*, 10, 122–126. <https://doi.org/10.1016/j.enmm.2018.05.010>
- Tan, X., Wei, H., Zhou, Y., Zhang, C., & Ho, S. H. (2022). Adsorption of sulfamethoxazole via biochar: The key role of characteristic components derived from different growth stage of microalgae. *Environmental Research*, 210, 112965. <https://doi.org/10.1016/j.envres.2022.112965>
- Tariq, S., Saeed, M., Zahid, U., Munir, M., Intisar, A., Asad Riaz, M., Riaz, A., Waqas, M., & Abid, H. M. W. (2022). Green and eco-friendly adsorption of dyes with organoclay: isothermal, kinetic and thermodynamic studies. *Toxin Reviews*, 41(4), 1105–1114. <https://doi.org/10.1080/15569543.2021.1975751>
- Teixeira, M., Almeida, Â., Calisto, V., Esteves, V. I., Schneider, R. J., Wrona, F. J., Soares, A. M. V. M., Figueira, E., & Freitas, R. (2017). Toxic effects of the antihistamine cetirizine in mussel *Mytilus galloprovincialis*. *Water Research*, 114, 316–326. <https://doi.org/10.1016/j.watres.2017.02.032>

- Teo, Y. S., Jafari, I., Liang, F., Jung, Y., Van der Hoek, J. P., Ong, S. L., & Hu, J. (2022). Investigation of the efficacy of the UV/Chlorine process for the removal of trimethoprim: Effects of operational parameters and artificial neural networks modelling. *Science of the Total Environment*, 812, 152551. <https://doi.org/10.1016/j.scitotenv.2021.152551>
- Thiebault, T., & Boussafir, M. (2019). Adsorption mechanisms of psychoactive drugs onto montmorillonite. *Colloid and Interface Science Communications*, 30, 100183. <https://doi.org/10.1016/j.colcom.2019.100183>
- Thirunavukkarasu, A., Nithya, R., & Sivashankar, R. (2021). Continuous fixed-bed biosorption process: A review. *Chemical Engineering Journal Advances*, 8, 100188. <https://doi.org/10.1016/j.ceja.2021.100188>
- Thommes, M., Kaneko, K., Neimark, A. V., Olivier, J. P., Rodriguez-Reinoso, F., Rouquerol, J., & Sing, K. S. W. (2015). Physisorption of gases, with special reference to the evaluation of surface area and pore size distribution (IUPAC Technical Report). *Pure and Applied Chemistry*, 87(9–10), 1051–1069. <https://doi.org/10.1515/pac-2014-1117>
- Tomašić, V., & Jović, F. (2006). State-of-the-art in the monolithic catalysts/reactors. *Applied Catalysis A: General*, 311, 112–121. <https://doi.org/10.1016/j.apcata.2006.06.013>
- Undabeytia, T., Nir, S., Polubesova, T., Rytwo, G., Morillo, E., & Maqueda, C. (1999). Adsorption–desorption of chlordimeform on montmorillonite: Effect of clay aggregation and competitive adsorption with cadmium. *Environmental Science & Technology*, 33(6), 864–869. <https://doi.org/10.1021/es980822k>
- Vallova, S., Plevova, E., Smutna, K., Sokolova, B., Vaculikova, L., Valovicova, V., Hundakova, M., & Praus, P. (2022). Removal of analgesics from aqueous solutions onto montmorillonite KSF. *Journal of Thermal Analysis and Calorimetry*, 147(3), 1973–1981. <https://doi.org/10.1007/s10973-021-10591-y>
- Vasilachi, I., Asimicesei, D., Fertu, D., & Gavrilescu, M. (2021). Occurrence and fate of emerging pollutants in water environment and options for their removal. *Water*, 13(2), 181. <https://doi.org/10.3390/w13020181>

- Vasseghian, Y., Sezgin, D., Nguyen, D. C., Hoang, H. Y., & Sari Yilmaz, M. (2023). A hybrid nanocomposite based on CuFe layered double hydroxide coated graphene oxide for photocatalytic degradation of trimethoprim. *Chemosphere*, 322, 138243. <https://doi.org/10.1016/j.chemosphere.2023.138243>
- Velde, B. (1992). *Introduction to clay minerals: Chemistry, origins, uses and environmental significance*. Editorial Chapman & Hall, London.
- Vergunst, T., Linders, M. J. G., Kapteijn, F., & Moulijn, J. A. (2001). Carbon-based monolithic structures. *Catalysis Reviews*, 43(3), 291–314. <https://doi.org/10.1081/CR-100107479>
- Vimonses, V., Lei, S., Jin, B., Chow, C. W. K., & Saint, C. (2009). Kinetic study and equilibrium isotherm analysis of Congo Red adsorption by clay materials. *Chemical Engineering Journal*, 148(2–3), 354–364. <https://doi.org/10.1016/j.cej.2008.09.009>
- Vivo-Vilches, J. F., Carrasco-Marín, F., Pérez-Cadenas, A. F., & Maldonado-Hódar, F. J. (2015). Fitting the porosity of carbon xerogel by CO₂ activation to improve the TMP/n-octane separation. *Microporous and Mesoporous Materials*, 209, 10–17. <https://doi.org/10.1016/j.micromeso.2015.01.010>
- Vivo-Vilches, J. F., Pérez-Cadenas, A. F., Maldonado-Hódar, F. J., Carrasco-Marín, F., Regufe, M. J., Ribeiro, A. M., Ferreira, A. F. P., & Rodrigues, A. E. (2018). Resorcinol–formaldehyde carbon xerogel as selective adsorbent of carbon dioxide present on biogas. *Adsorption*, 24(2), 169–177. <https://doi.org/10.1007/s10450-018-9933-6>
- Wan, Y., Bao, Y., & Zhou, Q. (2010). Simultaneous adsorption and desorption of cadmium and tetracycline on cinnamon soil. *Chemosphere*, 80(7), 807–812. <https://doi.org/10.1016/j.chemosphere.2010.04.066>
- Wang, C.-J., Li, Z., Jiang, W.-T., Jean, J.-S., & Liu, C.-C. (2010). Cation exchange interaction between antibiotic ciprofloxacin and montmorillonite. *Journal of Hazardous Materials*, 183(1–3), 309–314. <https://doi.org/10.1016/j.jhazmat.2010.07.025>

- Wang, K., Ye, Z., Li, X., & Yang, J. (2022). Nanoporous resorcinol-formaldehyde based carbon aerogel for lightweight and tunable microwave absorption. *Materials Chemistry and Physics*, 278, 125718. <https://doi.org/10.1016/j.matchemphys.2022.125718>
- Wang, M., & You, X. (2023). Efficient adsorption of antibiotics and heavy metals from aqueous solution by structural designed PSSMA-functionalized-chitosan magnetic composite. *Chemical Engineering Journal*, 454, 140417. <https://doi.org/10.1016/j.cej.2022.140417>
- Wang, W., Zheng, B., Deng, Z., Feng, Z., & Fu, L. (2013). Kinetics and equilibriums for adsorption of poly(vinyl alcohol) from aqueous solution onto natural bentonite. *Chemical Engineering Journal*, 214, 343–354. <https://doi.org/10.1016/j.cej.2012.10.070>
- Wang, X., Jing, J., Zhou, M., & Dewil, R. (2023). Recent advances in H₂O₂-based advanced oxidation processes for removal of antibiotics from wastewater. *Chinese Chemical Letters*, 34(3), 107621. <https://doi.org/10.1016/j.ccllet.2022.06.044>
- Wang, X., Lu, S., Chen, L., Li, J., Dai, S., & Wang, X. (2015). Efficient removal of Eu(III) from aqueous solutions using super-adsorbent of bentonite–polyacrylamide composites. *Journal of Radioanalytical and Nuclear Chemistry*, 306(2), 497–505. <https://doi.org/10.1007/s10967-015-4115-4>
- Wang, Y., Feng, H., Zhang, Y., Lin, C., Zheng, L., Ji, W., & Han, X. (2019). Suppression effects of hydroxy acid modified montmorillonite powders on methane explosions. *Energies*, 12(21), 4068. <https://doi.org/10.3390/en12214068>
- Wang, Y.-J., Jia, D.-A., Sun, R.-J., Zhu, H.-W., & Zhou, D.-M. (2008). Adsorption and cosorption of tetracycline and copper(II) on montmorillonite as affected by solution pH. *Environmental Science & Technology*, 42(9), 3254–3259. <https://doi.org/10.1021/es702641a>
- Weber, W. J., & Morris, J. C. (1963). Kinetics of adsorption on carbon from solution. *Journal of the Sanitary Engineering Division*, 89(2), 31–59. <https://doi.org/10.1061/JSEDAI.0000430>

- White, C. M., & Hernandez, A. V. (2021). Ranitidine and Risk of N - Nitrosodimethylamine (NDMA) Formation. *JAMA*, 326(3), 225.
- White, D., Lapworth, D. J., Civil, W., & Williams, P. (2019). Tracking changes in the occurrence and source of pharmaceuticals within the River Thames, UK; from source to sea. *Environmental Pollution*, 249, 257–266. <https://doi.org/10.1016/j.envpol.2019.03.015>
- Wicklein, B., Darder, M., Aranda, P., & Ruiz-Hitzky, E. (2010). Bio-organoclays based on phospholipids as immobilization hosts for biological species. *Langmuir*, 26(7), 5217–5225. <https://doi.org/10.1021/la9036925>
- Wilke, C. R., & Chang, P. (1955). Correlation of diffusion coefficients in dilute solutions. *AIChE Journal*, 1(2), 264–270. <https://doi.org/10.1002/aic.690010222>
- Wilkinson, J., Hooda, P. S., Barker, J., Barton, S., & Swinden, J. (2017). Occurrence, fate and transformation of emerging contaminants in water: An overarching review of the field. *Environmental Pollution*, 231, 954–970. <https://doi.org/10.1016/j.envpol.2017.08.032>
- Wojcieszńska, D., Guzik, H., & Guzik, U. (2022). Non-steroidal anti-inflammatory drugs in the era of the Covid-19 pandemic in the context of the human and the environment. *Science of the Total Environment*, 834, 155317. <https://doi.org/10.1016/j.scitotenv.2022.155317>
- Wu, H., Xie, H., He, G., Guan, Y., & Zhang, Y. (2016). Effects of the pH and anions on the adsorption of tetracycline on iron-montmorillonite. *Applied Clay Science*, 119, 161–169. <https://doi.org/10.1016/j.clay.2015.08.001>
- Wu, M., Zhao, S., Jing, R., Shao, Y., Liu, X., Lv, F., Hu, X., Zhang, Q., Meng, Z., & Liu, A. (2019). Competitive adsorption of antibiotic tetracycline and ciprofloxacin on montmorillonite. *Applied Clay Science*, 180, 105175. <https://doi.org/10.1016/j.clay.2019.105175>
- Wu, P., Wu, W., Li, S., Xing, N., Zhu, N., Li, P., Wu, J., Yang, C., & Dang, Z. (2009). Removal of Cd²⁺ from aqueous solution by adsorption using Fe-montmorillonite. *Journal of Hazardous Materials*, 169(1–3), 824–830. <https://doi.org/10.1016/j.jhazmat.2009.04.022>

- Xia, C., Lv, G., Mei, L., Song, K., Li, Z., Wang, X., Xing, X., & Xu, B. (2014). Removal of chlorpheniramine from water by birnessite. *Water, Air, & Soil Pollution*, 225(9), 2131. <https://doi.org/10.1007/s11270-014-2131-6>
- Xu, L., Zhang, H., Xiong, P., Zhu, Q., Liao, C., & Jiang, G. (2021). Occurrence, fate, and risk assessment of typical tetracycline antibiotics in the aquatic environment: A review. *Science of the Total Environment*, 753, 141975. <https://doi.org/10.1016/j.scitotenv.2020.141975>
- Xu, Y., Li, Z., Fang, F., E, Y., & Zhao, G. (2021). Novel visible-light-induced BiOCl/g-C₃N₄ photocatalyst for efficient degradation of metronidazole. *Inorganic Chemistry Communications*, 132, 108820. <https://doi.org/10.1016/j.inoche.2021.108820>
- Xue, Z., Feng, Y., Li, H., Xu, C., Ju, J., Dong, L., Yang, C., Bao, W., Wang, J., Wang, H., & Ma, R. (2023). Adsorption of trimethoprim and sulfamethoxazole using residual carbon from coal gasification slag: Behavior, mechanism and cost-benefit analysis. *Fuel*, 348, 128508. <https://doi.org/10.1016/j.fuel.2023.128508>
- Yamamoto, K., Shiono, T., Yoshimura, R., Matsui, Y., & Yoneda, M. (2018). Influence of hydrophilicity on adsorption of caffeine onto montmorillonite. *Adsorption Science & Technology*, 36(3–4), 967–981. <https://doi.org/10.1177/0263617417735480>
- Yang, S., Huang, Z., Li, C., Li, W., Yang, L., & Wu, P. (2020). Individual and simultaneous adsorption of tetracycline and cadmium by dodecyl dimethyl betaine modified vermiculite. *Colloids and Surfaces A: Physicochemical and Engineering Aspects*, 602, 125171. <https://doi.org/10.1016/j.colsurfa.2020.125171>
- Yang, Z., Li, J., Xu, X., Pang, S., Hu, C., Guo, P., Tang, S., & Cheng, H.-M. (2020). Synthesis of monolithic carbon aerogels with high mechanical strength via ambient pressure drying without solvent exchange. *Journal of Materials Science & Technology*, 50, 66–74. <https://doi.org/10.1016/j.jmst.2020.02.013>
- Yao, N., Li, C., Yu, J., Xu, Q., Wei, S., Tian, Z., Yang, Z., Yang, W., & Shen, J. (2020). Insight into adsorption of combined antibiotic-heavy metal contaminants on graphene oxide in water. *Separation and Purification Technology*, 236, 116278. <https://doi.org/10.1016/j.seppur.2019.116278>

- Yariv, S., Russell, J. D., & Farmer, V. C. (1966). Infrared study of the adsorption of benzoic acid and nitrobenzene in montmorillonite. *Israel Journal of Chemistry*, 4(5–6), 201–213. <https://doi.org/10.1002/ijch.196600034>
- Yılmaz, Ç., & Özcengiz, G. (2017). Antibiotics: Pharmacokinetics, toxicity, resistance and multidrug efflux pumps. *Biochemical Pharmacology*, 133, 43–62. <https://doi.org/10.1016/j.bcp.2016.10.005>
- Yin, K., Viana, P. Z., & Rockne, K. J. (2019). Organic contaminated sediments remediation with active caps: Nonlinear adsorption unveiled by combined isotherm and column transportation studies. *Chemosphere*, 214, 710–718. <https://doi.org/10.1016/j.chemosphere.2018.09.122>
- Yu, F., Li, Y., Han, S., & Ma, J. (2016). Adsorptive removal of antibiotics from aqueous solution using carbon materials. *Chemosphere*, 153, 365–385. <https://doi.org/10.1016/j.chemosphere.2016.03.083>
- Yu, L., Cao, W., Wu, S., Yang, C., & Cheng, J. (2018). Removal of tetracycline from aqueous solution by MOF/graphite oxide pellets: Preparation, characteristic, adsorption performance and mechanism. *Ecotoxicology and Environmental Safety*, 164, 289–296. <https://doi.org/10.1016/j.ecoenv.2018.07.110>
- Zainol, M. M., Asmadi, M., Iskandar, P., Wan Ahmad, W. A. N., Amin, N. A. S., & Hoe, T. T. (2021). Ethyl levulinate synthesis from biomass derivative chemicals using iron doped sulfonated carbon cryogel catalyst. *Journal of Cleaner Production*, 281, 124686. <https://doi.org/10.1016/j.jclepro.2020.124686>
- Zhang, D., Pan, B., Zhang, H., Ning, P., & Xing, B. (2010). Contribution of different sulfamethoxazole species to their overall adsorption on functionalized carbon nanotubes. *Environmental Science & Technology*, 44(10), 3806–3811. <https://doi.org/10.1021/es903851q>
- Zhang, H., Ma, J., Shi, M., Xia, M., Wang, F., & Fu, C. (2021). Adsorption of two β -blocker pollutants on modified montmorillonite with environment-friendly cationic surfactant containing amide group: Batch adsorption experiments and Multiwfn wave function analysis. *Journal of Colloid and Interface Science*, 590, 601–613. <https://doi.org/10.1016/j.jcis.2021.01.077>

- Zhang, L., Song, X., Liu, X., Yang, L., Pan, F., & Lv, J. (2011). Studies on the removal of tetracycline by multi-walled carbon nanotubes. *Chemical Engineering Journal*, 178, 26–33. <https://doi.org/10.1016/j.cej.2011.09.127>
- Zhang, P., Zhou, H., Li, K., Zhao, X., Liu, Q., Li, D., & Zhao, G. (2018). Occurrence of pharmaceuticals and personal care products, and their associated environmental risks in a large shallow lake in north China. *Environmental Geochemistry and Health*, 40(4), 1525–1539. <https://doi.org/10.1007/s10653-018-0069-0>
- Zhang, R., Zhang, R., Yu, K., Wang, Y., Huang, X., Pei, J., Wei, C., Pan, Z., Qin, Z., & Zhang, G. (2018). Occurrence, sources and transport of antibiotics in the surface water of coral reef regions in the South China Sea: Potential risk to coral growth. *Environmental Pollution*, 232, 450–457. <http://dx.doi.org/10.1016/j.envpol.2017.09.064>
- Zhang, R., Zheng, X., Chen, B., Ma, J., Niu, X., Zhang, D., Lin, Z., Fu, M., & Zhou, S. (2020). Enhanced adsorption of sulfamethoxazole from aqueous solution by Fe-impregnated graphitized biochar. *Journal of Cleaner Production*, 256, 120662. <https://doi.org/10.1016/j.jclepro.2020.120662>
- Zhang, W., Zhang, M., Lin, K., Sun, W., Xiong, B., Guo, M., Cui, X., & Fu, R. (2012). Eco-toxicological effect of Carbamazepine on *Scenedesmus obliquus* and *Chlorella pyrenoidosa*. *Environmental Toxicology and Pharmacology*, 33(2), 344–352. <https://doi.org/10.1016/j.etap.2011.12.024>
- Zhang, X., Yi, H., Bai, H., Zhao, Y., Min, F., & Song, S. (2017). Correlation of montmorillonite exfoliation with interlayer cations in the preparation of two-dimensional nanosheets. *RSC Advances*, 7(66), 41471–41478. <https://doi.org/10.1039/C7RA07816A>
- Zhang, Z., Chen, Y., Wang, Z., Hu, C., Ma, D., Chen, W., & Ao, T. (2021). Effective and structure-controlled adsorption of tetracycline hydrochloride from aqueous solution by using Fe-based metal-organic frameworks. *Applied Surface Science*, 542, 148662. <https://doi.org/10.1016/j.apsusc.2020.148662>
- Zhao, C., Hong, P., Li, Y., Song, X., Wang, Y., & Yang, Y. (2019). Mechanism of adsorption of tetracycline–Cu multi-pollutants by graphene oxide (GO) and

- reduced graphene oxide (rGO). *Journal of Chemical Technology & Biotechnology*, 94(4), 1176–1186. <https://doi.org/10.1002/jctb.5864>
- Zhao, Y., Gu, X., Gao, S., Geng, J., & Wang, X. (2012). Adsorption of tetracycline (TC) onto montmorillonite: Cations and humic acid effects. *Geoderma*, 183–184, 12–18. <https://doi.org/10.1016/j.geoderma.2012.03.004>
- Zhao, Y., Tan, Y., Guo, Y., Gu, X., Wang, X., & Zhang, Y. (2013). Interactions of tetracycline with Cd (II), Cu (II) and Pb (II) and their cosorption behavior in soils. *Environmental Pollution*, 180, 206–213. <https://doi.org/10.1016/j.envpol.2013.05.043>
- Zheng, H., Wang, Z., Zhao, J., Herbert, S., & Xing, B. (2013). Sorption of antibiotic sulfamethoxazole varies with biochars produced at different temperatures. *Environmental Pollution*, 181, 60–67. <https://doi.org/10.1016/j.envpol.2013.05.056>
- Zhou, A., Wu, X., Chen, W., Liao, L., & Xie, P. (2020). Fabrication of hydrophobic/hydrophilic bifunctional adsorbent for the removal of sulfamethoxazole and bisphenol A in Water. *Journal of Environmental Chemical Engineering*, 8(5), 104161. <https://doi.org/10.1016/j.jece.2020.104161>
- Zhou, S., Di Paolo, C., Wu, X., Shao, Y., Seiler, T. B., & Hollert, H. (2019). Optimization of screening-level risk assessment and priority selection of emerging pollutants – The case of pharmaceuticals in European surface waters. *Environmental International*, 128, 1–10. <https://doi.org/10.1016/j.envint.2019.04.034>
- Zind, H., Mondamert, L., Remaury, Q. B., Cleon, A., Leitner, N. K. V., & Labanowski, J. (2021). Occurrence of carbamazepine, diclofenac, and their related metabolites and transformation products in a French aquatic environment and preliminary risk assessment. *Water Research*, 196, 117052. <https://doi.org/10.1016/j.watres.2021.117052>
- Zoroufchi Benis, K., Sokhansanj, A., Hughes, K. A., McPhedran, K. N., & Soltan, J. (2023). An engineered biochar for treatment of selenite contaminated water: Mass transfer characteristics in fixed bed adsorption. *Chemical Engineering Journal*, 469, 143946. <https://doi.org/10.1016/j.cej.2023.143946>